ISBN 978-82-326-2460-7 (printed version)
ISBN 978-82-326-2461-4 (electronic version)
ISSN 1503-8181

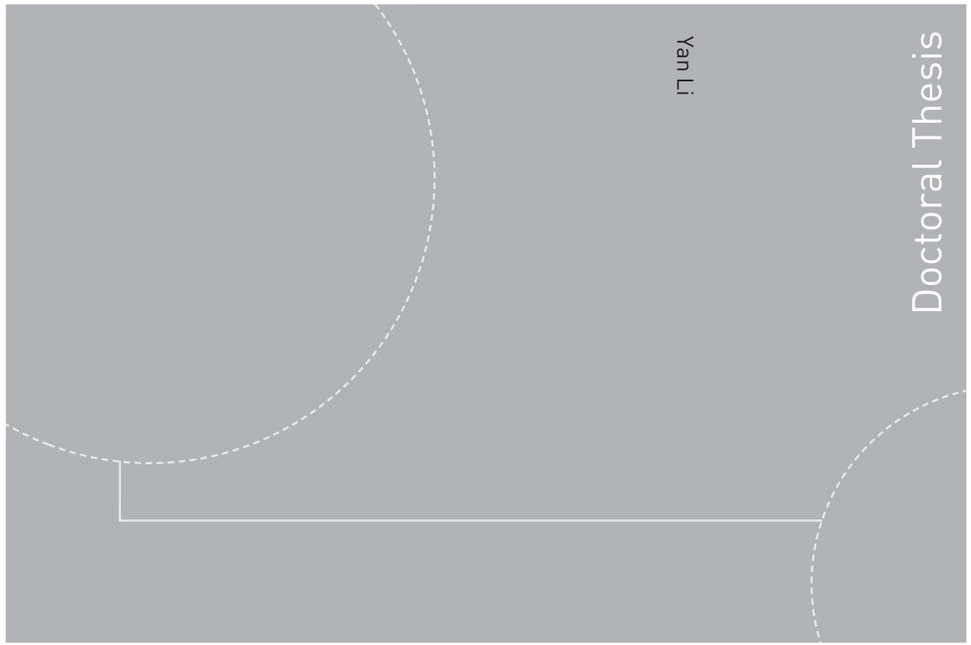

Doctoral theses at NTNU, 2017:194

Yan Li

Surface water waves on depth dependent flows

NTNU
Norwegian University of
Science and Technology
Faculty of Engineering
Science and Technology
Department of Energy and Process Engineering

NTNU
Norwegian University of
Science and Technology

Doctoral theses at NTNU, 2017:194

NTNU

NTNU
Norwegian University of
Science and Technology

Yan Li

Surface water waves on depth dependent flows

Thesis for the degree of Philosophiae Doctor

Trondheim, August 2017

Norwegian University of Science and Technology
Faculty of Engineering
Science and Technology
Department of Energy andProcess Engineering

NTNU
Norwegian University of
Science and Technology

NTNU
Norwegian University of Science and Technology

Thesis for the degree of Philosophiae Doctor

Faculty of Engineering
Science and Technology
Department of Energy andProcess Engineering

ISBN 978-82-326-2460-7 (printed version)
ISBN 978-82-326-2461-4 (electronic version)
ISSN 1503-8181

Doctoral theses at NTNU, 2017:194

Printed by Skipnes Kommunikasjon as

Abstract

The present thesis provides essential insights into surface water waves propagating atop a horizontal current whose magnitude and direction may vary arbitrarily with water depth. A comprehensive theory in this regard is developed in the framework of linear wave theory in three dimensions, being readily applied to a wide range of realistic circumstances. General theoretical solutions to different boundary value problems are presented. In particular, explicit expressions with regard to the surface elevation and the vertical velocity are derived. The boundary value problems include the Cauchy-Poisson problem, surface disturbances generated by an initial impulsive and a time-dependent pressure, and a steady pressure that normally works as the model of moving vessels and oscillating travelling sources. Efforts focus especially on the dispersion relation and the effects of a subsurface shear current on surface waves. A subsurface shear current is most often found to have significant effects on surface waves. In particular, the presence of a current of uniform vorticity is analysed in detail for the problems of ship waves, an oscillating advancing source and wave interferences.

A theory is especially presented to calculate waves from a general, time-dependent applied surface pressure acting on the surface of a horizontally directed shear current which may vary arbitrarily with depth in both direction and magnitude. It is based on deriving the response function in the context of waves generated by an impulsive applied pressure. Effective approaches to calculate wave resistance without undue difficulty are presented. Strikingly, a lateral radiation force – that is defined towards the starboard (right) – is firstly found apart from the well-known wave resistance along the stern-wise direction due to the presence of a shear current when a ship is making an oblique angle with the shear current. The lateral radiation force may amount to 20 percent of the normal wave resistance in some specific situations.

As for waves on a current in arbitrary variation of water depth, an implicit dispersion relation is derived, which poses potential challenges in obtaining analytical solutions. Several semi-analytical approaches to solve/approximate the dispersion relation are hence derived. In particular, a direct integration approach – that solves the linearised Rayleigh equation and implicit dispersion relation in a coupled way – and approximations based on a perturbation method are presented. The proper criteria under which different perturbed approximate dispersion relations are applicable are determined. Furthermore, the analytical solutions of the dispersion relation under limited circumstances are derived, e.g. for a shear current of uniform vorticity and stationary waves for a specific class of shear profiles of non-zero curvature.

Despite the fact that linear waves in the presence of a linear shear current have been extensively analysed in two dimensions, studies in three dimensions are scarce. This means that realistic three dimensional effects may be in some cases overlooked or yet discovered. The present thesis hence attempts to fill this gap based on theoretical as well as numerical analysis. Effects of a uniform vorticity are specially analysed in the context of ship waves, waves generated by an oscillating travelling source and interferences of waves generated by a two-point wavemaker of monohull ships. Fascinating and novel features are found due to the uniform vorticity S that is known either as the 'intrinsic shear Froude number' $\mathrm{Fr}_{\mathrm{sb}} = S\sqrt{L/g}$ or the 'shear Froude number' $\mathrm{Fr}_{\mathrm{s}} = |\mathbf{V}|S/g$ (L: the reference length; $|\mathbf{V}|$: moving speed of a wavemaker; g: the gravitational acceleration). In particular, asymmetrical ship wave patterns, the critical shear velocity above which the transverse ship waves vanish, the transitions between the sub-critical and supercritical situations due to the complex interplays of the shear current and seabed, non-constant Kelvin angles, and a somewhat similar effect as a finite water depth on wave interferences are shown for the problem of ship wakes. All of those novel features would not have been found if theoretical studies are constrained to 2D. Furthermore, the classical Doppler resonance occurs when the non-dimensional frequency $\tau = |\mathbf{V}|\omega/g$ (ω : the oscillating frequency) is equal to $1/4$ in the absence of a shear current, while there may be multiple Doppler resonances – as many as 4 – for $\mathrm{Fr}_{\mathrm{s}} > 1/3$ in deep water due to the presence of a linear shear current. It is also indicated that the Doppler resonance may be profoundly modified even for a linear current of weak vorticity.

Preface

This thesis is submitted for the degree of Doctor of Philosophy at the Norwegian University of Science and Technology (NTNU). The work included in the thesis started in August 2014 at the Department of Energy and Process Engineering (EPT), NTNU, and was completed in the beginning of June, 2017. The result of research undertaken during this period is under the supervision of Associate Professor Simen Å Ellingsen. Professor Dag Myrhaug from the Department of Marine Technology, NTNU, has been the co-supervisor. Apart from a stay of three months at the University of Shanghai Jiao Tong University (SJTU) in the summer of 2016, the research has been carried out in Trondheim. During the stay at SJTU, the research had been partially supervised by Professor Francis Noblesse from the School of Naval Architecture, Ocean & Civil Engineering, SJTU.

My fellowship during the PhD period has been provided by the faculty of Engineering Science and Technology at NTNU in connection with the project – 'Fluid Dynamics: Wave-Current Interactions'.

Acknowledgement

"It is the time you have wasted for your rose

that makes your rose so important."

Quoted from *The Little Prince*

I am approaching the end of my Phd period, which may lead to a completely new page for the rest of my life. This reminds me of a lot of people who have offered me great help and support especially during my Phd period.

Above all, I would like to express my most sincere gratitude to my supervisor – Associate Professor Simen Å Ellingsen, a young and highly talented scholar. I deeply feel it has been my honour to have worked for three years with him. During the PhD period, I have been deeply inspired by his wisdom, his broad knowledge and rigorous attitude to work and research. He opened a new door for me and guided me into a new world associated with my academic career, which has fostered my fruitful results and may continuously contribute to my future career. I appreciate especially the freedom that he has generously given during our working and collaboration period. I would also like to thank him for his generous support, guidance and suggestions throughout my research.

It has been my great pleasure to have worked in the group of Professor Francis Noblesse during my stay at Shanghai Jiao Tong University (SJTU). His generous and patient way to guide me to present research results are greatly appreciated. I have remarkably benefited from this. Moreover, I am especially thankful for his warm hospitality. Apart from him, I have been always very happy to work with the group members at SJTU, especially Zhu Yi who has been always like a big brother, Ma Chao and Hui Yu. Special thanks go to my classmates from my

college for their great help and support during my stay at SJTU.

Special thanks go to my colleagues who have been working in the same group as me at NTNU. Particularly, Benjamin K. Smeltzer, Dr. Andreas H. Akselsen, and Peter Maxwell are a group of kind and lovely people. It has been always my great pleasure to work with them. And I have greatly benefited from discussions, talks and meetings with them.

Without the company of my dearest friends and their generous support and help, my life would have been less colourful and a lot of happiness would have faded. My special thanks go to Liu Xinting, Zhao Lihao, Fu Chao, Yu Zhaolong, Wang Mao, Yang Limin, Deng Han, Yang Kun, Liu Peng, Li Tian, Tu Ying, Wang Xiao, Sebastian Schafhirt, and David Jose. In particular, Lihao and Chao has been always like big brothers and it has been my great honour to meet them and to work with them in the same department. Thanks to Yang Limin for his kindness of treating me like a younger sister. Special thanks go to Sebastian Schafhirt for the special journey we have been on. Especially, my life may be more bright and colourful because of the possibilities with you in future. Things are sometimes more beautiful and fantastic due to uncertainties and unpredictable elements, although admitting they may go to other directions too. There are plenty of friends that are not listed here but I would also like to thank them all.

Finally, my greatest gratitude goes to my family for their selfless support and encouragement. Wish them the greatest happiness in the world and May I be able to thank and repay them with my practical actions in the future.

Contents

Publications

A list of appended papers

1. **Li, Y.** and Ellingsen, S. Å. (2017a). Direct integration method for surface waves on a depth dependent flow.(submitted).

2. **Li, Y.** (2017). Wave-interference effects on far-field ship waves in the presence of a shear current. *Journal of ship research*. (under review).

3. **Li, Y.**, Smeltzer, B. K., and Ellingsen, S. Å. (2017). Transient wave resistance upon a real shear current. *European Journal of Mechanics / B Fluids*. (accepted).

4. Ellingsen, S. Å. and **Li, Y**[1]. (2017). Approximate dispersion relations for waves on an arbitrary shear flow. *Journal of Geophysical Research – Oceans*. (under review).

5. **Li, Y.** and Ellingsen, S. Å. (2016a). Multiple resonances of a moving oscillating surface disturbance on a shear current. *Journal of Fluid Mechanics*, 808:668-689.

6. **Li, Y.** and Ellingsen, S. Å. (2016b). Ship waves on uniform shear current: wave resistance and finite water depth. *Journal of Fluid Mechanics*, 791:539-567.

7. **Li, Y.** and Ellingsen, S. Å. (2016c). Effect of anisotropic shape on ship wakes in presence of shear current of uniform vorticity. *In ASME 2016 35th International Conference on Ocean, Offshore and Arctic Engineering*, volume 7: Ocean Engineering.

[1]The authors are considered to be joint first authors, ordered alphabetically

8. **Li, Y.** and Ellingsen, S. Å. (2015a). Initial value problems for water waves in the presence of a shear current. *In Proceedings of the twenty-fifth International Ocean and Polar Engineering Conference (Proceedings of ISOPE)*.

Additional papers and abstracts

1. **Li, Y.** and Ellingsen, S. Å. (2015b). Waves in presence of shear current with uniform vorticity. *In Proceedings of MekIT'15 Eighth National Conference on Computational Mechanics*.

2. Ellingsen, S. Å. and **Li,Y.** (2015c). Ship waves at finite depth in the presence of uniform vorticity. *the International Workshop on Water Waves and Floating Bodies (IWWWFB)*.

3. **Li,Y.** and Ellingsen, S. Å. (2016d). Dispersion relations of waves generated by a travelling oscillating disturbance on a shear current. *the International Workshop on Water Waves and Floating Bodies (IWWWFB)*.

4. **Li,Y.** and Ellingsen, S. Å. (2016e). Multiple resonances for moving periodic wave source in shear current. 11^{th} *European Fluid Mechanics Conference*.

5. **Li,Y.**, Ellingsen, S. Å. and Francis Noblesse (2016), Wave-interference effects in the presence of a shear current, *the Division of Fluid Dynamics 16 Meeting of The American Physical Society*.

6. Smeltzer, B. K., **Li, Y.**, and Ellingsen, S. Å. (2017). Effects on Doppler resonance from a near-surface shear layer. *In ASME 2017 36th International Conference on Ocean, Offshore and Arctic Engineering*.

7. **Li,Y.** and Ellingsen, S. Å. (2017b), Approximate dispersion relation for surface waves on current with arbitrary depth dependence, *European Geosciences Union General Assembly*.

Chapter 1

Introduction

1.1 Research background

Better understandings of water waves are key to a wide range of areas such as marine, offshore, ocean engineering and oceanography. Particularly, sea loads due to waves have remarkable effects on a large number of marine vessels, and fixed, floating or moored installations. Water waves themselves display fascinating features, for instance being capable of carrying energy over long distances, and the dispersive properties in finite and deep water [1]. A couple of relevant examples are named here, for instance, the striking V shaped wake generated by a travelling duck or a marine vessel [2, 3, 4], the beautiful wave ripples formed by winds, and natural occurring giant waves [5], indicating both rich physics and practical applications about water waves. There are many factors that may affect the propagation of waves, including viscosity, gravity, surface tension, the presence of sub-surface flows, the wind induced force, the seabed, the density of fluid, etc [6]. Interactions of water waves with those factors may pose potential challenges in terms of both theoretical analysis as well as real world applications. The present thesis primarily focuses on the complex interactions between waves and a sub-surface shear current, which are of essential significance, as will be indicated below.

It is well known that water surface waves and currents widely coexist in coastal and offshore environments, especially in the regions of tidal, ocean, fjord, and discharge currents [7]. In particular, the interactions between waves and currents are pivotal to a wide range of applications, such as offshore installations, the design of large ocean structures and coastal breakwaters, and sea loads on ocean slender structures [8]. Compared to circumstances in the absence of a current, wave forces on offshore structures may be considerably different when a current is present.

Dalrymple [8] and Dalrymple et al. [9] indicate that the exclusion of currents, noticeably due to the wind actions, ocean circulations and tidal forces, may cause a significant underestimate drag force acting on an under-design offshore structure. For example, including the current of 12.5% of the maximum speed –16 ft/s– of a design wave may result in the increase of drag force by 25%, while a current of 18.75% of this maximum speed may lead to an increase over 40%. In addition, the presence of a sub-surface current may also have a profound effect on data measured about waves, which may attract particular attention from oceanographers. It is thus essential to raise awareness concerning the non-trivial interactions between waves and currents.

Currents have been known for a long time to induce a couple of noticeable effects on water waves, such as the effects on the refraction in shallow water, the dispersed properties, wave height or steepness, exchange of energy and momentum, etc. There is extensive literature which has indicated a large amount of examples for the wave-current interactions, e.g. Jonsson [7], Isaacs and Johnson [10], Taylor [11], Lighthill [12], Jonsson and Skovgaard [13], Jonsson and Wang [14], Hedges [15], Kirby and Chen [16], Smith [17], Lamb [18], Hjelmervik [19]. For instance, Isaacs and Johnson [10] reveal a couple of such phenomena observed during navigations, especially with respect to the refraction in areas such as the entrance channel to estuaries and coastal regions. Furthermore, it is indicated in a series of references by Longuet-Higgins and Stewart [20, 21, 22, 23] that exchanges of wave energy between water waves and currents widely exist in real environments. Meanwhile, one key concept called 'radiation stress' is introduced that has considerably contributed to explain the close interactions between waves and currents, especially in terms of its physical interpretation. Waves interacting with horizontal currents that are uniform over water depth have been extensively studied during the period from 1940s to 1990s, see references [15, 24, 25, 26, 27] and references therein. Modelling a current with the uniform profile over water depth is likely because of the wide recognition with respect to tidal currents and large ocean circulations of the nature that varies negligibly with water depth.

Moreover, several studies, e.g. [7, 28, 29, 30] and references therein, have shown that the presence of a current may noticeably affect the wave height or steepness. Especially, it has been indicated that an opposing current may closely relate to the formation mechanism of giant waves [30]. There are many sources which have documented notable outcomes or serious accidents that happened while there were currents present. For instance, Fig.1.1 depicts an accident that occurred due to a giant wave in the Agulhas current, off the eastern coast of South Africa [7, 31]. The strong tidal currents in Moskenes Sound, Norway, are recorded in Grabbe et al. [32] for the dangers in pulling ships down and swallowing them up. Other

Figure 1.1: A picture of the tanker damaged by encountering an advancing giant wave when going in the Agulhas Current on May. 17, 1974, from [7].

examples of waves encountering currents are documented in Holthuijsen and Tolman [33] regarding the Gulf stream, in Mathiesen [34] with respect to the current whirl in the Norwegian coastal current, and in Isaacs and Johnson [10] about the ebb and flood currents in the estuaries. As for more extensive literature regarding the wave-current interactions before 1990, readers are directed to some of the comprehensive reviews, e.g. [6, 7, 8, 27].

There are many types of naturally occurring currents, including for instance the tidal currents, wind-induced currents, wave-induced flows, the currents induced by fluid-density gradients,etc.[8, 27]. Normally, the tidal currents or the large scale ocean currents have negligible variations of water depth and thus are widely modelled as uniform flows in theoretical studies [6, 19]. Primary sites for subsurface flows are normally in the areas of rivers, continental shelves, ocean areas after natural hurricanes, ocean delta, or river/ocean mouth (estuaries), ocean areas where strong winds exist, coastal inlets, fjords (noticeably the fjords in Norway [34]), harbours, straits, etc.

In terms of the variations with respect to physical space, current models used for studies may be categorized into the following groups, including uniform currents independent of physical space [35], horizontal currents uniform over water depth [14, 36], currents varying linearly with water depth [37], bilinear shear currents consisting of two layers of linear profile [11], exponential /logarithmic shear current [38], depth-dependent shears uniform in the horizontal plane [16] and spiral currents that may vary both the magnitude and direction with water depth [39]. The present thesis primarily pays attention to horizontal currents whose magnitude and

direction may vary with water depth.

1.2 Depth dependent flows

In natural areas either near coastal zones or in continental shelves especially, currents are normally strongly sheared, particularly due to wind actions, as observed in [40, 41]. The vertically sheared profiles are primarily due to seabed friction, density gradient and wind stress at the free surface [6, 27]. Due to its relevance to various real-world applications, such as submerged slender structures like risers and pipes, it is important to obtain a deeper understanding of wave interactions with currents that vary with water depth.

Although the importance of depth dependent flows has been recognised, challenges have also been widely known in the theoretical, experimental and field-investigation perspectives, due to the unsteady/complicated nature of flows in real environments. Above all, there is a lack of proper models of fully and general 3D flows. Theoretical solutions in this regard are thus currently not available. It is not only because of the complicated nature of the flows, but also due to the difficulty in solving the fully 3D governing equations for waves in the presence of a sub-surface shear current of a general form with respect to water depth. What makes the problem even more challenging is that experimental and field data is scarce, resulting in a lack of validation/verification data to the theoretical results.

Theoretically, much simpler models have been widely used. Not only may each simpler model embrace the virtue of being more straightforward to obtain analytical results, but also it provides essential insights into the nature of a problem and thus contributes to draw the complete picture of a more complicated natural case. A large body of literature hence exists in this regard . A couple of the comprehensive literature reviews regarding waves propagating atop a shear current in variation of water depth can be noticeably found in the second half of the 20th century, e.g. [6, 7, 8, 27, 42].

1.2.1 Linear and bilinear shear currents

Above all, the simplest model is to describe the shear that varies linearly with water depth, either of zero vorticity – uniform flow – or of a non-zero constant vorticity. The effect of a uniform flow on surface waves as a Doppler shift has been well recognised [12, 36]. Relevant reviews in this regard are thus excluded in this subsection. A somewhat modified model of a uniform current is to use multiple layers of uniform flows of different velocities within each layer, noticeably aiming at modelling currents in stratified fluids [43, 44].

The interplays of a linear shear current and surface linear waves have been exten-

sively studied in two dimensions. Especially, analytical solutions to describe the system of linear waves atop a linear shear current can be obtained. In particular, the dispersion relation is first derived in Thompson [45] where a piecewise linear approximation (PLA) to analyse linear waves propagating on a depth varying shear current is also introduced, having led to extensions to more general circumstances, e.g. the study made in Zhang [46]. The dispersion relation obtained in Thompson [45] agrees with the results independently derived in Biesel [47]. Tsao [48] has derived the expressions of surface elevation and particle velocities for waves in the presence of a linear shear current. Taylor [11] analyses the effects on wave stopping from two special bilinear shear profiles that may work as breakwaters. This study is extended by Brevik [49] where the additional effect from a seabed is taken into consideration. Parameters, e.g. wave length and wave height, of waves on a linear shear current and a surface jet are studied in Kantardgi [50] where agreement with previous studies is shown. Dalrymple [8] derives a comprehensive theory about small amplitude waves when a current of uniform vorticity is present. In recently, the roles of surface tension and shallow water and the wave stopping effect in the presence of a linear shear current are studied in Ellingsen and Brevik [51]. Furthermore, a classical problem of waves generated by an oscillating source with a background one-line shear profile is studied in Tyvand and Lepperød [52], which is extended via the additional consideration of a Doppler effect in Tyvand and Lepperød [53]. The problem of an oscillating point source is analysed in Ellingsen and Tyvand [54].

Currently, linear waves in the presence of a current of uniform vorticity have yet been studied extensively in 3D and there are only a few limited references, e.g. [55]. Particularly, small amplitude waves propagating in an oblique angle with a shear is analysed for the first time in Dalrymple [8] on a 2D basis. It is confirmed in Peregrine [6] that the effect of a linear shear on linear waves making an oblique angle θ with the shear current can be simply considered in a manner that applies the projection of the shear in the wave-vector direction, i.e. by a factor of $\cos\theta$. Nevertheless, although simple and straightforward enough, this approach may overlook the 3D effects in realistic circumstances. Recently a general solution to 3D linear waves on a vertically sheared current of uniform vorticity was derived in Ellingsen [56] where effects of the uniform vorticity on the 3D propagation of linear waves are analysed. The theory derived in Ellingsen [56] is of essential significance in revealing valuable insights and its extensions to a wide range of real world applications are readily obtained in this regard. The results obtained in Ellingsen [56] are later confirmed by Li and Ellingsen [57] in which the solution to linear waves generated by an initial impulsive pressure is derived. Furthermore, the theory is applied to solve problems of ship wakes both in infinite water [58] and finite water [59, 60], an oscillating travelling source [61], an oscillating point source [62] and

wave interferences [63]. Detailed analysis regarding the effects due to a current of uniform vorticity on 3D linear water waves is further presented in the following.

The presence of a linear shear current has been found to have profound effects on the surface linear waves and novel features are introduced due to the uniform non-zero vorticity, as especially indicated in recently based on studies in 3D [58]. The degree to which a train of progressive linear wave is affected by the vorticity depends on a couple of factors, including the seabed, parameters of the wave and the surface tension. Particularly, Ellingsen [56] indicates an asymmetric effect on the ring waves whose directions following or opposing the current are the mostly affected by the shear. A side-on shear shows no effect on a single train of progressive wave. Fascinating and novel features are introduced to the problem of ship wakes as a consequence of the presence of a uniform vorticity [58, 60]. Previous observations and a recent study by Rabaud and Moisy [64] regarding ship waves have led to the revival of studies in the classical problem of ship wave pattern. There has been many times that the semi-angle of the wake sector generated by a wavemaker is observed to be smaller than the one of a striking V-ship wake whose semi-angle is predicted to be constant – 19.47^o independent of the moving speed and scales of a wavemaker – by Thomson [2] in ideal and deep water, which have aroused the interests in seeking theoretical explanations, as shown in [65, 66, 67, 68, 69]. It is also shown that the presence of a linear shear may considerably modify the ship wave pattern [58, 60]. In particular, asymmetric ship wakes and non-constant Kelvin angles are introduced due to the uniform vorticity [58, 59, 60]. Transitions between a sub-critical and supercritical situation are found when the shear Froude number $\mathrm{Fr}_s = |\mathbf{V}|S/g$ ($\mathbf{V}$: velocity of the ship motion, S : vorticity of the shear, g : gravitational acceleration) increases in finite water [59, 60]. Furthermore, a critical intrinsic shear Froude number $\mathrm{Fr}_{sb} = S\sqrt{b/g}$ (b : the reference length) above which the transverse waves vanishes is found in Ellingsen [58], Li and Ellingsen [60]. The classical problem of waves generated by an oscillating and travelling surface disturbance is considered in Li and Ellingsen [61]. Particularly, a striking feature that multiple Doppler resonances - as many as 4 - may exist is found due to the constant vorticity while the classical nondimensional frequency $\tau = |\mathbf{V}|\omega/g$ (ω : the frequency of an oscillating disturbance) is equal to $1/4$ when the Doppler resonance occurs in the absence of a shear current. Additionally, it is also shown that even a current of weak vorticity may have profound effects on the Doppler resonance. This work is extended to finite water depth and to a bilinear shear current in [70] which confirms the result that a current of weak vorticity may show significant effects on the Doppler resonance.

Studies also exist regarding nonlinear waves propagating on a linearly sheared current, e.g. [37, 71, 72, 73]. Dalrymple [8] and Dalrymple [74] derive the solu-

tions to finite amplitude waves on a linear current, the latter of which additionally works on a bilinear shear profile whose effects on wave forces calculated by the Morrison equation are analysed. Brevik [75] extends the study in Brevik [49] to obtain higher-order solutions of nonlinear waves in the presence of a current of uniform vorticity in deep water. Jonsson and Skovgaard [13] additionally consider effects of a slowly varying bed and solve the waves to the second order of the wave amplitude. Via a weakly nonlinear approximation, numerical studies regarding the properties of gravity waves are presented in Simmen [76] and Simmen and Saffman [77]. Nevertheless, studies in 3D in this regard are scarce with only a few scattered exceptions, e.g. [78, 79].

1.2.2 Shear profiles of non-zero curvature

Realistic currents normally possess a much more complicated form than a linear profile. As was noted previously, challenges exist in terms of fully solving problems of 3D waves in the presence of a general depth varying current. More additional efforts are thus demanding. Studies have been made especially regarding much more simplified situations, which gradually form an in-depth understanding in this regard. In particular, extensive literature exists for 2D cases. Abdullah [80] attempts to, for the first time, obtain the dispersion relation for waves atop a wind-drift shear current that decreases exponentially with water depth. Liu et al. [81] investigate the interactions of progressive waves of different parameters in the presence of an exponentially sheared current. Other attempts are made towards other shear profiles, including a one seventh power of depth [38, 82], a hyperbolic sine varying current [83], a cosine velocity profile [84], vertically logarithmic steady currents [85], etc. Burns [86] is a classical paper where an approximate approach to the problem of long waves on an arbitrary shear current is derived.

Perturbation techniques are widely used when trying to seek solutions of waves on a vertically dependent flow. Stewart and Joy [87] derive an approximation to the dispersion relation based on the assumption of a weak shear / fast propagating waves in deep water, which is further analysed and also extended to a finite water depth by Skop [88] where several examples of different shear profiles are shown. Kirby and Chen [16] generalize the theories developed in Stewart and Joy [87], Skop [88] to obtain higher-order approximations to the dispersion relation of linear waves on a depth dependent shear current, which have been widely used and tested for vertically sheared currents of weak vorticity. The theory in Kirby and Chen [16] is applied in Dong and Kirby [89] where numerical results are obtained for real circumstances where a current is strongly sheared at the Columbia River mouth. Based on the 'near-potentiality condition' that assumes the leading behaviour of waves on a depth dependent flow follows potential theory, Shrira [90] derives exact solutions to short waves via a Neumann series in the presence of a

current in arbitrary variation of water depth. Different from Kirby and Chen [16], Swan and James [91] presents a perturbation analysis which shows a good agreement with the experimental results in Swan et al. [92] for small amplitude waves on shear currents of considerable strong vorticity.

Apart from perturbation methods a piecewise linear approximation (PLA) has also been widely used for the problem of waves when in the presence of a current in variation of water depth. It is, however, also accompanied with spurious solutions at the layer interfaces, which may lead to challenges in numerical implementations and additional computational cost [46]. Thompson [45] firstly proposes this approach. More recent references where PLA is used include Zhang [46], Caponi et al. [93], Smeltzer and Ellingsen [94] in which Smeltzer and Ellingsen [94] is one of the scarce 3D references. Modelling a shear flow with the bilinear profile essentially implies the nature of the PLA, e.g. [8, 11].

In addition, Dalrymple and Cox [95] have derived theories about finite amplitude waves atop a current of vorticity that varies with the stream function. Mellor [96] obtains the wave equations on a depth-averaged basis and in particular the radiation stress and Doppler velocity are defined in 3D in the presence of a depth dependent current. Other references regarding waves interacting with a vertically sheared current can also be found, for instance, [97, 98] and the references therein.

1.2.3 Stability

Especially for strongly sheared currents, instability may take place due to a possible critical layer that exists below the water surface as a consequence of interactions between waves and currents, possibly resulting in profound effects on surface waves when the critical layer is near enough to the water surface [90, 99]. There is extensive literature that has studied the instability of a shear flow, e.g. a series made by Miles [100, 101, 102, 103], Rayleigh [104], Velthuizen and Van Wijngaarden [105], Morland et al. [106] and references therein. The piecewise linear model is widely used in the stability analysis [107, 108]. A few references that have applied smooth shear models for instability are Ellingsen and Li [99] and [90], where it is found that instability of the flow is considerably affected by the sign of the curvature of a shear profile. Numerical analysis regarding unstable models can be found in [106].

1.2.4 Experimental investigations

There are quite limited references where experimental and field studies regarding waves on vertically sheared flows are presented. Investigations in the 1960s can be found in Yu [109], Sarpkaya [110]. Experimental data for several current profiles is present in Thomas [111, 112] where linear and nonlinear waves opposing currents

are analysed, respectively. Efforts have been made towards laboratory investigations regarding waves interacting with a shear current of a time-averaged vorticity in Cummins and Swan [113] in which a good agreement with results from a piecewise linear model is shown. Swan [114] has experimentally investigated waves on a strongly shear current, whose data has been applied for analytical models, e.g. [92]. In addition, wave lengths and frequencies are observed in a laboratory flume when a current in variation of water depth is present. The parameters of unsteady waves on the breaking onset are experimentally observed in Yao and Wu [115] when negative and positive sheared currents are present separately.

1.3 Thesis motivations and objectives

As was noted above, waves are of essential importance in realistic circumstances, having motivated numerous studies in order to acquire a better understanding. The presence of a subsurface shear current may be a key factor that profoundly affects wave propagations and thus leads to considerable effects on wave forces acting on offshore structures. This reveals that interactions between waves and currents are non-trivial both in the theoretical and realistic regard. Nevertheless, problems of surface water waves in the presence of a subsurface flow that possesses a general profile with respect to water depth have yet been fully understood. In particular, waves propagating on a depth dependent current are insufficient in three dimensions, even to a linear order, which has motivated the studies made in the present thesis.

The present thesis primarily aims at providing essential insights into complex interplays of linear surface water waves and a depth dependent flow. In particular, in order to achieve this goal, the following attempts have been made, which are briefly depicted in Fig.1.2 that gives a general idea about what the papers are about as well as the primary work that has been included in the present thesis. It includes two key parts – a current that varies linearly with water depth and a more general case regarding a flow whose magnitude and direction may vary with water depth. Detailed information is shown in the following section.

1.4 Summary of thesis articles

Fig.1.2 depicts how the papers are structured and organised. Two primary parts are included regarding linear surface water waves on a linear current as well as on a depth dependent flow, which are respectively introduced in §1.4.1 and §1.4.2.

1.4.1 Linear waves on a general depth dependent flow

Efforts focus on a comprehensive theory regarding surface linear water waves propagating on a vertically sheared current, forming a fundamental basis to fur-

ther extensions and applications. In particular, different approximate methods to the dispersion relation are derived for which appropriate criteria are also given based on a perturbation method. Moreover, a direct integration method (DIM) is further introduced d to obtain numerical solutions to the linearised Rayleigh equation and the implicit dispersion relation in a coupled way. The DIM is found of distinctive advantages, capable of obtaining the velocity and pressure of the entire fluid field and of dealing with cases where a critical layer exists in a straightforward approach. General solutions for implementing the DIM are also derived. The primary work in this regard is especially given in *Paper I*, *Paper II*, and *Paper VI* where the effects of a vertically sheared current are analysed on surface water waves, indicating that the effects closely relate to the varying depth of a shear below water surface in relative to the wavelength of a train of progressive wave.

1.4.2 Linear waves on a current of uniform vorticity

Attempts have been made especially towards linear waves atop a linear shear current. It embraces the virtue of being possible to obtain explicit theoretical solutions, which is somewhat a benchmark in this sense.

A general solution to the linear waves generated by an initial impulsive pressure is derived in the presence of a current of uniform vorticity, given in *Paper VII*. The solution obtained works as a response function that is readily extended and applied for more realistic circumstances. For instance, it is a classical way to form steady ship wakes by considering the accumulated ring waves generated by continuous impulses that advances along a certain course. Especially, this provides an alternative to develop the theory in *Paper IV*, *Paper VI* and *Paper VIII*.

Efforts also focus on ship waves as well as wave resistance when a linear shear current is present, as shown in *Paper IV*, *Paper V*, *Paper VI* and *Paper VIII*. It is particularly found that the interplays of ship wakes, seabed and the uniform vorticity are non-trivial. Novel and fascinating features have been introduced due to the additional consideration of uniform vorticity while compared to cases in the absence of a linear shear current. In particular, asymmetrical ship wakes whose semi-angle may be as large as 180 degrees for a side-on shear current are introduced for ships moving in an oblique angle with the shear, denoting non-constant Kelvin angle that is widely known as 19.47 degrees, independent of the moving speed and length scales, for the wakes generated by a wavemaker advancing in ideal deep water . Moreover, a critical velocity above which the transverse waves vanish is derived, below which is called sub-critical situation while above is called supercritical situation. Transitions between the sub-critical and supercritical situations are found for different combinations of the parameters including the magnitude of the uniform vorticity, the angle between the motion axis and the current,

moving speed, and the water depth. Particularly due to the vorticity, a lateral wave resistance normal to the motion axis is found as a consequence of the asymmetric waves radiated from a wavemaker. Moreover, a transient feature that transient waves vanish at different rates when a ship is making different angles with the shear current is also introduced, posing potential challenges to manoeuvring of a ship. In addition, effects of a linear shear current on the interferences between waves generated by a two-point wavemaker of monohull ships are shown in a manner that is somewhat similar to a finite depth.

A fundamental problem of waves generated by an oscillating and advancing surface disturbance atop a linearly sheared flow is considered in *Paper III*. A general dispersion relation is analysed. In particular, wave sectors due to the vorticity of a linear shear current exist, in which waves may vanish for stronger vorticity in relative to the oscillating frequency of an oscillating disturbance. A striking feature that multiple Doppler resonances - as many as 4 - exist is also introduced due to the constant vorticity while the classical nondimensional frequency $\tau = |\mathbf{V}|\omega/g$ is equal to $1/4$ when the Doppler resonance occurs in the absence of a shear current. Additionally, it is shown that even a current of weak vorticity may have profound effects on the Doppler resonance. The study in *Paper III* is further extended to a more general case in [94] where a linear surface jet or a finite water is considered. Studies for the case in a finite water can also be found [94] when a linear shear current in present.

1.4.3 The appended articles

Paper I Direct integration method for surface waves on a depth dependent flow

This paper introduces a direct integration method (DIM) that is used to seek solutions of problems of linear surface water waves on a current whose magnitude and direction may vary with water depth. As essentially a numerical method, it is capable of fully describing the entire fluid field for the problems of interest and of dealing with cases where a critical layer exist in a straightforward way. Different from other approximations whose criteria required for applicability considerably depend on the wavelength range and the shear profile, this approach shows no limitation in this regard. Compared to the piecewise linear approximation, the DIM provides equivalent, if not higher, accuracy, introduces no spurious solutions and deals with the critical layer in a simple approach. General solutions for a couple of typical boundary conditions are derived for implementing the DIM. Error estimates of different approximate dispersion relations are made. The validation and verification are also presented for the DIM.

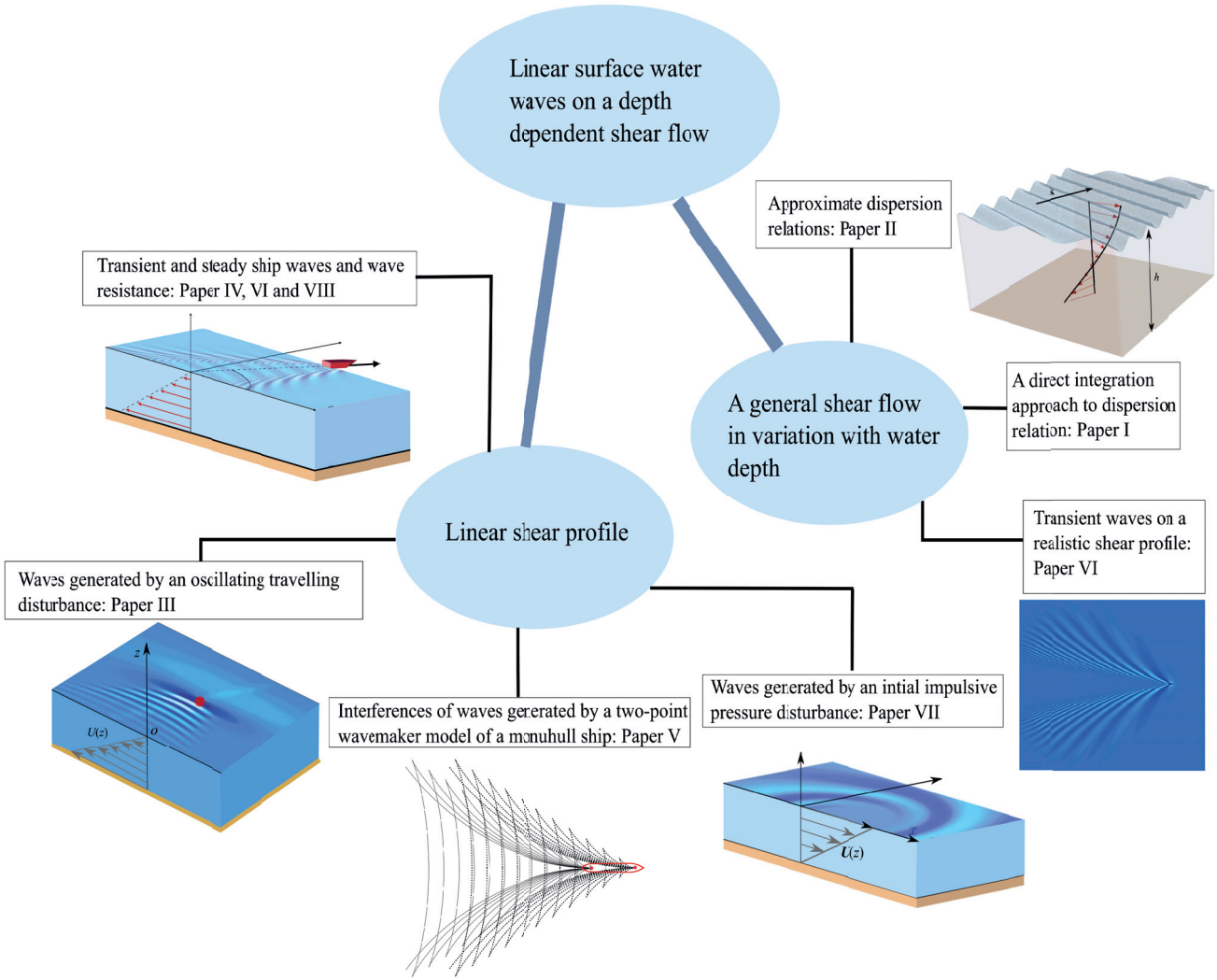

Figure 1.2: A sketch of the papers appended;

Paper II Approximate dispersion relations for waves on an arbitrary shear flow

This article derives an approximate dispersion relation for linear surface waves propagating on a shear current that may vary arbitrarily with depth in both the magnitude and direction. Based on the perturbation method, both the first- and second- order approximation to the dispersion relation are derived, the former of which is shown to be good at all wavelengths for a wide range of naturally occurring shear flows as well as widely used model flows, while the latter of which can provide significantly improved accuracy especially for the long and medium wavelengths. In addition, this article extends a widely used approximation by Kirby & Chen [1989] in 2D to 3D. The (3D generalisation of) first-order Kirby & Chen approximate method provides equivalently good applicability and accuracy as the newly derived 1st-order model, while the exact criteria for its applicability has yet been known for it may work for cases where its assumption based on which the approximation is derived is strongly violated. The article thus comes up with the reasonable criteria that explain the wide application of the Kirby & Chen approximation. In addition, the article also argues that the newly derived approximation is more robust for it succeeds in cases where the Kirby & Chen model fails. When compared to the second-order of the Kirby & Chen model, the newly derived 2nd-order scheme embraces advantages such as an explicitly known criterion of accuracy, arguably significantly simpler and more physically transparent in terms of the implementations.

Paper III Multiple resonances of a moving oscillating surface disturbance on a shear current

This article extends a classical problem by considering waves generated by an oscillating pressure source that advances at a constant speed when a shear flow is present with uniform horizontal vorticity of magnitude S. This article starts with a detailed analysis of the dispersion relation for the wave-current interactions and focuses on how the presence of a linear shear profile may affect the dispersion relation in both finite and infinite water depth. For the latter case, different far-field waves that exist in different sectors of wave-vector space are shown under difference circumstances. It is well known that a Doppler resonance occurs when $\tau = |\mathbf{V}|\omega_0/g$ is equal to the critical value $1/4$ ($\mathbf{V}$: velocity of disturbance, ω_0 : oscillation frequency, g : gravitational acceleration), which is shown to be considerably different due to the presence of the shear. Not only does the resonant value of τ depend strongly on the angle between $\mathbf{V}$ and the current' s direction and the 'shear-Froude number' $\mathrm{Fr}_s = |\mathbf{V}|S/g$, multiple resonant values - as many as four- can occur for some directions of motion when $\mathrm{Fr}_s > 1/3$. The minimum

resonance frequency tends to zero at sufficient large Fr_s for most of the directions of motion, denoting the critical velocity of ship waves.

Paper IV Ship waves on uniform shear current at finite depth: Wave resistance and critical velocity

This article extends the work of Ellingsen (2014) [58] to a more general case and presents a comprehensive theory for linear gravity-driven ship waves when a shear current of uniform vorticity is present in finite water. The critical velocity at which the transverse waves become vanishing is derived, showing non-trivial interplays of the seabed and the shear. Especially, the transition between the sub-critical situation where both transverse and divergent waves exist, and the super-critical situation under which the transverse waves vanish, are found when the 'shear-Froude number' $\mathrm{Fr}_s = |\mathbf{V}|S/g$ increases for different water depths and angles between the ship motion and the current ($\mathbf{V}$: velocity of the ship motion, S : vorticity of the shear, g : gravitational acceleration). Moreover, this article calculates the wave resistance in the presence of a linear shear for the first time, by which a non-zero lateral component is found due to the shear for oblique angles between the shear and the ship motion. In particular, the lateral component can amount to 10-20% of the normal wave resistance for a side-on shear and $S\sqrt{b/g}$ – b : the characteristic length of the ship – of order of unity. Furthermore, this article presents theory that properly deals with ship waves from the far-field contributions by the Cauchy' s integral theorem, exposing potential pitfalls with respect to a slightly different method (Sokhotsky-Plemelj) used in several previous works.

Paper V Wave-interference effects on far-field ship waves in the presence of a shear current

This article presents wave-interference effects in the presence of a shear current for a 2-point wavemaker model of monohull ships. Interesting and non-trivial effects on ship waves are shown, as also found in the analysis of wave interferences in finite water depth. The effect of shear on the far-field waves created by a 2-point wavemaker model of a monohull ship greatly depends on the shear Froude number VS/g, where V is the speed of the ship, S is the uniform vorticity of the shear and g is the gravitational acceleration, as well as the angle between the shear current and the direction of motion of the ship. There are various circumstances under which the ray angles of the highest waves that result from constructive wave interferences are much narrower than the Kelvin angles (the angles of the cusps or the asymptotes) of the wave patterns formed by a 1-point wavemaker. In particular, Kelvin shear Froude numbers $\mathrm{Fr}_{s_\mathrm{K}}$ for which the ray angles of the highest waves are equal to the Kelvin angles are determined. The ray angles of the highest waves for $\mathrm{Fr}_\mathrm{s} > \mathrm{Fr}_{s_\mathrm{K}}$ are considerably smaller than the Kelvin angles.

Paper VI Transient wave resistance upon a real shear current

This article presents a general theory to calculate waves and wave resistance in the presence of a depth dependent flow and studies the wave radiation forces, including wave-making resistance, for different model ships in a real, measured current in the Columbia River delta. The theory allows for calculation of waves from a general, time-dependent applied surface pressure acting on the water surface. Because momentum is imparted to radiated waves a well-known resistance force is experienced by the ship, yet for ships moving at oblique angles with the sub-surface shear, the wave radiation force also has a lateral component, since wave momentum is radiated at different rates to starboard and port. We focus here on the transient ship waves and the corresponding wave resistance and lateral wave radiation for a ship which suddenly appears and moves steadily thereafter. We consider both a simple model current with linear depth dependence, and a reasonably realistic model "ship" travelling on a real, measured shear current with a complicated velocity profile. The simple, linear profile has the virtue of allowing analytical results, which is used to compare to a numerical study of the more general case. Ship waves on an arbitrary shear currents are calculated via a piecewise-linear approximation. Close correspondence is found between the two shear currents at a qualitative and, with appropriately selected shear, quantitative level. Of particular interest is the initial peak wave resistance shortly after appearance. The lateral radiation force peaks more strongly than does the resistance force and for a short period reaches values comparable to the stern-wise resistance. It is concluded that the transient lateral force can be of considerable importance during manoeuvring in sheared conditions, especially for slender ships.

Paper VII Initial value problems for water waves in the presence of a shear current

This paper derives a general solution for the initial value problems of linear water waves that are generated by an initial impulsive pressure in the presence of a shear current of uniform vorticity beneath the surface. The analytical solution obtained in the paper is fundamental and can be applied in a wide range of realistic problems, e.g. forming the solution for the problems of both transient and stationary waves generated by a moving disturbance. Numerical results based on the analytical solution agrees with the results in the absence of a shear current, and asymmetry between upstream and downstream is shown.

Paper VIII Effect of Anisotropic Shape on Ship Wakes in Presence of Shear Current of Uniform Vorticity

This paper extends the work of Li & Ellingsen (2016) [60] to a more general case where a more realistic ship model is used. It primarily presents interactions between a subsurface shear current of uniform vorticity and gravity surface waves generated by a moving wavemaker of an anisotropic shape. Different from the model used in [60] where only one dominant length is used for modelling a ship, the paper additionally considers the aspect ratio of a ship. Waves contribution from far fields and expression of Mach angle based on the asymptotic approximation at high Froude numbers are derived. In addition, the Kelvin and Apparent wake angle at moderate Froude numbers under different combinations of the shear strengths and the aspect ratio are also calculated by numerical approach.

Chapter 2

Theory and numerical results

This chapter focuses on the fundamental theory regarding linear waves atop a horizontal current whose magnitude and direction may arbitrarily vary with water depth. The geometry of a wave-current system is initially introduced. Next, the linearised Rayleigh equation and boundary conditions both at the free surface and seabed are derived to describe waves atop a vertically sheared current. General solutions, especially of the surface elevation and vertical velocity, are obtained. The resistance due to waves generated by an advancing and oscillating wavemaker is thereafter described in a general form.

The dispersion relation to describe linear surface waves atop a depth dependent flow is derived in an implicit form. Due to the challenges in obtaining analytical solutions to the implicit dispersion relation, a couple of approximate techniques to solve the dispersion relation, e.g. the direct integration approach and different approximations based on a perturbation method, are thereafter presented. Under which situations each approximation may embrace distinct advantages are explained in detail and the applicability criteria, if there is any, are also derived. Analytical solutions to the dispersion relation under limited circumstances are presented, including when in the presence of a shear current that possesses a linear shear profile and problems of stationary waves atop a special class of nonlinear shear profiles.

Next, particular solutions under different classical boundary conditions at the free water surface are derived. In particular, two initial cases – that include the Cauchy-Poisson problem and waves generated by an initial impulsive disturbance on the water surface, transient waves generated by a time-dependent pressure disturbance and stationary waves either in the context of ship wakes and waves generated by

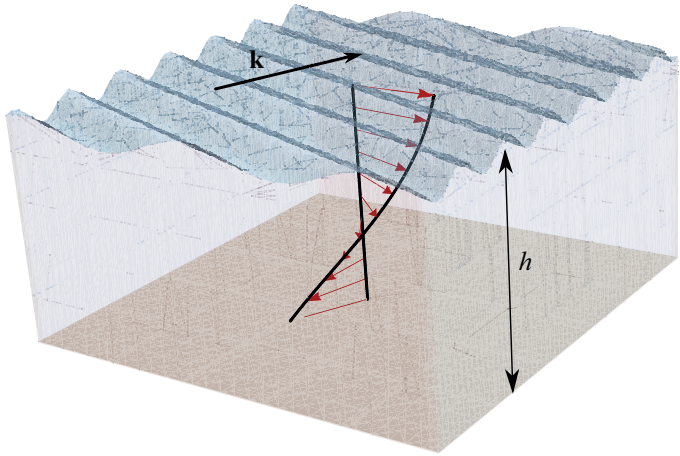

Figure 2.1: Geometry of a three-dimensional wave and current system in a uniform water depth h.

an oscillating and travelling source are presented. In addition, a few examples that show novel features due to the presence of a shear current are given.

Only part of the numerical solutions from the thesis articles are presented either for convenience or for further references such that unnecessary repetitions may be avoided. This chapter ends with the recommendations to future researches. Readers are directed to different thesis articles for more detailed information.

2.1 Geometry and description of the system

Three dimensional water waves in the presence of a vertically sheared flow are considered in the framework of linear wave theory. Assume incompressible and inviscid flow. Geometry of a wave-current system is depicted in Fig. 2.1 where a flat seabed of depth h is considered. The Cartesian coordinate system is used. The free water surface is lying at $z = 0$ when everything is at rest such that the surface elevation $\hat{\zeta}(\mathbf{r}, t)$ is depicted $z = \hat{\zeta}(\mathbf{r}, t)$ due to disturbances, where z is the vertical axis, $\mathbf{r} = (x, y)$ is the position in the horizontal plane, and t is the time. Consider a plane progressive wave with wave vector $\mathbf{k} = k(\cos\theta, \sin\theta)$ ($k = |\mathbf{k}|$) propagating atop a depth dependent shear current – $\mathbf{U}(z) = (U_x(z), U_y(z))$. It is assumed that waves may be affected by the presence of a shear current, but not vice versa. The velocity and pressure field are described respectively by $(\hat{u}(\mathbf{r}, z, t), \hat{v}(\mathbf{r}, z, t), \hat{w}(\mathbf{r}, z, t))$ and $\hat{P}(\mathbf{r}, z, t)$ due to waves. Let $\hat{p} = \hat{P} - \rho g z$ where $\hat{p}$ is the dynamic pressure, ρ is the fluid density and g is the gravitational acceleration. All of the physical quantities are assumed to be small so that all solutions are obtained to the linear order.

2.1.1 Governing equations

Before seeking general solutions, we may make the ansatz that all of the physical solutions depend on an overall oscillating factor $\mathrm{e}^{-\mathrm{i}\omega t}$ where ω is the frequency of a plane wave propagating in the θ direction. The Fourier transform is taken for all of the physical quantities in the horizontal plane

$$\left[\ \hat{u}, \hat{v}, \hat{w}, \hat{p}, \hat{p}_{\text{ext}}(\mathbf{r}, t), \hat{\zeta}\ \right] = \int \frac{\mathrm{d}^2 k}{(2\pi)^2} \left[\ u, v, w, p, p_{\text{ext}}, \zeta\ \right] \mathrm{e}^{\mathrm{i}(\mathbf{k}\cdot\boldsymbol{r}-\omega t)}, \tag{2.1}$$

where $\hat{p}_{\text{ext}}$ is the external pressure on the free surface; $u, v, w, p, p_{\text{ext}}$ and ζ are independent of t.

As for the particular wave-current model considered in the present thesis, the continuity and Euler equation in the physical plane are

$$\nabla \cdot \hat{\mathbf{u}} = 0, \tag{2.2a}$$

$$(\partial_t + \hat{\mathbf{u}} \cdot \nabla)\hat{\mathbf{u}} = -\nabla \hat{P}/\rho + \mathbf{g}. \tag{2.2b}$$

where $\hat{\mathbf{u}} = (\hat{u} + U_x, \hat{v} + U_y, \hat{w})$, the nabla operator is defined $\nabla = (\partial_x, \partial_y, \partial_z)$ and the gravitational acceleration vector $\mathbf{g} = (0, 0, -g)$.

Next, (2.2) is linearised and the Fourier transform is thereafter taken. It then yields

$$\mathrm{i}k_x u + \mathrm{i}k_y v + w' = 0, \tag{2.3a}$$

$$\mathrm{i}(\mathbf{k}\cdot\mathbf{U} - \omega)u + U_x' w = -\mathrm{i}k_x p/\rho, \tag{2.3b}$$

$$\mathrm{i}(\mathbf{k}\cdot\mathbf{U} - \omega)v + U_y' w = -\mathrm{i}k_y p/\rho, \tag{2.3c}$$

$$\mathrm{i}(\mathbf{k}\cdot\mathbf{U} - \omega)w = -p'/\rho, \tag{2.3d}$$

where the prime is the derivative with respect to z.

Reorganising u, v, $w$and p in (2.3) yields

$$(\partial_z^2 - k^2)w = \frac{\mathbf{k}\cdot\mathbf{U}''}{\mathbf{k}\cdot\mathbf{U} - \omega} w, \tag{2.4}$$

$$(\mathbf{k}\cdot\mathbf{U} - \omega)w' - \mathbf{k}\cdot\mathbf{U}' w = \mathrm{i}k^2 p/\rho, \tag{2.5}$$

$$\mathrm{i}k_x[\mathbf{k}\cdot\mathbf{U}' w - (\mathbf{k}\cdot\mathbf{U} - \omega)w'] - \mathrm{i}k^2 U_x' w = k^2(\omega - \mathbf{k}\cdot\mathbf{U})u, \tag{2.6}$$

$$\mathrm{i}k_y[\mathbf{k}\cdot\mathbf{U}' w - (\mathbf{k}\cdot\mathbf{U} - \omega)w'] - \mathrm{i}k^2 U_y' w = k^2(\omega - \mathbf{k}\cdot\mathbf{U})v. \tag{2.7}$$

(2.4) is called the Rayleigh equation (or the inviscid Orr-Sommerfeld equation). Noticeably, an analytical solution to (2.4) may only be obtained under quite limited circumstances as the solutions are considerably dependent on the shear current

profile $\mathbf{U}$. [6, 56, 58, 60, 61] and references therein present most of the limited cases where analytical solutions are available. Despite that challenges exist in obtaining the analytical solutions to (2.4) in the presence of a general shear current, other alternatives are possible, for instance the direct integration method that is essentially a numerical method, as will be indicated later in §2.2.1. It is worth to notice that analytical solutions of problems of waves in the presence of a linear shear current in 3D are somewhat a benchmark in the manner that analytical solutions and extensive applications are readily available for references.

2.1.2 Boundary conditions

Before seeking general solutions under various occasions, the boundary conditions both at the free surface and at the seabed should be specified. The former boundary condition includes the kinematic condition that states fluid particles remain on the free surface and the dynamic condition that denotes pressure right above the free surface equals to the pressure just below. Hereby, the linearised boundary conditions read

$$k^2 p_{\text{ext}}/\rho = -\mathrm{i}(\mathbf{k}\cdot\mathbf{U}-\omega)w' + \mathrm{i}\mathbf{k}\cdot\mathbf{U}'w - (gk^2+\sigma k^4/\rho)\zeta, \text{ at } z=0 \tag{2.8a}$$

$$w = \mathrm{i}(\mathbf{k}\cdot\mathbf{U}-\omega)\zeta(\mathbf{k},t), \text{ at } z=0, \tag{2.8b}$$

$$w = 0, \text{ at } z=-h. \tag{2.8c}$$

where σ is the surface tension coefficient.

For later references and convenience, we make

$$\mathbf{U}_0 = \mathbf{U}(0), \mathbf{U}_0 = \mathbf{U}'(0), \tilde{c}(\mathbf{k}) = \omega(\mathbf{k})/k - \mathbf{k}\cdot\mathbf{U}_0/k, \Delta\mathbf{U} = \mathbf{U}-\mathbf{U}_0, w_0 = w(\mathbf{k},0).$$

The kinematic and dynamic boundary conditions at the free surface $z=0$ together yield the combined boundary condition

$$(\mathbf{k}\cdot\mathbf{U}_0-\omega)^2 w_0' - [\mathbf{k}\cdot\mathbf{U}_0'(\mathbf{k}\cdot\mathbf{U}_0-\omega)+gk^2+\sigma k^4/\rho]w_0 = \mathrm{i}(\mathbf{k}\cdot\mathbf{U}_0-\omega)k^2 p_{\text{ext}}/\rho. \tag{2.9}$$

2.1.3 General solutions

As was noted, when a shear current is of a linear profile, i.e. $\mathbf{U}''=0$, analytical solutions (2.3) are available. Particularly, the solution of the vertical velocity is of a form with unit amplitude - $G(\mathbf{k},z) = \sinh k(z+h)/\sinh kh$ that satisfies the boundary condition at the seabed (2.8c) and the linearised Rayleigh equation (2.4) (or Laplace Equation for this specific case).

Performing Green's formula on the quantities w and G yields

$$w_0'G_0 - G_0'w_0 = \int_{-h}^{0} \mathrm{d}z \frac{\mathbf{k}\cdot\mathbf{U}''wG}{(\mathbf{k}\cdot\mathbf{U}-\omega)w_0}. \tag{2.10}$$

Inserting the combined boundary condition (2.9) into (2.10) further gives

$$w_0(\mathbf{k})\Delta_R(\mathbf{k},\omega(\mathbf{k})) = \frac{\mathrm{i}(\mathbf{k}\cdot\mathbf{U}_0-\omega)kp_{\text{ext}}\tanh kh}{\rho}, \tag{2.11}$$

where

$$\Delta_R = (1+I_g)k^2\tilde{c}^2 + \tilde{c}\mathbf{k}\cdot\mathbf{U}_0'\tanh kh - \left(gk+\frac{\sigma k^3}{\rho}\right)\tanh kh, \tag{2.12a}$$

$$I_g = \int_{-h}^{0} \mathrm{d}z \frac{\mathbf{k}\cdot\mathbf{U}''\bar{w}(\mathbf{k},z)\sinh k(z+h)}{k(\mathbf{k}\cdot\Delta\mathbf{U}-k\tilde{c})\cosh kh}, \tag{2.12b}$$

$$\tag{2.12c}$$

in which $\bar{w}(\mathbf{k},z) = w(\mathbf{k},z)/w_0$, called the unity vertical velocity, will be analysed more in detail in §2.2.1. Possible poles may occur in the integrand in (2.12b) due to possible critical layers that need careful treatment, as will be indicated in §2.3. When the current has no curvature, we have $I_g = 0$. Thereby, Δ_R is explicit with respect to $\tilde{c}$. More analysis can be found in §2.2.4 where a linear shear current is considered.

The general solutions of amplitude of the vertical velocity and the surface elevation are, respectively

$$w_0(\mathbf{k}) = \frac{\mathrm{i}(\mathbf{k}\cdot\mathbf{U}_0-\omega)kp_{\text{ext}}\tanh kh}{\rho\Delta_R(\mathbf{k},\omega(\mathbf{k}))}, \tag{2.13}$$

$$\zeta(\mathbf{k}) = \frac{p_{\text{ext}}k\tanh kh}{\rho\Delta_R(\mathbf{k},\omega(\mathbf{k}))}. \tag{2.14}$$

The inverse Fourier transform as described in (2.1) may then be taken to obtain the solutions in the physical plane. Despite that analytical expressions have been derived, the system is not fully described since the dispersion relation and how to solve $\bar{w}$ are yet determined. Discussions in this regard will be presented in §2.2 where possible approaches to approximate/solve both the dispersion relation and the Rayleigh equation are presented.

2.1.4 Wave resistance

When a travelling disturbance is advancing at a constant speed on the water surface, the wavemaker feels a resistance force due to the energy that is conveyed to radiate waves. The present thesis focuses on the wave resistance due to wave making while the friction resulting from viscosity is neglected. The wave resistance acting on an advancing pressure distribution due to wave making is defined in [116, 117]. It is equivalent to the resultant force acting on an imagined rigid cover that perfectly fits the elevated water surface due to small amplitude waves. Strikingly, the force vector may have two non-zero components along both the stern-wise and starboard-wise for a symmetric disturbance while a sub-surface shear current is present [60, 118] and the wavemaker is making an oblique angle with the shear current. As for the particular wave-current system described here, the wave resistance $R_\parallel$ – that is along the stern-wise direction – and the lateral radiation force $R_\perp$ – that is towards the starboard (right) – are defined, respectively, where

$$\begin{aligned}\begin{pmatrix} R_\parallel \\ R_\perp \end{pmatrix} &= -\frac{1}{|\mathbf{U}_0|}\int \mathrm{d}^2 r \hat{p}_{\text{ext}} \begin{pmatrix} \mathbf{U}_0 \\ \mathrm{e}_z \times \mathbf{U}_0 \end{pmatrix} \cdot \nabla\hat{\zeta} \\ &= -\frac{1}{|\mathbf{U}_0|}\int \frac{\mathrm{d}^2 k}{(2\pi)^2} \mathrm{i}\mathbf{k} \cdot \begin{pmatrix} \mathbf{U}_0 \\ \mathrm{e}_z \times \mathbf{U}_0 \end{pmatrix} \frac{p^*_{\text{ext}} p_{\text{ext}} \tanh kh}{\rho\Delta(\mathbf{k})} \mathrm{e}^{\mathrm{i}(\mathbf{k}\cdot\boldsymbol{r}-\omega t)}\end{aligned} \tag{2.15}$$

in which the asterisk denotes the complex conjugate. Particularly, different ω may represent different situations. For instance, $\omega = 0$ normally solves the wave resistances of a vessel advancing at constant velocity and implies a stationary condition that the waves propagate at the phase speed that equals to moving speed of the vessel such that the waves can keep up with the vessel.

2.2 Dispersion relation

As was noted above, additional conditions are required in order to fully describe the system introduced in §2.1. The eigenvalue problem given by the linear homogeneous conditions for the system described by (2.4), (2.5) and (2.8) then gives $\tilde{c}(\mathbf{k})$ (or $\omega(\mathbf{k})$) via the implicit dispersion relation

$$\Delta_R(\mathbf{k}, \tilde{c}(\mathbf{k})) = 0, \tag{2.16}$$

which itself is not closed since both $\tilde{c}$ and $\bar{w}$ are unknown but is indeed a fruitful starting point for further approximate methods presented below.

Based on the homogeneous conditions obtained from (2.9), (2.12a), (2.12b) and the dispersion relation (2.16), we yield

$$w_0'(\mathbf{k}) = k(1 + I_g(\mathbf{k}))w_0(\mathbf{k}) \coth kh, \tag{2.17}$$

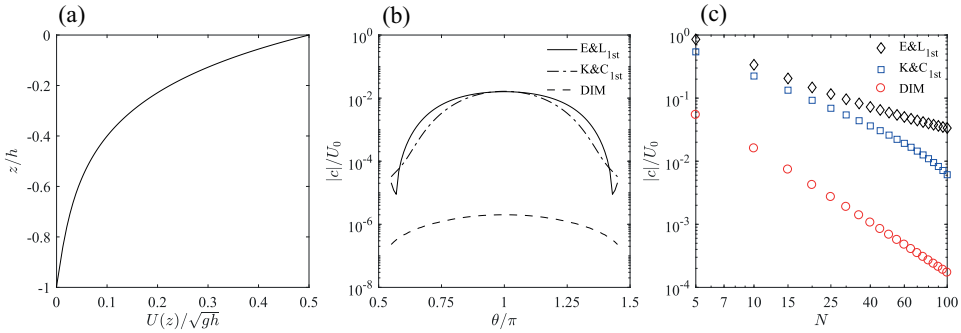

Figure 2.2: Stationary waves in different propagating directions θ [119]. In the figure, (a) the current is with the parameters $|\mathbf{U}|_0/\sqrt{gh} = 0.5$ and $\sqrt{\alpha}h = 4$; (b) The phase velocities approximated by three different methods: the DIM, (2.30)(E&L) and (2.32)(K&C); (c) the phase velocity as function of the discrete number N for $\theta = \pi$.

which may be used for further applications, as will be used in §2.4.2.

2.2.1 Semi-analytical approaches

Several attempts have been made to seeking the solutions of (2.16). As was noted previously, analytical solutions are only available in special cases. For instance, the linear shear profile [50, 56] and a class of specific shear profiles of the form $\mathbf{U}'' = \alpha\mathbf{U}$ where α is a constant. The latter is introduced in [6] for steady waves.

The present work has no ambition to achieve the completeness in solving analytically the dispersion relation with respect to plane waves propagating atop a depth dependent flow that possesses a general form. Nevertheless, a few of the 3D approaches are presented, which provide essential insights into how the dispersion relation may be properly solved based on, if there is any, reasonable criteria. The author argues that the approximate dispersion relations presented here are good, or to some extent excellent, for a wide range of naturally occurring shear flows as well as much-used theoretical model flows. Comments regarding which is superior under some specific situations will be made in the following, despite that it is, to some extent, a point of preference under some circumstances. It is nevertheless worth to point out that the DIM is capable of giving exact solutions to the dispersion relation (2.16) and of solving the fluid field completely, as will be indicated below. The author argues that the DIM is most often superior than the piecewise linear approximation (PLA) for several reasons. The former requires less computational cost as the latter introduces spurious solutions and extra computation efforts are needed in order to obtain the two physical eigenvalues out of an amount of solutions that increases with the layers used. Additionally, the DIM is capable of easily dealing with specific cases where a critical layer exist while

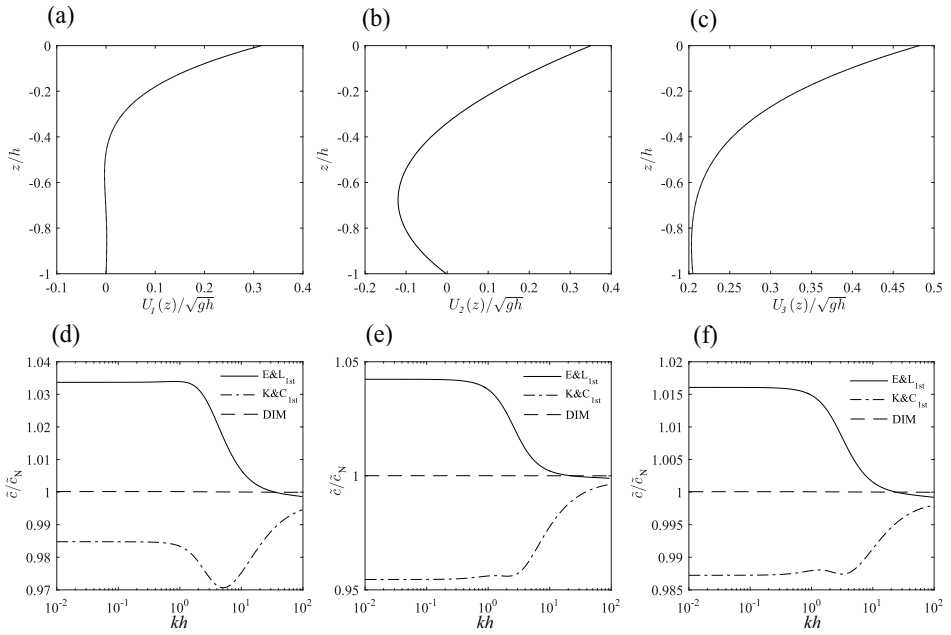

Figure 2.3: Phase velocities in variation of the dimensionless wave number kh while three natural appearing wind-induced shear currents (a)-(c), whose data is from [92], are presented [119]. In the figure, solutions of the DIM, the first-order approximation from [16] (K&C) and [99] (E&L) are scaled by the solutions obtained from the piecewise linear approximation in [94]; (d), (e), and (f) are calculated when $U_1(z)$, $U_2(z)$ and $U_3(z)$ are present, respectively.

the PLA needs much more complicated numerical techniques.

The corresponding methods are presented in the following to solve the implicit dispersion relation. The readers are directed to relevant thesis articles for more details.

(i) Direct integration method

As noticed and introduced above, $\bar{w}$ – the unity vertical velocity – is described by the following equations

$$(\partial_z^2 - k^2)\bar{w} = \mathbf{k}\cdot\mathbf{U}''\bar{w}/(\mathbf{k}\cdot\mathbf{U} - \omega), \text{for} - h < z < 0, \tag{2.18a}$$

$$\bar{w}_0 = 1,\ \bar{w}(\mathbf{k}, -h) = 0. \tag{2.18b}$$

Provided that both $\mathbf{k}$ and ω are prescribed, the above second-order ordinary differential equation (ODE) (2.18a) with respect to z are readily solved with the Dirichlet boundary condition described by (2.18b).

Despite that there are only limited cases where an analytical expression to $\bar{w}$ is available, a direct numerical approach under a general circumstance to obtain solutions of $\bar{w}$ described by (2.18a) and (2.18b) is possible, owing to the rapid development of computational science. To the best knowledge of the author, [89] is one of the scarce exceptions that have used a numerical method to solve the problem of interest here, although the derivations are constrained to a narrow banded wave train. It is worth to note that when a uniform/linear shear current is present, $\bar{w}$ is expressed $\bar{w} = \sinh k(k+z)/\sinh kh$.

The *Direct Integration Method* (DIM) obtains numerical solutions of $\bar{w}$ and $c(\mathbf{k})$ simultaneously for a prescribed shear current based on the boundary value problem described by (2.18) and the implicit dispersion relation (2.16). *Paper I* [119] has introduced more details regarding the DIM.

Different from the approximations introduced below and [16], where limitations for each approximate method exist due to the close dependence of a realistic shear profile and wavelength regions and where theoretical error may not be avoided, the DIM contains no theoretical error and is independent of wavelengths and of whatever a shear profile that is present. In this sense, the DIM shows surely a competitive edge. Moreover, solutions from the DIM in the Fourier $\mathbf{k}$ plane may form a database of $c(\mathbf{k})$ and $\bar{w}(\mathbf{k})$ with respect to $\mathbf{k}$ in the frequency domain, which are readily for further references and transforms to the physical plane. This suggests that a one-time calculation in the Fourier plane for a prescribed shear profile is sufficient for use, independent of boundary conditions at the free surface.

Moreover, as an implicit form of which (2.16) possesses, the DIM is generally open to all of the reasonable initial guesses of $c(\mathbf{k})$ as well as to numerical techniques to solve $\bar{w}$, although approximate methods introduced in [99] may serve as an initial guess of $\omega(\mathbf{k})$ while using the DIM. As for a specific case where a critical layer exists – that introduces a pole in the integration path of the integral (2.12b), using the DIM is also straightforward to give exact solutions, as will be indicated in §2.3.

Additionally, as for steady waves where $\omega = \omega_0$ is understood as a prescribed condition, solving (2.18a) after inserting $\omega = \omega_0$ into (2.18a) is sufficient when using the DIM

Figs.2.2 – 2.4 verify the DIM with the results from the piecewise linear approximation in the presence of different shear profiles. In particular, extremely strongly sheared profiles are considered in Fig. 2.4 . It is shown that the DIM is capable of giving exact solutions and meanwhile provides solutions with an accuracy in order of N^{-2} where N is the discrete number, despite that the accuracy essentially depends on the numerical approaches adopted. For more detailed analysis, one may

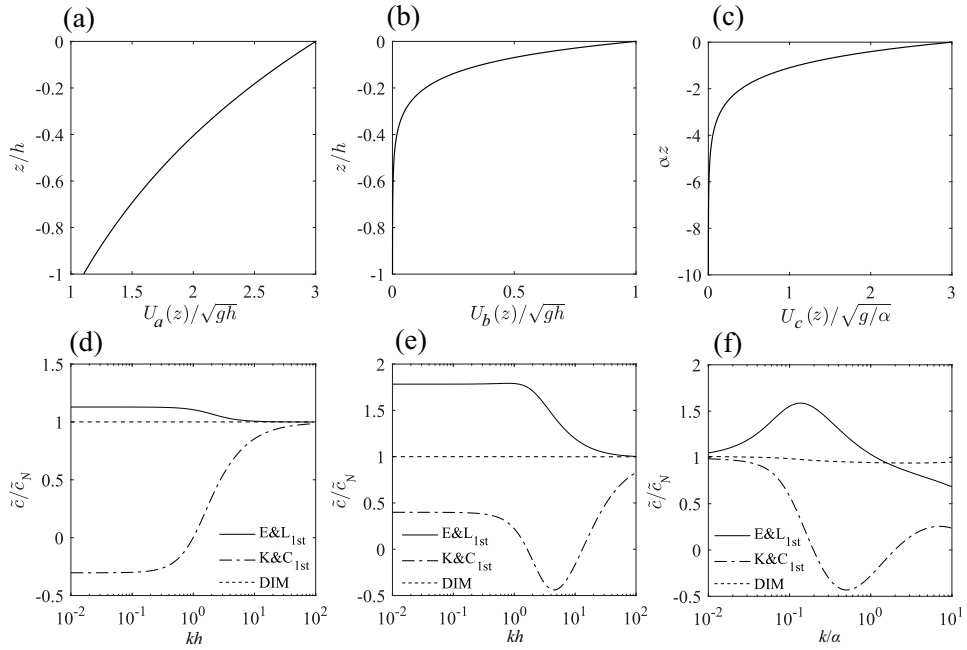

Figure 2.4: Phase velocities in variation of the dimensionless wave number in the presence of $U_a(z)$, $U_b(z)$ and $U_c(z)$, respectively [119].

refer to *Paper I* [119].

(ii) Perturbation method

It is natural to seek approximations to either $\tilde{c}$ or $\bar{w}$ when it is challenging to obtain the analytical solutions to (2.16) in the presence of a general depth dependent flow, provided the corresponding criteria can be met. Under this circumstance, a perturbation method is an option to proceed if it begins with a reasonable assumption. In particular, the *near-potentiality* assumption that is introduced in [90] is made so that the leading order and higher orders of the approximations to w will be obtained via recursion relations. The fundamental point of the assumption states that the term in the right-hand of the Rayleigh equation (2.4) (or (2.18a)) is relatively small compared to the other terms, indicating that the system is nearly a potential one and that the presence of a shear current provides small corrections to all of the physical quantities due to the linear waves. In this sense, iterative solutions can be made to obtain successively better approximations [120].

A small ordering parameter ϵ is introduced in the beginning and will be determined

later. The perturbation expansion of $\bar{w}$ can now be written in powers of ϵ

$$\bar{w} = \sum_{n=0}^{\infty} \epsilon^n \bar{w}^{(n)}. \tag{2.19}$$

Substituting (2.19) in (2.18a) and then collecting the same order of ϵ yields

$$\bar{w}^{(0)}(z) = \frac{\sinh k(z+h)}{\sinh kh}, \tag{2.20}$$

$$\bar{w}^{(1)}(z) = \int_{-h}^{z} \frac{\mathbf{k}\cdot\mathbf{U}''(\xi)}{\mathbf{k}\cdot\Delta\mathbf{U}(\xi) - k\tilde{c}} \frac{\sinh k(\xi+h)\sinh k(z-\xi)}{k\sinh kh} \mathrm{d}\xi. \tag{2.21}$$

Next, inserting $\bar{w} = \bar{w}^{(0)} + \epsilon\bar{w}^{(1)} + \mathcal{O}(\epsilon^2)$ to (2.16) gives

$$\tilde{c}^2 + 2c_0\tilde{c}\delta - c_0^2 + c_0^2\Delta(\tilde{c}) + \ldots = 0 \tag{2.22}$$

with

$$\delta(\mathbf{k}) = \int_{-h}^{0} \frac{\mathbf{k}\cdot\mathbf{U}'(z)\sinh 2k(z+h)}{kc_0\sinh 2kh}\mathrm{d}z, \tag{2.23}$$

$$\Delta(\tilde{c}) = -\frac{2\tilde{c}}{kc_0^2}\int_{-h}^{0} \frac{\mathbf{k}\cdot\mathbf{U}''(z)}{\mathbf{k}\cdot\Delta\mathbf{U}(z) - k\tilde{c}} \frac{\sinh k(z+h)\sinh kz}{\sinh kh}\left[\tilde{\mathbf{U}}(\mathbf{k}) - \tilde{u}(z)\right]\mathrm{d}z, \tag{2.24}$$

$$\tilde{\mathbf{U}}(\mathbf{k}) = \int_{-h}^{0} \frac{2\mathbf{k}\cdot\mathbf{U}(z)\cosh 2k(z+h)}{\sinh 2kh}\mathrm{d}z, \tag{2.25}$$

$$\tilde{u}(z) = -\frac{\sinh kh}{\sinh kz}\int_{z}^{0} \frac{2\mathbf{k}\cdot\mathbf{U}(\zeta)\cosh k(2\xi+h-z)}{\sinh 2kh}\mathrm{d}\xi, \tag{2.26}$$

and $c_0 = \sqrt{(g/k)\tanh kh + \sigma k/\rho\tanh kh}$.

Equations from (2.20) $\sim$ (2.26) are derived and presented in more details in the appendix A.1.1 in *Paper II* [99]. In accordance with the 'near–potentiality' assumption we essentially presume $|\Delta(\tilde{c})| \ll 1$. Now we know naturally that $\mathcal{O}(\epsilon) = \mathcal{O}(\Delta)$.

After eliminating the higher orders in (2.22), we yield

$$\tilde{c} \approx c_0(\sqrt{1+\delta^2-\Delta} - \delta). \tag{2.27}$$

Before proceeding to different approximate expressions, it is understood that the criterion for an approximation $\tilde{c}_{\text{app}}$ to be good is $|\tilde{c} - \tilde{c}_{\text{app}}| \ll |\tilde{c}_{\text{app}}|$ which is the fundamental point to obtain criteria (2.30) and (2.32).

(ii-1) the EL approximate method.

The criteria for this approximate method is now quite straightforward. Assume that

$$|\Delta(\tilde{c})| \ll 2|\delta\sqrt{1+\delta^2} - 1 - \delta^2|, \tag{2.28}$$

whose sufficient and far simpler criterion is that

$$|\Delta(\tilde{c})| \ll 1 \tag{2.29}$$

Hence it reads $\tilde{c} \approx \tilde{c}_{\text{EL}} + \epsilon\tilde{c}_{\text{EL,2nd}}$ where

$$\tilde{c}_{\text{EL}}(\mathbf{k}) = c_0\left(\sqrt{1+\delta^2} - \delta\right), \tag{2.30}$$

$$\tilde{c}_{\text{EL,2nd}} = -\frac{c_0\Delta(\tilde{c}_{\text{EL}})}{2\sqrt{1+\delta^2}}. \tag{2.31}$$

To calculate $\Delta(\tilde{c})$ in practice for (2.31), the first order estimate is inserted for $\tilde{c}$, as indicated in (2.31). Generally speaking, (2.31) is good to provide essential improvement to (2.30) for most of the natural appearing current flows. (2.30) and (2.31) suggest that the leading order involves the slope contributions of a shear while the second-order approximation includes the curvature contributions of a flow over the whole water depth.

(ii-2) the 3DKC approximate method.

As was noted previously, KCA is good at all wavelengths for a wide range of shear currents while the exact criteria to explain this phenomenon are only introduced in [99] where it is explained why KCA may work for a number of cases where the assumption of KCA is strongly violated.

Here the three dimensional generation of KCA (3DKCA) is derived. The 3DKCA gives

$$\tilde{c}_{\text{KC}}(\mathbf{k}) = c_0(1-\delta). \tag{2.32}$$

The criterion that works for (the 3D generation of) KCA is

$$\mathcal{O}(\frac{\delta^2 - \Delta}{2(1-\delta)}) \ll 1, \tag{2.33}$$

assuming $\delta < 1$.

A sufficient criterion for this to hold is the *double* criterion

$$|\Delta| \ll 1 \text{ and } \delta^2 \ll 1. \tag{2.34}$$

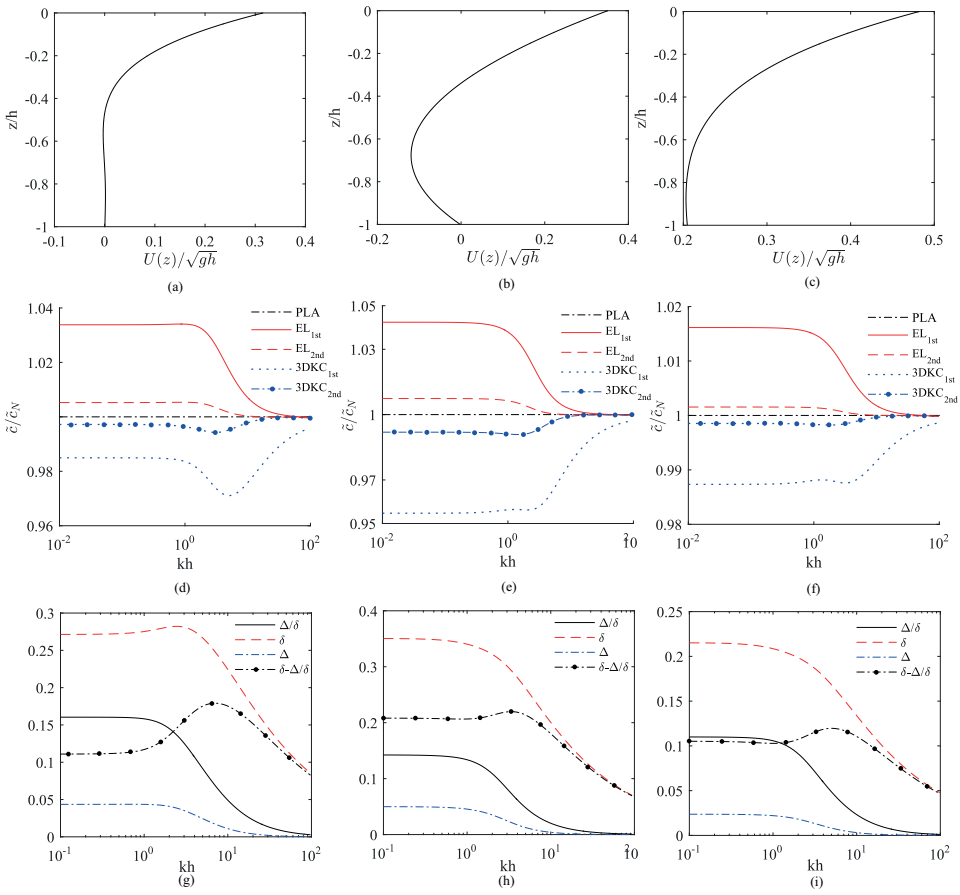

Figure 2.5: Approximate dispersion relations applied to different wind-drift shear currents [99] (The data of the shear profiles is from [92]). Results for the shear profiles in panels (a,b,c) are found in their respective columns. (d,e,f) show calculated estimates of intrinsic velocity $\tilde{c}$ relative to the "exact" value calculated with the piecewise–linear method (PLA) from [94]. Results are calculated for the 1st and 2nd order approximations found herein in (2.30) and (2.31), respectively, and those due to Kirby and Chen [16]. Panels (g,h,i) show the parameters relevant to applicability of the approximations. $\Delta(\tilde{c})$ was calculated from the PLA value of $\tilde{c}$.

Particularly, in cases where $|\Delta| \ll 1$ is satisfied but $\mathcal{O}(|\delta|) \sim 1$, (2.30) is most often superior. Nevertheless, circumstances exist where (2.32) works good even when δ is not so small due to another sufficient criterion implying (2.33) that is

$$|\delta^2 - \Delta| \ll 1 \text{ and } 2(1-\delta) \sim \mathcal{O}(1). \tag{2.35}$$

In such cases cancellation occurs in the next order correction to (2.32), indicating it may be accurate even when δ^2 and Δ are not so small respectively.

Examples in *Paper II* [99] have showed that the criterion (2.33) indeed provides a reasonable explanation of KCA that works for wave regions where its assumption is strongly violated.

(ii-3) the second-order extended KC approximate method.

The 2nd-order extended KC approximation slightly differs from the 2nd-order approximation derived in [16] in two aspects. The former is based on a more well-defined assumption and the latter arguably holds a much more complicated form. Again, based on the criterion (2.33), we yield that $\tilde{c} \approx \tilde{c}_{\text{KC}} + \tilde{c}_{\text{e}}^{(2)}$ where

$$c_{\text{e}}^{(2)} = c_0[\delta^2 - \Delta(\tilde{c}_{\text{KC}})]/2, \tag{2.36}$$

which is supposed to have an equivalent accuracy as (2.31).

Before proceeding to the next subsection, it is worth to notice that the approximations (2.30) and (2.32) are essentially equivalently good in terms of the complexity, the computational effort and the accuracy. As for a wide range of shear flows, the first order approximations, e.g. (2.30) and (2.32), are sufficient. As for which of the two is to use, it is somewhat a point of preference. Nevertheless, it has indicated in *Paper II* [99] that (2.30) is superior for strongly sheared flows and for cases where δ is not small when compared to $\mathcal{O}(1)$. Especially when $|\delta| > 1$, the results given by (2.32) is physically unacceptable, as indicated in Fig. 2.6.

Moreover, compared to the second order approximate scheme derived in [16], (2.31) (or (2.36)) is, in the author's opinion, of a much simpler form. Meanwhile, it contains essential physical implications. Note that criteria (2.33) only explain why (2.32) has a wide range of applicability while the criteria for which the second order approximation derived in [16] works have yet been known.

All of the discussions in the previous two paragraphs are confirmed by Figs. 2.5 and 2.6. Detailed analysis with respect to Figs. 2.5 and 2.6 is, however, not presented to avoid too much repetition, and readers are directed to *Paper II* [99].

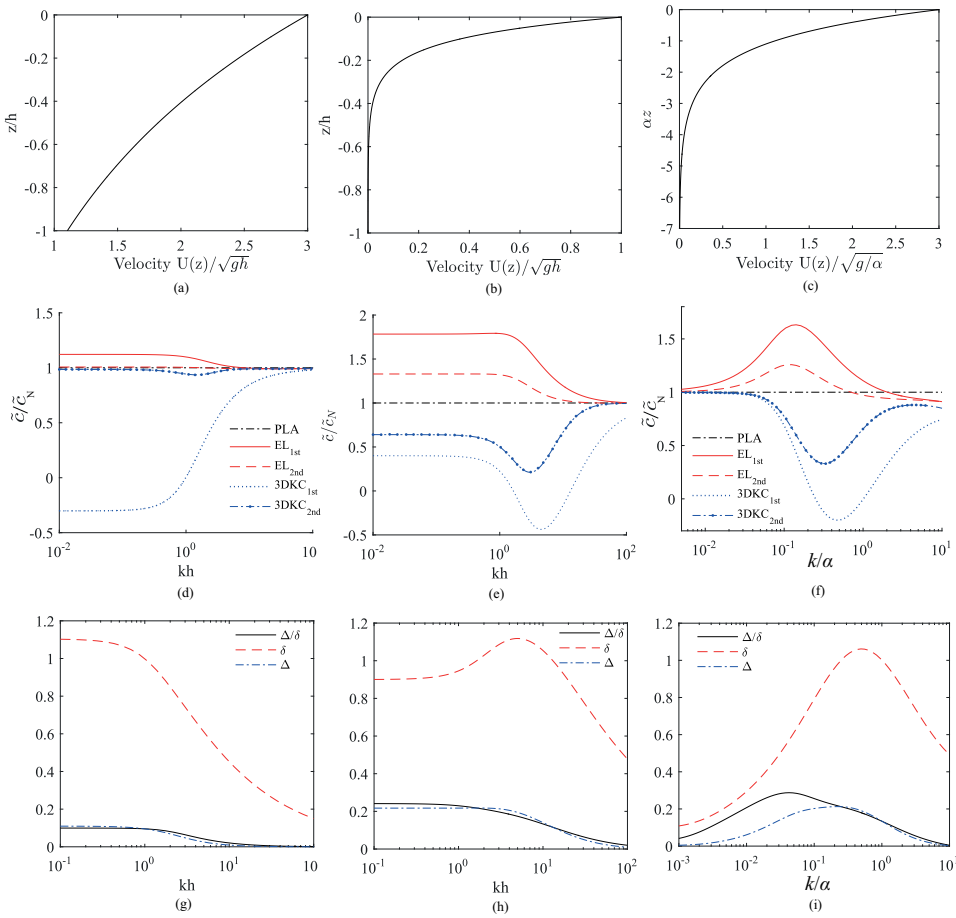

Figure 2.6: Comparison of different approximation models for three strongly sheared velocity profiles [99]. (a,d,g) pertain to profile 1, e.g. $U_1(z) = 3\sqrt{gh}\exp(z/h)$, (b,e,h) to profile 2, e.g. $U_2(z) = \sqrt{gh}\exp(10z/h)$, and (c,f,i) to profile 3, e.g. $U_3(z) = 3\sqrt{g/\alpha}\exp(\alpha z)$. (a,b,c): Velocity profiles. (d,e,f): 1st and 2nd order estimates using the present model to first and second order, respectively $\mathrm{EL}_{1\mathrm{st}}$ [(2.30)], and EL_{2nd} [(2.31)], as well as the 1st and 2nd order approximations of Kirby and Chen [16] ($\mathrm{3DKC}_{1st}$ and $\mathrm{3DKC}_{2nd}$, respectively), relative to the high accuracy calculation with the piecewise linear approximation (PLA). (e) and (f): applicability parameters for the models as discussed in this subsection.

2.2.2 Error estimates

We may find the Taylor series for (2.16) about $c = c_{\approx}$ where $c_{\approx}$ represents any of the approximations to the phase velocity, provided that $\tilde{c}_{\approx}$ is a good approximation to the accurate $\tilde{c}$. It thus yields

$$\Delta_R(\mathbf{k}, \tilde{c}_{\approx} + \tilde{c} - \tilde{c}_{\approx}) = \Delta_R(\mathbf{k}, \tilde{c}_{\approx}) + (\tilde{c} - \tilde{c}_{\approx}) \left.\frac{\partial \Delta_R}{\partial c}\right|_{\tilde{c}=\tilde{c}_{\approx}} + \mathcal{O}((\tilde{c} - \tilde{c}_{\approx})^2) = 0. \tag{2.37}$$

The relative error of the leading order then reads

$$R_{\text{err}} = \frac{\tilde{c} - \tilde{c}_{\approx}}{\tilde{c}} \cong -\left.\frac{\partial \Delta_R / \partial c}{\tilde{c}_{\approx} \Delta_R}\right|_{\tilde{c}=\tilde{c}_{\approx}} \tag{2.38}$$

As for approximations (2.30) and (2.32), error estimates can be roughly made by the next order in relative to the leading order. Hence the rough errors are expressed, respectively,

$$\text{err}_{\text{EL}} = \frac{c_0 |\Delta(\tilde{c}_{\text{EL}})|}{2\tilde{c}_{\text{EL}}\sqrt{1+\delta^2}}, \ \text{err}_{\text{KC}} = \frac{|\delta^2 - \Delta(\tilde{c}_{\text{KC}})|}{2(1-\delta)}. \tag{2.39}$$

2.2.3 Phase and group velocity

As was noted and introduced above, the phase velocity describes the speed at which the crest or phase of a progressive wave propagates. Here, we further derive the group velocity which denotes the speed at which the wave energy propagates. Based on the implicit dispersion relation (2.16), we yield

$$\mathbf{c}_g = \nabla_k \omega(\mathbf{k}) = -\frac{\nabla_k \Delta_R}{\partial \Delta_R / \partial \omega} \tag{2.40}$$

in which the operator $\nabla_k = \dfrac{\partial}{\partial k}\mathbf{e}_k + \dfrac{\partial}{k\partial\theta}\mathbf{e}_\theta$. (2.40) is an implicit expression but uncomplicated to obtain numerical results.

2.2.4 The analytical solutions to special cases

(i). a linear shear current.

Waves atop a linear shear current have been extensively studied. An analytical approach to solve the 3D linear waves propagating on a current of uniform vorticity is initially introduced in [56, 58]. The linear shear profile is expressed $\mathbf{U} = \mathbf{U}_0 + (Sz, 0)$ where S ($S > 0$ is normally assumed for convenience) is the uniform vorticity. As for the particular case, the dispersion relation reads

$$\omega - \mathbf{k}\cdot\mathbf{U}_0 = \pm\sqrt{k^2 c_0^2 + \left(\frac{\mathbf{k}\cdot\mathbf{U}_0' \tanh kh}{2k}\right)^2} - \frac{\mathbf{k}\cdot\mathbf{U}_0' \tanh kh}{2k}, \tag{2.41}$$

The physical implications of (2.41) either for different strengths of vorticity or for different water depths are introduced in detail in *paper III* [61]. In infinite water depth, the dispersion relation is readily given by taking the limit $kh \to \infty$

$$\omega - \mathbf{k}\cdot\mathbf{U}_0 = \pm\sqrt{k^2c_0^2 + \left(\frac{\mathbf{k}\cdot\mathbf{U}_0'}{2k}\right)^2} - \frac{\mathbf{k}\cdot\mathbf{U}_0'}{2k} = \Sigma_{\pm}(K)\sqrt{\frac{g}{b}}, \tag{2.42}$$

where b is a reference length that can be chosen for better reference and $K = kb$. (2.42) yields an explicit solution of k for a given oscillating frequency $\omega = \omega_0$,

$$\begin{aligned} K_{C,E} &= \frac{\tau\cos\gamma - 0.5(1 - \mathrm{Fr_s}\cos\theta\cos\gamma) + \sqrt{D_k}}{\mathrm{Fr}^2\cos^2\gamma}, \\ K_{B,D} &= \frac{\tau\cos\gamma - 0.5(1 - \mathrm{Fr_s}\cos\theta\cos\gamma) - \sqrt{D_k}}{\mathrm{Fr}^2\cos^2\gamma}, \end{aligned} \tag{2.43}$$

in which $\tau = |\mathbf{U}_0|\omega/g$, $\mathrm{Fr_s} = |\mathbf{U}_0||\mathbf{U}_0'|/g$, $\mathrm{Fr} = |\mathbf{U}_0|/\sqrt{gb}$, γ is the angle between the propagating direction of a wave train and $\mathbf{U}_0$ ($\mathbf{U}_0 = |\mathbf{U}_0|(\cos\beta, \sin\beta)$), $D_k = (1 - \mathrm{Fr_s}\cos\gamma\cos\theta)^2 - 4\tau\cos\gamma$ is the discriminant of (2.42) as a quadratic function of k after a little bit effort of reorganising, the subscribes B, C, D and E are marked in Fig. 2.7. Fig. 2.7 depicts the graphical solutions of (2.42). More detailed information can be found in *Paper III* [61] where more physical implications are also presented. (2.43) agrees with [36] when the shear current is not present.

Physically, a *Doppler resonance* occurs when

$$\mathbf{c}_g = 0, \tag{2.44}$$

which implies that wave energy is held stationary in space. The resonance condition described by (2.44) and together with the dispersion relation (2.41) or (2.42) is sufficient to yield the Doppler resonance τ_{res}. More discussions regarding the dispersion relation and Doppler resonance can be found in *Paper III* [61]. A figure that depicts the multiple Doppler resonances is shown in Fig.2.8.

(ii). steady waves on a special class of shear profiles.

There is a special class of shear profiles for which the analytical solutions to problems of steady waves can be obtained. Generally, this class of shear current is expressed $\mathbf{U}''(z) = \alpha\mathbf{U}(z)$. When steady waves are the problem of interest, it gives $c(\mathbf{k}) = 0$ (or $\omega = 0$). Under this specific situation, the Rayleigh equation (2.4) yields

$$w(\mathbf{k}, z) = \sinh k_\alpha(z + h)/\sinh k_\alpha h, \tag{2.45}$$

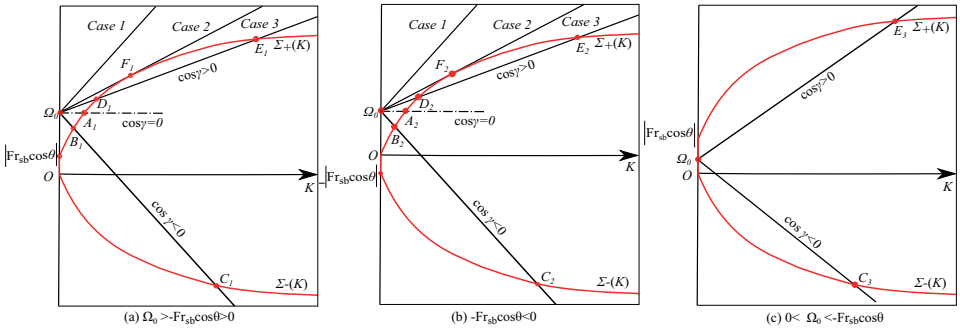

Figure 2.7: Graphical solutions of dispersion relation in deep waters [61]. In the figures, slope of the tangent of curve $\Sigma_{\pm}(K)$ denotes component of non-dimensional and intrinsic group velocity, $C_{gK}(K) = \partial\Sigma_{\pm}/\partial K$; Slope of the line connecting one point on curve $\Sigma_{\pm}(K)$ and origin denotes intrinsic phase velocity, $C(K) = \Sigma_{\pm}/K$; Slope of the straight line $\Omega_0 + K\mathrm{Fr}\cos\gamma$ is the projected component of non-dimensional moving speed of the source along direction of wave propagating - $\mathrm{Fr}\cos\gamma$.

where $k_\alpha = \sqrt{k^2 + \alpha}$.

Hence, the dispersion relation now reads

$$(\mathbf{k}\cdot\mathbf{U}_0)^2 k_\alpha \coth k_\alpha h - [\mathbf{k}\cdot\mathbf{U}_0'\mathbf{k}\cdot\mathbf{U}_0 + gk^2 + \sigma k^4/\rho] = 0; \tag{2.46}$$

which is not complex to seek solutions.

2.3 Critical layer

As was noted above, a critical layer may exist at a critical depth z_c that satisfies the relation $\mathbf{k}\cdot\mathbf{U}(z_c) = kc$. If z_c is close enough to the water surface, the critical layer may have profound effects on surface water waves. Otherwise the effects could be somewhat neglected when the critical layer exists in a deep depth in relative to the wavelength. A critical layer normally introduces an imaginary part of the eigenvalues, possibly resulting in instability of the flow. The instability depends on the sign of the imaginary part of the phase velocity. A piecewise linear model is widely used to study the instability of the flow [106, 107, 108]. Additional consideration of the viscosity brings a more realistic model, which shows nontrivial effects on the unstable modes [105, 121].

When a critical layer exists, $\tilde{c}$ becomes complex that can be written as $\tilde{c} = \tilde{c}_r + \mathrm{i}c_i$. we may obtain the leading behaviour of c_i from the implicit dispersion relation (2.16). It reads

$$c_i \approx -\tilde{c}_{\approx} I_i/(2\sqrt{1+\delta^2}). \tag{2.47}$$

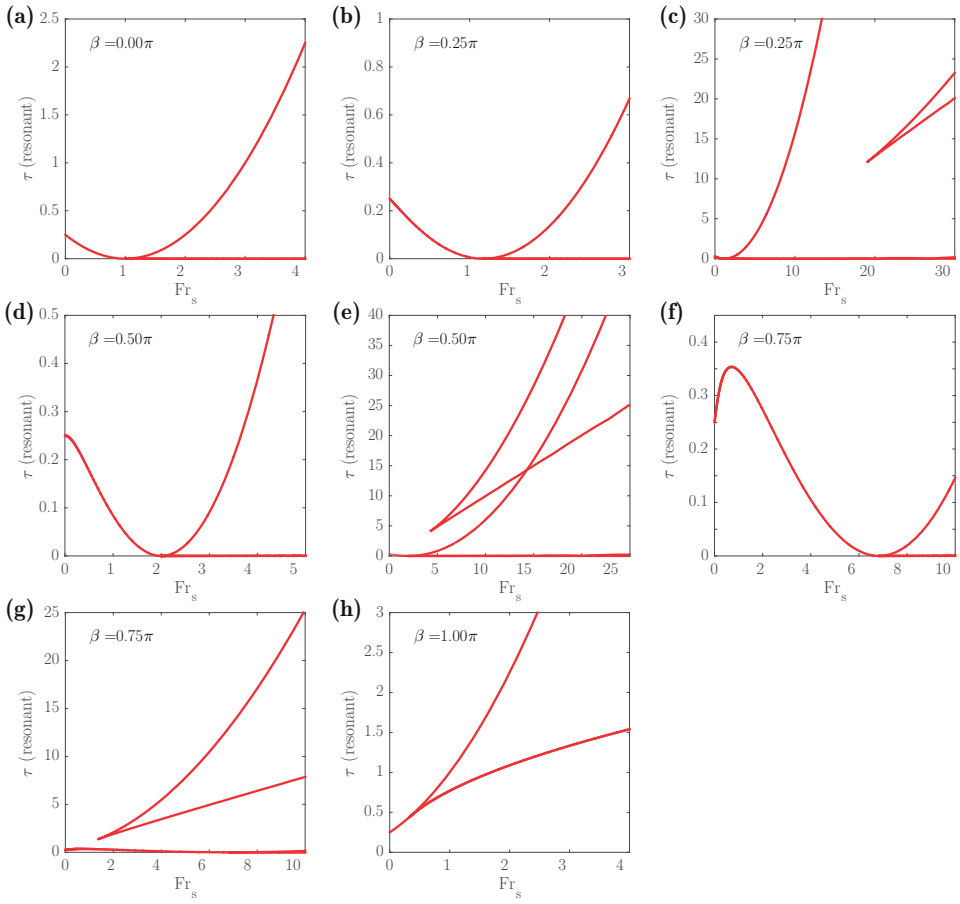

Figure 2.8: Doppler resonant frequencies τ_{res} as a function of Fr_s for different directions of motion β with the shear current [61]. Where two panels show the same β $((b,c),(d,e),(f,g))$, the first is a zoom of behaviour for small and moderate Fr_s while the second shows the full picture appearing at large Fr_s.

where

$$I_i = \frac{2\pi \mathbf{k}\cdot\mathbf{U}_c'' \sinh^2 k(z_c+h)}{k|\mathbf{k}\cdot\mathbf{U}_c'|\sinh 2kh},$$

which is the imaginary part of I_g due to the critical layer after using the Sokhotski-Plemelj theorem. (2.47) implies that instability occurs when $\mathbf{k}\cdot\mathbf{U}_c'' < 0$ and its deep-water version agrees with the result in [90]. More detailed analysis can be found in the appendix in *Paper II* [99].

Additionally, it is straightforward to yield c_i by the DIM. The only difference is that the DIM obtains only $c(\mathbf{k})$ that is real when there is no critical layer but it solves $c(\mathbf{k})$ that additionally includes an imaginary part when a critical layer exists. For more details in this regard, one may refer to *Paper I*[119].

2.4 Boundary value problems

2.4.1 The Cauchy-Poisson problem

As for a Cauchy - Poisson problem, the initial surface elevation relevant quantities – $\hat{\zeta}(\mathbf{r}, t=0) = \hat{\zeta}_0$ and its derivative with respect to the time - $\dot{\hat{\zeta}}(\mathbf{r},t)|_{t=0} = \dot{\hat{\zeta}}_0$ – are understood to be prescribed conditions. For this particular initial condition, we may assume the solution of surface elevation of the form

$$\zeta(\mathbf{k},t) = D_+(\mathbf{k})\mathrm{e}^{-\mathrm{i}\omega_+ t} + D_-(\mathbf{k})\mathrm{e}^{-\mathrm{i}\omega_- t}, \tag{2.48}$$

in which $\omega_\pm$ should satisfy the dispersion relation (2.16) that gives two roots of ω, satisfying the relation $\omega_+(\mathbf{k}) = -\omega_-(-\mathbf{k})$ that indicates an identical ω propagating in two opposite directions, i.e. $\mathbf{k}$ and $-\mathbf{k}$.

Next, we insert (2.48) into the initial condition introduced here and then yield

$$D_+ + D_- = \zeta_0; \tag{2.49a}$$

$$-\mathrm{i}\omega_+ D_+ - \mathrm{i}\omega_- D_- = \dot{\zeta}_0. \tag{2.49b}$$

where ζ_0 and $\dot{\zeta}_0$ are the Fourier transform of $\hat{\zeta}_0$ and $\dot{\hat{\zeta}}_0$, respectively. The kinematic and dynamic conditions at the free surface then give the vertical velocity distribution w and hydrodynamic pressure p, respectively.

Until now, the Cauchy-Poisson problem has been solved, in which $D_\pm(\mathbf{k})$ and $\omega_\pm$ are the primary physical unknowns. The inverse Fourier transform then yields the solutions in the physical plane.

2.4.2 Initial impulsive pressure

The solution obtained from an initial impulsive pressure works as an impulse response function which can be widely applied in realistic situations [122]. For

instance, this is one of the classical ways to form the steady ship waves [35, 36]. Similar to §3.5 discussed in [118], an initial impulsive pressure on the water surface is normally considered of the form $p_I(\mathbf{k}, t) = I(\mathbf{k})\delta(t)$ where δ is the Dirac delta function and I is normally equal to unity in units of pressure.

Before proceeding to seeking the impulse response function of the surface elevation, $[\tilde{w}, \tilde{\zeta}] = [w, \zeta]\mathrm{e}^{-\mathrm{i}\omega t}$ is defined. Rewriting the boundary conditions at the free surface now yields

$$-(\partial_t + \mathrm{i}\mathbf{k}\cdot\mathbf{U})\tilde{w}' + \mathrm{i}\mathbf{k}\cdot\mathbf{U}'\tilde{w} - (gk^2 + \sigma k^4/\rho)\tilde{\zeta} = k^2 p_I/\rho, \text{ at } z = 0, \quad (2.50a)$$

$$(\partial_t + \mathrm{i}\mathbf{k}\cdot\mathbf{U})\tilde{\zeta}(\mathbf{k}, t) = \tilde{w}, \text{ at } z = 0, \quad (2.50b)$$

It is physically reasonable that all of the physical quantities are assumed to be finite at $t = 0^+$. The integration of both sides of (2.50a) and (2.50b) over an infinitesimal interval $t = 0^-$ to 0^+ yields

$$\tilde{w}' = -k^2 I/\rho, \text{at } t = 0^+ \text{and } z = 0, \quad (2.51a)$$

$$\tilde{\zeta}_0 = 0, \text{ for } z = 0, \quad (2.51b)$$

$$\dot{\tilde{\zeta}}_0 = \tilde{w}, \text{at } t = 0^+ \text{and } z = 0. \quad (2.51c)$$

Based on (2.17) and (2.51a), we yield

$$w_0(\mathbf{k})(1 + I_g) = -kI \tanh kh/\rho \quad (2.52)$$

which gives the expression of $w_0(\mathbf{k})$. In addition, I is normally set to 1. From (2.51b) and (2.51c), we notice that an initial impulsive pressure gives an initial vertical velocity distribution or the initial $\dot{\zeta}_0$. (2.52) together with the dispersion relation (2.16) – that provides an additional condition – are sufficient to fully solve the problem. Further solutions of $\zeta(\mathbf{k}, t)$ and $\omega_\pm$ can be thereafter obtained by referring to §2.4.1.

For convenience, a $H(k, t)$ function is used from now on to represent a general solution obtained for the particular boundary condition considered here and a subscript is added to denote different physical quantities. For instance, H_ζ denotes the response function of the surface elevation obtained here. As was noted previously, solutions obtained in this subsection may serve as a response function that may be directly used to form solutions in different boundary conditions. This is straightforward and physical transparent. Here, H_ζ reads

$$H_\zeta(\mathbf{k}, t) = \frac{\mathrm{i}kI \tanh kh}{2\rho\omega_{\text{div}}(1 + I_g)}\left(\mathrm{e}^{-\mathrm{i}\omega_- t} - \mathrm{e}^{-\mathrm{i}\omega_+ t}\right) \quad (2.53)$$

where I is normally in units of pressure, $\omega_{\text{div}} = \omega_+ - \omega_-$ and $\Delta_R = (1 + I_g)(\omega - \omega_+)(\omega - \omega_-) = 0$ that denotes the dispersion relation.

2.4.3 Transient waves generated by a time dependent pressure disturbance

When an external pressure disturbance is depressing on the free water surface, solutions can be formed based on the response function obtained in the previous subsection. It then yields

$$G(\mathbf{k},t)=\int_{-\infty}^{t}\mathrm{d}\tau p_{\text{ext}}(\mathbf{k},\tau)H_G(\mathbf{k},t-\tau), \tag{2.54}$$

where $G(\mathbf{k},t)$ may represent any of the physical quantities for an external time dependent pressure disturbance.

Fig.2.9 depicts one example regarding how waves – that are generated by a suddenly starting ship – develop as time advances in the presence of a linear shear current with the shear Froude number Fr_s equal to 0.8. For more details regarding the transient waves generated by a time dependent wavemaker, readers are directed to *Paper VI* [118].

2.4.4 Steady waves

As for stationary waves, it is understood that $\omega=\omega_0$ is known. Particularly, $\omega_0=0$ denotes the ship waves, indicating the stationary condition [60]. When $\omega\neq 0$, it may be used to represent waves generated by a source oscillating with a single frequency ω_0. In particular, it is a well-known approach to deal with the radiation problem of a floating structure in the sea.

A. Radiation condition.

With a readily known ω, (2.13) and (2.14) should be sufficient to give solutions. Nevertheless, the uniqueness of the physical problems requires an extra condition that serves to meet the boundary condition in the infinite far field, or to gradually develop the initial transient waves into the, somewhat, artificial stationary ones. The radiation condition discussed in [12] is simple and extensively used. It simply replaces $\omega=\omega_0$ with $\omega=\omega_0+\mathrm{i}\epsilon$, where ϵ is an infinitesimal positive parameter which will ultimately set to zero. This constrains the direction of wave propagating to a one-way oriented, i.e. waves are limited to be radiated away from a wavemaker instead of the other way around. This is physically transparent and quite straightforward to understand.

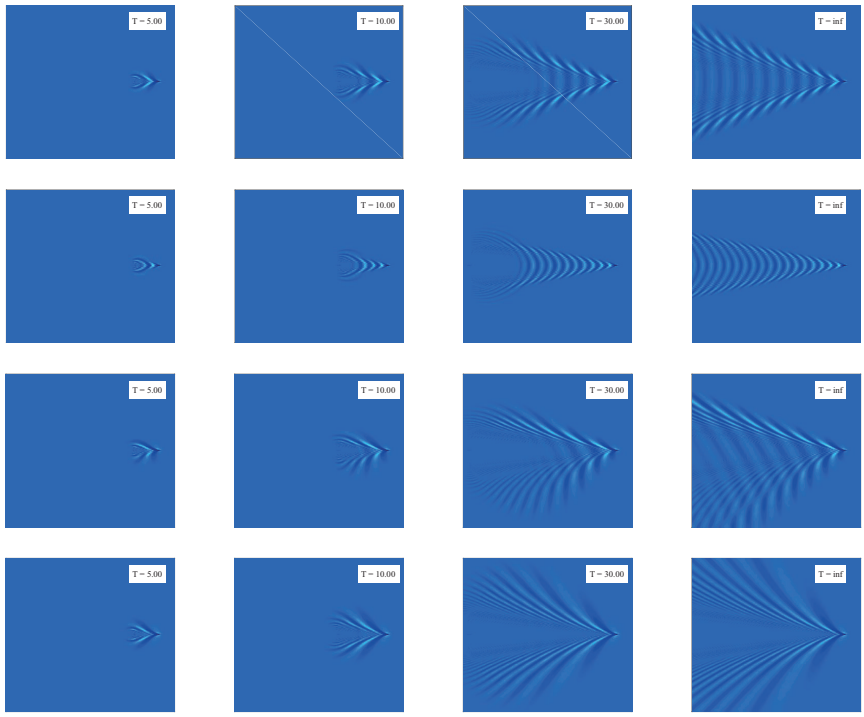

Figure 2.9: Wave patterns of modelling ship suddenly set in motion from rest at $T = 0$, at increasing nondimensional time $T = t\sqrt{g/L}$ where L is the ship length [118]. The ship is modelled as a super-Gaussian of aspect ratio $L/b = 6$. First row: no shear; second row: $\beta = 0$; third row: side-on shear $\beta = \pi/2$; fourth row: $\beta = \pi$. The shear Froude number $\mathrm{Fr}_\mathrm{s} = 0.8$.

Hence, we obtain

$$\hat{w}(\mathbf{r},z,t)=\int\frac{\mathrm{d}^2k}{(2\pi)^2}\frac{\mathrm{i}(\mathbf{k}\cdot\mathbf{U}_0-\omega)kp_{\text{ext}}\tanh kh}{\rho\Delta_R(\mathbf{k},\omega_0+\mathrm{i}\epsilon)}\mathrm{e}^{\mathrm{i}(\mathbf{k}\cdot\boldsymbol{r}-\omega_0 t)}, \tag{2.55}$$

$$\hat{\zeta}(\mathbf{r},t)=\int\frac{\mathrm{d}^2k}{(2\pi)^2}\frac{p_{\text{ext}}k\tanh kh}{\rho\Delta_R(\mathbf{k},\omega_0+\mathrm{i}\epsilon)}\mathrm{e}^{\mathrm{i}(\mathbf{k}\cdot\boldsymbol{r}-\omega_0 t)}, \tag{2.56}$$

which gives the solutions of problems in the context of ship wakes when $\omega_0=0$ and $\mathbf{U}_0\neq 0$ in a relative coordinate system that is fixed on a moving wavemaker.

(2.56) can also be obtained by inserting (2.53) and $p_{\text{ext}}(\mathbf{k})$ into (2.54).

The wave resistance is readily obtained by replacing ω with $\omega_0+\mathrm{i}\epsilon$ in (2.15). In particular, $\omega_0=0$ for ship wave resistance. A general expression of the wave resistance of a ship moving atop a current of an arbitrarily vertically sheared form is derived in [98] in 2D. However, the expression derived in [98] is not closed itself for one unknown exists and no approach is suggested to solve this in a general case. Regarding this particular point, the present work has not only indicated an proper approach but also derived the expression in a far more general case – finite water depth in 3D.

B. ***Ship waves*** $\omega_0=0$.

When $\omega_0=0$, (2.56) solves the problem of stationary ship waves on a depth dependent flow. This means that (2.56) can be directly used for further studies in the context of ship waves on a subsurface flow. Moreover, a stationary condition is satisfied by nature from $\omega_0=0$, stating that the waves that can keep up with a ship propagate at the speed of the ship's motion.

Next, we proceed to the special cases associated with ship waves in the presence of a linear shear current in finite water depth. Here follows a summary of novel features that are introduced due to the uniform vorticity, which are found in *paper IV*[60] and *paper V* [63] where more details are presented.

- ▷ Asymmetric ship wakes and non-constant Kelvin angles – as large as 180^o – are introduced. Fig.2.10 and Fig.2.11 depict the ship wakes and Kelvin angles under different combinations of the parameters Fr_s and Fr_h for different values of β, respectively. Detailed analysis can be found in *paper IV* [60].

- ▷ A critical velocity is found above which the transverse waves vanish. Physically, this means that the fastest transverse waves cannot keep up with the ship any more. Generally a situation refers to a *supercritical situation*

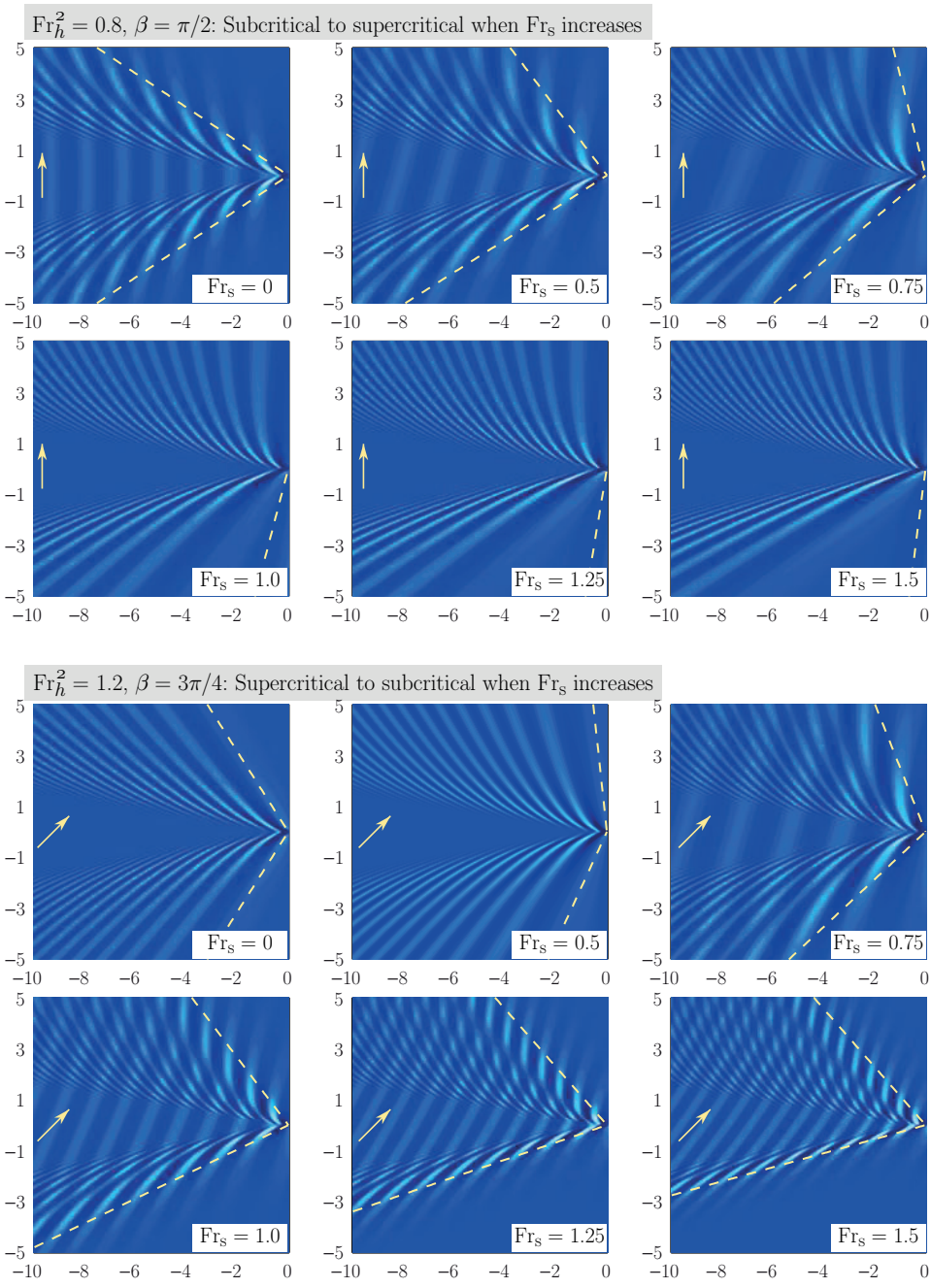

Figure 2.10: Increasing the shear S (and therefore Fr_s) can cause transition from subcritical to supercritical situation (top 6 panels) or from supercritical to subcritical (bottom 6 panels) depending on the value of $\mathrm{Fr}_h = |\mathbf{U}_0|/\sqrt{gh}$ and β [60]. In deep waters ($\mathrm{Fr}_h = 0$) only the former transition is possible. In all graphs $\mathrm{Fr} = 0.8$. Arrows indicate direction of shear flow in the system where the surface is at rest, $\mathrm{Fr}_h = |\mathbf{U}_0|/\sqrt{gh}$ and Fr_s.

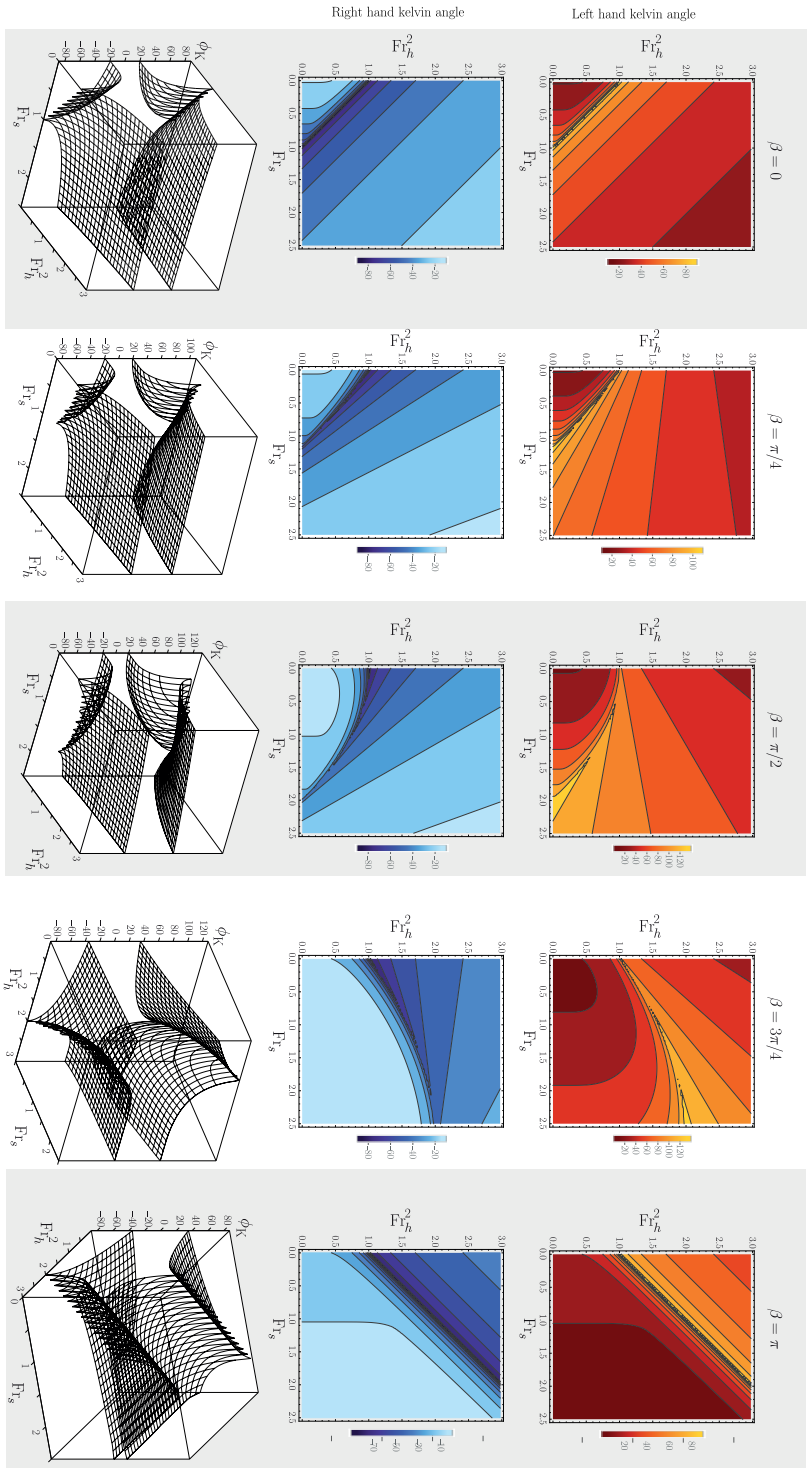

Figure 2.11: Kelvin angles for different values of Fr_s and Fr_h^2 [60].

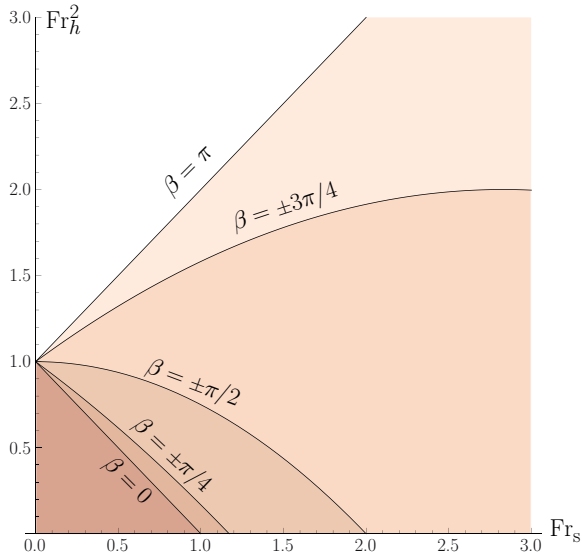

Figure 2.12: Critical lines as function of Fr_s and Fr_h for different values of β. The shaded regions below the critical lines are sub-critical [60].

when no transverse waves exist, otherwise it denotes a *sub-critical situation*. When both a finite water depth and a current of uniform water depth are present, the critical velocity reads

$$\mathrm{Fr}_\mathrm{crit} = \frac{V_\mathrm{crit}}{\sqrt{gb}} = \frac{\sqrt{\mathrm{Fr}_\mathrm{sb}^2 + 1/H} - \mathrm{Fr}_\mathrm{sb}\cos\beta}{1/H + \mathrm{Fr}_\mathrm{sb}^2 \sin^2\beta}. \tag{2.57}$$

where $H = h/b$. Fig.2.12 shows the critical lines for different values of β as function of Fr_s and Fr_h, below which a sub-critical situation is shown.

▷ The transitions between sub-critical and supercritical situations can be observed as Fr_s increases when the ship is moving in different angles with the shear current, as shown in Fig.2.10.

▷ Interplays between the shear current and wave-interference effects, for deep water, are found to be complex and to result in different wave-interference regimes, in a manner that is somewhat similar to the complex interplays between the seabed and wave-interference effects, as depicted in Fig.2.13. Detailed analysis can be found in *Paper V* [63].

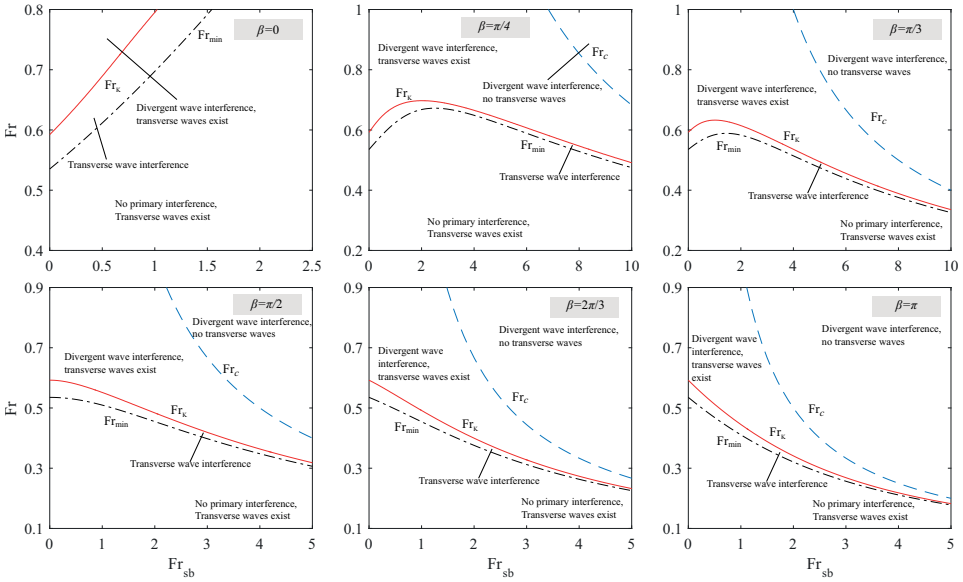

Figure 2.13: Wave-interference regimes when a ship is moving in the directions $0,\ \pi/4,\ \pi/3,\ \pi/2,\ 2\pi/3$ and π with the shear current [63].

2.4.5 Wave resistance

Due to the asymmetric ship wake in the presence of a shear current, a lateral radiation force is firstly introduced. Compared to the normal wave resistance along the stern-wise direction, the lateral radiation force is defined towards the starboard (right) and equals to zero for a symmetric ship hull in the absence of a shear current.

The forces felt by a moving wavemaker due to the energy conveyed for radiating waves are analysed at two stages, including the transient stage of a ship suddenly set in motion and the stationary phase when wave pattern generated by a wavemaker advancing at constant speed is relatively steady to its motion. The former is considered in *paper VI* [118] and the latter in *paper IV* [60].

The thesis does not intend to cover every detail found about the wave resistance in the thesis articles. Hence, detailed analysis with respect to each relevant figure is not present here and only primary findings associated with the wave resistance for different applications are listed below.

- ▷ The lateral radiation force can amount to $10 \sim 20$ percent of the wave resistance under some circumstances, as indicated in Figs.2.14 and 2.15.

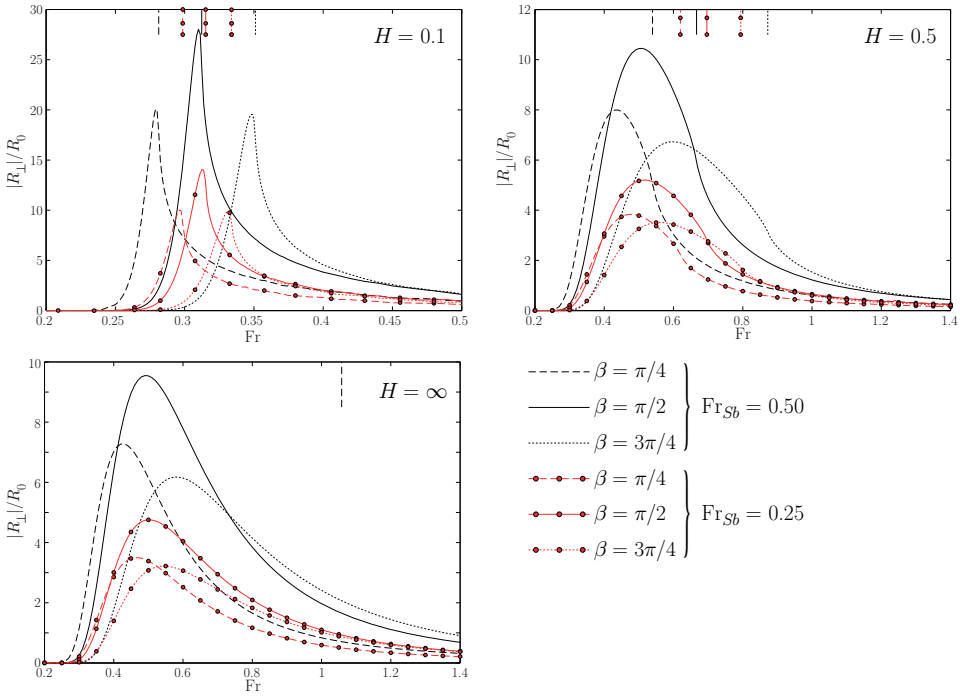

Figure 2.14: Lateral radiation force felt by a ship modelled as a Gaussian pressure distribution varies with Fr [60]. In the figure, $\mathrm{Fr}_{sb} = S\sqrt{l/g}$, (a) $H = h/l = 0.1$ (shallow water); (b) $H = 0.5$ (finite water); (c) $H = \infty$.

▷ The presence of a linear shear current tends to increase wave resistance for upstream ship motion and decrease it for downstream motion, although interference effects between bow waves and stern waves can alter this for certain Froude numbers. Also the value of Fr at which $R_{\|}$ is maximal is lowered for upstream and increased for downstream directions of ship motion, as indicated in Fig.2.15.

▷ The presence of a shear current can noticeably moderate the rate – at which the transient wave resistance $R_{\|}(t)$ dies out – and alter its oscillating frequency, as depicted in Fig.2.16. This is due to the fact that both the phase velocity and phase velocity depend significantly on the shear current that is present.

For more information, one may refer to *paper IV* [60] and *paper VI* [118].

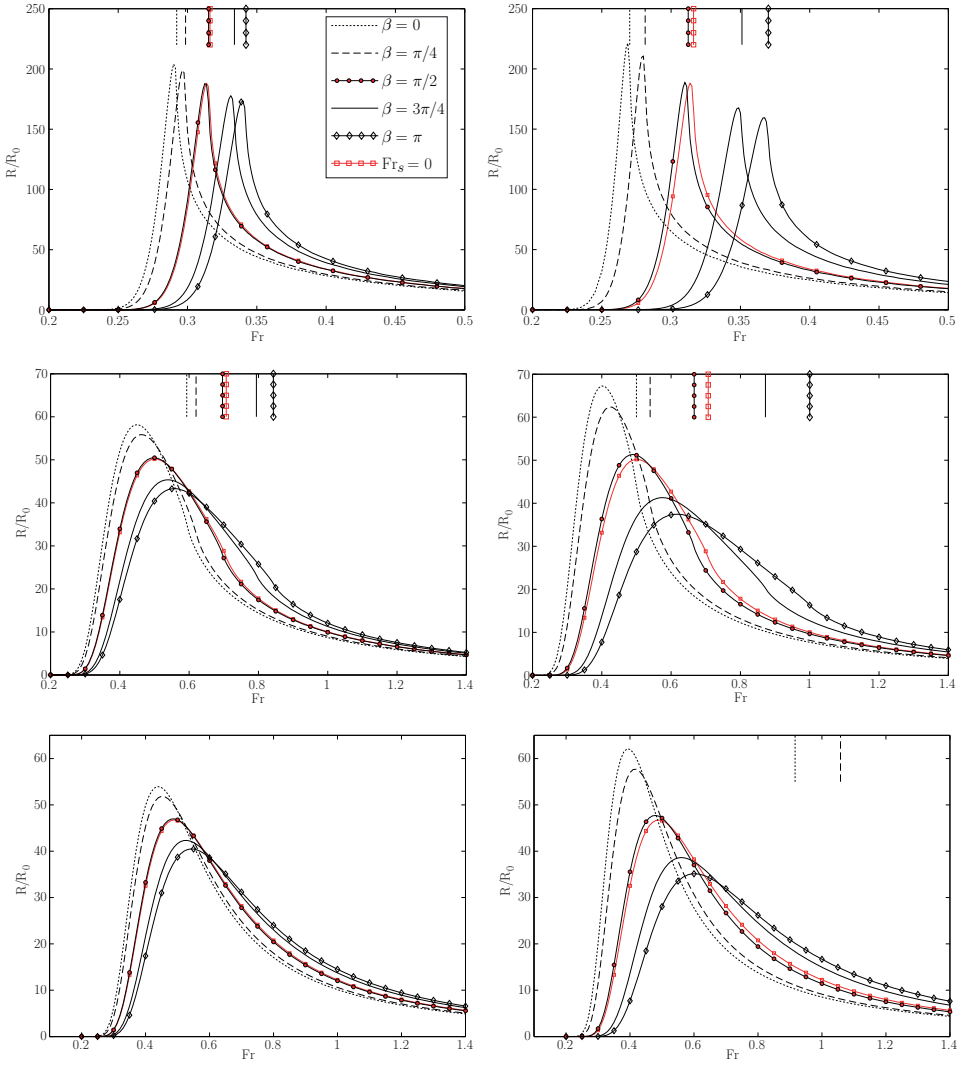

Figure 2.15: Wave resistance felt by a ship modelled as a Gaussian pressure distribution varies with Fr [60]. In the figure, depth $H = 0.1$ (a,b), 0.5 (c,d) , ∞ (e,f) for $\mathrm{Fr}_{sb} = 0.25$ (a,c,e) and 0.5 (b,d,f). The vertical lines show the critical Froude numbers as given in (2.57).

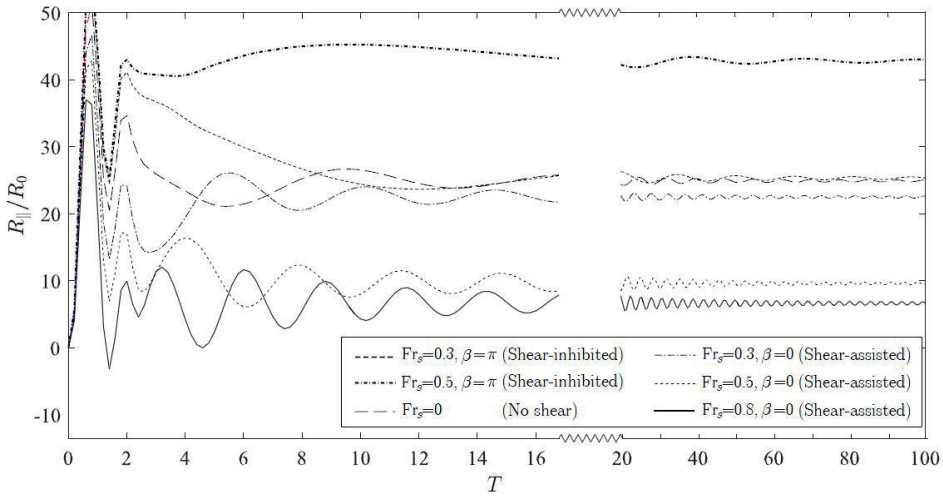

Figure 2.16: Transient wave resistance on a ship set suddenly in motion as a function of nondimensional time $T = t\sqrt{L/g}$, for different cases where a linear shear current is present in deep water [118]. The "ship" is modelled as an ellipsoidal, super-Gaussian surface pressure of aspect ratio 6 and $L = 1$ (arbitrary units), moving with $\mathrm{Fr} = 0.3$. Note that the abcissa is scaled differently for $T > 20$.

2.5 Recommendations for future topics

In the author's opinion, a couple of topics suggested below are beneficial for applications and thus can be used for future studies.

1. Applications based on the fundamental theory derived in the thesis. For instance, Doppler resonance affected by a realistic shear flow, energy flux, and etc.

2. Nonlinear waves on a depth-dependent flow in three dimensions. Especially, how the presence of a vertically sheared current may affect the wave steepness.

3. Laboratory and field observations are required, necessary, and desirable;

4. Engineering applications, such as the design of offshore structures, effects from the shear current on sea loads on offshore installations, larger structures such as the floating platforms, drilling and transporting vessels, etc.

Bibliography

[1] M. Lighthill, On waves generated in dispersive systems to travelling forcing effects, with applications to the dynamics of rotating fluids, in: Hyperbolic Equations and Waves, Springer, 1970, pp. 124–152.

[2] S. W. Thomson, On ship waves, Proceedings of the Institution of Mechanical Engineers 38 (1887) 409–434.

[3] T. H. Havelock, The propagation of groups of waves in dispersive media, with application to waves on water produced by a travelling disturbance, Proceedings of the Royal Society of London. Series A, Containing Papers of a Mathematical and Physical Character 81 (1908) 398–430.

[4] D. Peregrine, A ship's waves and its wake, Journal of Fluid Mechanics 49 (1971) 353–360.

[5] V.-S. Kharif, Christian, R. Thomas, the effect of a vertically sheared current on rogue wave properties, in: Proceedings of the 28^th International Workshop of Water Waves and Floating Bodies (IWWWFB), 2013.

[6] D. Peregrine, Interaction of water waves and currents, Advances in applied mechanics. 16 (1976) 9–117.

[7] I. G. Jonsson, Wave-current interactions, The sea 9 (1990) 65–120.

[8] R. A. Dalrymple, Water wave models and wave forces with shear currents., Ph.D. thesis, The University of Florida, 1973.

[9] R. A. Dalrymple, et al., Models for nonlinear water waves on shear currents, in: Offshore Technology Conference, Offshore Technology Conference, 1974.

[10] J. Isaacs, J. Johnson, Discussion of âĂIJrefraction of surface waves by currentsâĂİ, Eos, Transactions American Geophysical Union 29 (1948) 739–742.

[11] G. Taylor, The action of a surface current used as a breakwater, Proceedings of the Royal Society of London. Series A. Mathematical and Physical Sciences 231 (1955) 466–478.

[12] J. Lighthill, Waves in fluids. 1978, Cumbridge Uni-versity Press, Cambridge (1978).

[13] I. G. Jonsson, O. Skovgaard, Wave refraction across a shearing current, in: Coastal Engineering 1978, 1978, pp. 722–741.

[14] I. G. Jonsson, J. D. Wang, Current-depth refraction of water waves, Ocean Engineering 7 (1980) 153–171.

[15] T. Hedges, Combinations of waves and currents: an introduction, Proceedings of the Institution of Civil Engineers 82 (1987) 567–585.

[16] J. T. Kirby, T.-M. Chen, Surface waves on vertically sheared flows: approximate dispersion relations, Journal of Geophysical Research: Oceans (1978–2012) 94 (1989) 1013–1027.

[17] J. A. Smith, Wave–current interactions in finite depth, Journal of Physical Oceanography 36 (2006) 1403–1419.

[18] H. Lamb, Hydrodynamics, Cambridge university press, 1993.

[19] K. B. Hjelmervik, Wave-current interactions in coastal tidal currents (2009).

[20] M. S. Longuet-Higgins, R. Stewart, Changes in the form of short gravity waves on long waves and tidal currents, Journal of Fluid Mechanics 8 (1960) 565–583.

[21] M. S. Longuet-Higgins, R. Stewart, The changes in amplitude of short gravity waves on steady non-uniform currents, Journal of Fluid Mechanics 10 (1961) 529–549.

[22] M. S. Longuet-Higgins, R. Stewart, Radiation stress and mass transport in gravity waves, with application to âĂŸsurf beatsâĂŹ, Journal of Fluid Mechanics 13 (1962) 481–504.

[23] M. S. Longuet-Higgins, R. Stewart, Radiation stresses in water waves; a physical discussion, with applications, in: Deep Sea Research and Oceanographic Abstracts, volume 11, Elsevier, 1964, pp. 529–562.

[24] J. Johnson, The refraction of surface waves by currents, Eos, Transactions American Geophysical Union 28 (1947) 867–874.

[25] R. S. Arthur, Refraction of shallow water waves: the combined effect of currents and underwater topography, Eos, Transactions American Geophysical Union 31 (1950) 549–552.

[26] I. G. Jonsson, J. B. Christoffersen, Current depth refraction of regular waves, in: Coastal Engineering 1984, 1985, pp. 1103–1117.

[27] D. H. Peregrine, I. G. Jonsson, Interaction of Waves and Currents., Technical Report, DTIC Document, 1983.

[28] R. Smith, Giant waves, Journal of Fluid Mechanics 77 (1976) 417–431.

[29] J. K. Mallory, Abnormal waves on the south east coast of south africa, The International Hydrographic Review 51 (1974).

[30] C. Kharif, E. Pelinovsky, Physical mechanisms of the rogue wave phenomenon, European Journal of Mechanics-B/Fluids 22 (2003) 603–634.

[31] E. Schumann, Changes in energy of surface gravity waves in the agulhas current, in: Deep Sea Research and Oceanographic Abstracts, volume 23, Elsevier, 1976, pp. 509–518.

[32] M. Grabbe, E. Lalander, S. Lundin, M. Leijon, A review of the tidal current energy resource in norway, Renewable and Sustainable Energy Reviews 13 (2009) 1898–1909.

[33] L. Holthuijsen, H. Tolman, Effects of the gulf stream on ocean waves, Journal of Geophysical Research: Oceans 96 (1991) 12755–12771.

[34] M. Mathiesen, Wave refraction by a current whirl, Journal of Geophysical Research: Oceans 92 (1987) 3905–3912.

[35] J. J. Stoker, Water waves: The mathematical theory with applications, volume 36, John Wiley & Sons, 2011.

[36] J. V. Wehausen, E. V. Laitone, Surface waves, Springer, 1960.

[37] A. Da Silva, D. Peregrine, Steep, steady surface waves on water of finite depth with constant vorticity, Journal of Fluid Mechanics 195 (1988) 281–302.

[38] J. Fenton, Some results for surface gravity waves on shear flows, IMA Journal of Applied Mathematics 12 (1973) 1–20.

[39] V. W. Ekman, et al., On the influence of the earth's rotation on ocean-currents. (1905).

[40] X. Yang, K. A. Haas, H. M. Fritz, S. P. French, X. Shi, V. S. Neary, B. Gunawan, National geodatabase of ocean current power resource in usa, Renewable and Sustainable Energy Reviews 44 (2015) 496–507.

[41] B. Lund, H. C. Graber, H. Tamura, C. Collins, S. Varlamov, A new technique for the retrieval of near-surface vertical current shear from marine x-band radar images, Journal of Geophysical Research: Oceans 120 (2015) 8466–8486.

[42] G. Thomas, G. Klopman, Wave-current interactions in the near shore region, INTERNATIONAL SERIES ON ADVANCES IN FLUID MECHANICS 10 (1997) 255–319.

[43] X. Zhang, Mathematical modelling of nonlinear ring waves in a stratified fluid, Ph.D. thesis, © Xizheng Zhang, 2015.

[44] K. R. Khusnutdinova, X. Zhang, Long ring waves in a stratified fluid over a shear flow, Journal of Fluid Mechanics 794 (2016) 17–44.

[45] P. D. Thompson, The propagation of small surface disturbances through rotational flow, Annals of the New York Academy of Sciences 51 (1949) 463–474.

[46] X. Zhang, Short surface waves on surface shear, Journal of Fluid Mechanics 541 (2005) 345–370.

[47] F. Biesel, Etude théorique de la houle en eau courante, La Houille Blanche (1950) 279–285.

[48] S. Tsao, Behaviour of surface waves on a linearly varying flow, Tr. Mosk. Fiz.-Tekh. Inst. Issled. Mekh. Prikl. Mat 3 (1959) 66–84.

[49] I. Brevik, The stopping of linear gravity waves in currents of uniform vorticity, Phys. Norvegica 8 (1976) 157–162.

[50] I. Kantardgi, Effect of depth current profile on wave parameters, Coastal engineering 26 (1995) 195–206.

[51] S. Å. Ellingsen, I. Brevik, How linear surface waves are affected by a current with constant vorticity, European Journal of Physics 35 (2014) 025005.

[52] P. A. Tyvand, M. E. Lepperød, Oscillatory line source for water waves in shear flow, Wave Motion 51 (2014) 505–516.

[53] P. A. Tyvand, M. E. Lepperød, Doppler effects of an oscillating line source in shear flow with a free surface, Wave Motion 52 (2015) 103–119.

[54] S. Å. Ellingsen, P. A. Tyvand, Oscillating line source in a shear flow with a free surface: critical layer-like contributions, Journal of Fluid Mechanics 798 (2016) 201–231.

[55] J. P. McHugh, Surface waves on an inviscid shear flow in a channel, Wave motion 19 (1994) 135–144.

[56] S. Å. Ellingsen, Initial surface disturbance on a shear current: The cauchy-poisson problem with a twist, Physics of Fluids 26 (2014) 082104.

[57] Y. Li, S. A. Ellingsen, Initial value problems for water waves in the presence of a shear current, in: Proceedings of the twenty-fifth International Ocean and Polar Engineering Conference (Proceedings of ISOPE), 2015.

[58] S. Å. Ellingsen, Ship waves in the presence of uniform vorticity, Journal of Fluid Mechanics 742 (2014) R2.

[59] Y. Li, S. A. Ellingsen, Waves in presence of shear current with uniform vorticity, in: Proceedings of MekIT'15 Eighth National Conference on Computational Mechanics, 2015.

[60] Y. Li, S. A. Ellingsen, Ship waves on uniform shear current: wave resistance and finite water depth, Journal of Fluid Mechanics 791 (2016) 539–567.

[61] Y. Li, S. A. Ellingsen, Multiple resonances of a moving oscillating surface disturbance on a shear current, Journal of Fluid Mechanics 808 (2016) 668–689.

[62] S. Å. Ellingsen, P. A. Tyvand, Waves from an oscillating point source with a free surface in the presence of a shear current, Journal of Fluid Mechanics 798 (2016) 232–255.

[63] Y. Li, Wave-interference effects on far-field ship waves in the presence of a shear current (2017). (under review.

[64] M. Rabaud, F. Moisy, Ship wakes: Kelvin or mach angle?, Physical review letters 110 (2013) 214503.

[65] F. Noblesse, J. He, Y. Zhu, L. Hong, C. Zhang, R. Zhu, C. Yang, Why can ship wakes appear narrower than kelvinâĂŹs angle?, European Journal of Mechanics-B/Fluids 46 (2014) 164–171.

[66] M. Benzaquen, A. Darmon, E. Raphaël, Wake pattern and wave resistance for anisotropic moving objects, arXiv preprint arXiv:1404.1699 (2014).

[67] A. Darmon, M. Benzaquen, E. Raphaël, Kelvin wake pattern at large froude numbers, Journal of Fluid Mechanics 738 (2014) R3.

[68] F. Dias, Ship waves and kelvin, Journal of Fluid Mechanics 746 (2014) 1–4.

[69] R. Pethiyagoda, S. W. McCue, T. J. Moroney, What is the apparent angle of a kelvin ship wave pattern?, Journal of Fluid Mechanics 758 (2014) 468–485.

[70] B. K. Smeltzer, Y. Li, S. Å. Ellingsen, Effect on doppler resonance from a near-surface shear layer, in: ASME 2017 36th International Conference on Ocean, Offshore and Arctic Engineering, 2017.

[71] R. Baddour, S. Song, The rotational flow of finite amplitude periodic water waves on shear currents, Applied Ocean Research 20 (1998) 163–171.

[72] W. Choi, Nonlinear surface waves interacting with a linear shear current, Mathematics and Computers in Simulation 80 (2009) 29–36.

[73] A. Constantin, K. Kalimeris, O. Scherzer, Approximations of steady periodic water waves in flows with constant vorticity, Nonlinear Analysis: Real World Applications 25 (2015) 276–306.

[74] R. A. Dalrymple, A finite amplitude wave on a linear shear current, Journal of Geophysical Research 79 (1974) 4498–4504.

[75] I. Brevik, Higher-order waves propagating on constant vorticity currents in deep water, Coastal Engineering 2 (1978) 237–259.

[76] J. A. Simmen, Steady Deep-Water Waves on a Linear Shear Current, Ph.D. thesis, California Institute of Technology, 1984.

[77] J. A. Simmen, P. Saffman, Steady deep-water waves on a linear shear current, Studies in Applied Mathematics 73 (1985) 35–57.

[78] A. D. Craik, Resonant gravity-wave interactions in a shear flow, Journal of Fluid Mechanics 34 (1968) 531–549.

[79] R. Johnson, Ring waves on the surface of shear flows: a linear and nonlinear theory, Journal of Fluid Mechanics 215 (1990) 145–160.

[80] A. J. Abdullah, Wave motion at the surface of a current which has an exponential distribution of vorticity, Annals of the New York Academy of Sciences 51 (1949) 425–441.

[81] Z. Liu, Z. Lin, S. Liao, Phase velocity effects of the wave interaction with exponentially sheared current, Wave Motion 51 (2014) 967–985.

[82] J. Hunt, Gravity waves in flowing water, in: Proceedings of the Royal Society of London A: Mathematical, Physical and Engineering Sciences, volume 231, The Royal Society, 1955, pp. 496–504.

[83] J. Eliasson, F. Engelund, Gravity waves in rotational flow, Progr. Rep. No. 26, Inst. of Hydrodynamics and Hydr. Eng. Tech. Univ. of Denmark (1972) 15–22.

[84] J. Fredsøe, Rotational channel flow over small three-dimensional bottom irregularities, Journal of Fluid Mechanics 66 (1974) 49–66.

[85] S. Patil, V. Singh, Effect of vertically logarithmic steady currents on shallow surface waves, Physical Oceanography 18 (2008) 133–153.

[86] J. Burns, Long waves in running water, in: Mathematical Proceedings of the Cambridge Philosophical Society, volume 49, Cambridge Univ Press, 1953, pp. 695–706.

[87] R. H. Stewart, J. W. Joy, Hf radio measurements of surface currents, in: Deep Sea Research and Oceanographic Abstracts, volume 21, Elsevier, 1974, pp. 1039–1049.

[88] R. A. Skop, Approximate dispersion relation for wave-current interactions, Journal of Waterway, Port, Coastal, and Ocean Engineering 113 (1987) 187–195.

[89] Z. Dong, J. T. Kirby, Theoretical and numerical study of wave-current interaction in strongly-sheared flows, Coastal Engineering Proceedings 1 (2012) 2.

[90] V. I. Shrira, Surface waves on shear currents: solution of the boundary-value problem, Journal of Fluid Mechanics 252 (1993) 565–584.

[91] C. Swan, R. James, A simple analytical model for surface water waves on a depth-varying current, Applied ocean research 22 (2000) 331–347.

[92] C. Swan, I. Cummins, R. James, An experimental study of two-dimensional surface water waves propagating on depth-varying currents. part 1. regular waves, Journal of Fluid Mechanics 428 (2001) 273–304.

[93] E. Caponi, M. Caponi, P. Saffman, H. Yuen, A simple model for the effect of water shear on the generation of waves by wind, in: Proceedings of the Royal Society of London A: Mathematical, Physical and Engineering Sciences, volume 438, The Royal Society, 1992, pp. 95–101.

[94] B. K. Smeltzer, S. Å. Ellingsen, Surface waves on arbitrary vertically-sheared currents, Physics of Fluids 29 (2017) 047102.

[95] R. A. Dalrymple, J. C. Cox, Symmetric finite-amplitude rotational water waves, Journal of Physical Oceanography 6 (1976) 847–852.

[96] G. Mellor, The three-dimensional current and surface wave equations, Journal of Physical Oceanography 33 (2003) 1978–1989.

[97] O. G. Nwogu, Interaction of finite-amplitude waves with vertically sheared current fields, Journal of Fluid Mechanics 627 (2009) 179–213.

[98] M. Benzaquen, E. Raphael, Capillary-gravity waves on depth-dependent currents: Consequences for the wave resistance, EPL (Europhysics Letters) 97 (2012) 14007.

[99] S. A. Ellingsen, Y. Li, Approximate dispersion relations for waves on an arbitrary shear flow (2017). (under review).

[100] J. Miles, A note on surface waves generated by shear-flow instability, Journal of Fluid Mechanics 447 (2001) 173–177.

[101] J. W. Miles, On the generation of surface waves by shear flows, Journal of Fluid Mechanics 3 (1957) 185–204.

[102] J. W. Miles, On the generation of surface waves by shear flows. part 2, Journal of Fluid Mechanics 6 (1959) 568–582.

[103] J. W. Miles, On the generation of surface waves by shear flows part 3. kelvin-helmholtz instability, Journal of Fluid Mechanics 6 (1959) 583–598.

[104] L. Rayleigh, Viii. on the question of the stability of the flow of fluids, The London, Edinburgh, and Dublin philosophical magazine and journal of science 34 (1892) 59–70.

[105] H. Velthuizen, L. Van Wijngaarden, Gravity waves over a non-uniform flow, Journal of Fluid Mechanics 39 (1969) 817–829.

[106] L. Morland, P. Saffman, H. Yuen, Waves generated by shear layer instabilities, in: Proceedings of the Royal Society of London A: Mathematical, Physical and Engineering Sciences, volume 433, The Royal Society, 1991, pp. 441–450.

[107] S. Y. Gertsenshtein, N. Romashova, V. Chernyavski, On the generation and development of wind waves, Izv. Akad. Nauk. SSSR Mekh. Zhid. i Gaza 3 (1988) 163–169.

[108] P. G. Drazin, W. H. Reid, Hydrodynamic stability, Cambridge university press, 2004.

[109] Y.-Y. Yu, Breaking of waves by an opposing current, Eos, Transactions American Geophysical Union 33 (1952) 39–41.

[110] T. Sarpkaya, Oscillatory gravity waves in flowing water, Trans. Amer. Soc. Civ. Eng. (1950) 564–285.

[111] G. Thomas, Wave-current interactions: an experimental and numerical study. part 1. linear waves, Journal of Fluid Mechanics 110 (1981) 457–474.

[112] G. Thomas, Wave–current interactions: an experimental and numerical study. part 2. nonlinear waves, Journal of Fluid Mechanics 216 (1990) 505–536.

[113] I. Cummins, C. Swan, Vorticity effects in combined waves and currents, in: Coastal Engineering 1994, 1995, pp. 113–127.

[114] C. Swan, An experimental study of waves on a strongly sheared current profile, in: Coastal Engineering 1990, 1991, pp. 489–502.

[115] A. Yao, C. H. Wu, Incipient breaking of unsteady waves on sheared currents, Physics of Fluids 17 (2005) 082104.

[116] T. Havelock, Periodic irrotational waves of finite height, Proceedings of the Royal Society of London. Series A 95 (1918) 38–51.

[117] E. Raphaël, P.-G. De Gennes, Capillary gravity waves caused by a moving disturbance: wave resistance, Physical Review E 53 (1996) 3448.

[118] Y. Li, B. K. Smeltzer, S. A. Ellingsen, Transient wave resistance upon a real shear current, European Journal of Mechanics-B/Fluids (2017).

[119] Y. Li, S. A. Ellingsen, Direct integration method for surface waves on a depth dependent flow (2017). (submitted).

[120] C. M. Bender, S. A. Orszag, Advanced mathematical methods for scientists and engineers I: Asymptotic methods and perturbation theory, volume 1, Springer, 1999.

[121] S. Kawai, On the generation of wind waves relating to the shear flow in water-a preliminary study (1977).

[122] W. Cummins, The impulse response function and ship motions, Technical Report, DTIC Document, 1962.

Research articles in full text

Paper I

Direct integration method for surface waves on a depth dependent flow

Is not included due to copyright

Paper II

Approximate dispersion relations for waves on an arbitrary shear flow

Is not included due to copyright

Paper III

Multiple resonances of a moving oscillating surface disturbance on a shear current

Is not included due to copyright

Paper IV

Ship waves on uniform shear current at finite depth:
Wave resistance and critical velocity

Is not included due to copyright

Paper V

Wave-interference effects on far-field ship waves in the presence of a shear current

Is not included due to copyright

Paper VI

Transient wave resistance upon a real shear current

Transient wave resistance upon a real shear current

Yan Li[a,*], Benjamin K. Smeltzer[a,**], Simen Å. Ellingsen[a]

[a]*Department of Energy and Process Engineering, Norwegian University of Science and Technology, N-7491 Trondheim, Norway*

Abstract

We study the waves and wave–making forces acting on ships travelling on currents which vary as a function of depth. Our concern is realism; we consider a real current profile from the Columbia River, and model ships with dimensions and Froude numbers typical of three classes of vessels operating in these waters. To this end we employ the most general theory of waves from surface sources on shear current to date, which we derive and present here. Expressions are derived for ship waves which satisfy an arbitrary dispersion relation and are generated by a wave source acting on the surface, with the source's shape and time-dependence is also being arbitrary. Practical calculation procedures for numerically calculating dispersion on a shear current which may vary arbitrarily with depth both in direction and magnitude, are indicated.

For ships travelling at oblique angle to a shear-current, the ship wave pattern is asymmetrical, and wave–making radiation forces have a lateral component in addition tot he conventional wave resistance, the sternward component. No corresponding lateral force exists in the absence of shear. We consider the dependence of wave resistance and lateral force for upstream, downstream and cross–stream motion on the Columbia River current, both in steady motion and during two different maneouvres: a ship suddenly set in motion, and a ship turning through 360°. We find that for smaller ships (tugboats, fishing–boats) the wave resistance can differ drastically from that in quiescent water, and depends strongly on Froude number and direction of motion. For Froude numbers typical of such boats, wave resistance can vary by a factor 3 between upstream and downstream motion, and the strong Froude number dependence is made more complicated by interference effects. The lateral radiation force is approximately 20% of the wave resistance for cross–current motion for these ships, and can reach more than 50% for short periods during maneouvring; this is by no means a small force, and will have an effect on seakeeping, economy and optimal choice of route. For an example ship (tugboat) doing a turning motion, both the lateral force and wave resistance are predicted to undergo variations whose amplitude amounts to approximately 100% of their constant values in quiescent water.

Keywords: Wave resistance, Shear flow, Transient ship waves

1. Introduction

Typically, more than 30% of the fuel consumption of ocean–going ships is from making waves [1]. A resistance is felt due to the work done by the ship on the surrounding water, which propagates away in the form of wave energy. While going back over a century [2, 3, 4, 5, 6, 7, 8], wave resistance on ships has also been the focus of recent investigations [9].

Two of us recently showed that the wave resistance acting on a ship in steady motion can be significantly altered by the presence of a shear current beneath the water surface [10]. In conditions with no shear, wave resistance typically becomes important for Froude numbers around 0.3 and peaks in the vicinity of 0.5 before decreasing again as the wake becomes dominated by diverging waves. When a sub-surface shear current is present, however, both the Froude number at which wave resistance sets in, and the value at which it peaks, are in general changed, with opposite effects whether the ship travels along, against, or across the current [10]. Moreover, subsurface shear causes the angle made by the ship waves to differ from Lord Kelvin's classic 19.47°, being smaller for shear-assisted and larger for shear-inhibited motion, and asymmetric around the line of motion when the angle with the current is oblique [11]. In the latter case momentum is imparted to the water at different rates to starboard and port, and the corresponding wave radiation force experienced by the ship obtains a lateral component in addition to the conventional sternward wave resistance [10]. No corresponding phenomenon exists in rectilinear motion if the current has depth-uniform velocity profile.

Our concern in this paper is to introduce realism, compared to previous studies which have considered idealised models. We study how the shear of a real, measured current may affect the wave radiation forces on actual ships. We use an example shear profile measured in the Columbia

*Corresponding author.

**YL and BKS are to be considered joint first authors, in alphabetical order.

Email address: yan.li@ntnu.no (Yan Li)

River delta. These waters are crossed by thousands of ships each year, and we study model ships with dimensions and velocities typical of different vessel types operating there. This includes not only the forces acting during steady motion, but also transient forces from manoeuvring motions. To this end, the most general theory of linear ship waves (or waves from surface sources more generally) to date has been developed, and is presented here, allowing a shear current to vary arbitrarily with respect to depth both in direction and magnitude, as long as it may be considered uniform in horizontal directions.

We demonstrate in Section 3 how a real shear current can have a very significant effect on the wave–making forces acting on real ships. At typical Froude numbers we find for smaller boats (tugboats, fishing boats) that the wave resistance can differ by a factor 3 or more between upstream and downstream motion at the same velocity relative to the surface. The lateral radiation force acting when travelling across the shear is also very significant; it is typically around 20% of the sternward resistance force in steady motion, but can momentarily reach more than 50% of the wave resistance during maneouvring. These are by no means small effects, and will affect the seakeeping and the optimal choice of velocity and route of travel.

This paper contains two major sections, one theoretical, one of an applied nature. The reader primarily interested in what the practical effect of shear in real–life situations might be, may wish to refer directly to the numerical results in Section 3 bearing in mind the system definitions in Section 1.2. The theoretical foundations and framework is laid out in Section 2; it has been presented, as far as we have been able to, so as to be useful to readers who wish to employ the formalism for their own purposes.

Studies of transient wave resistance go back a long time. Whenever a ship undergoes changes in velocity during acceleration or manoeuvring, transient waves are emitted, and the wave radiation force correspondingly will be time dependent for the duration during which the created transient ring-wave remains in the immediate vicinity of the ship. A century ago, Havelock studied the wave resistance in 2 dimensions due to a suddenly appearing ship, modelled as a distribution of additional pressure at the water's surface, suppressing the surface approximately as would a ship [12]. The resistance force was found to increase from zero to a peak value before relaxing in an oscillatory manner to its static value. The speed of relaxation was found to depend closely on the aspect ratio of the disturbance, since the bow and stern waves from a more slender ship tend to cancel, causing a quicker relaxation to steady conditions and a more stable steady wave resistance. On the other hand a circular "ship" with little such interference, experienced a very slow relaxation rate. A study of the resistance felt by a submerged cylinder starting suddenly from rest revealed similar results [13]. Studies of ships in various kinds of acceleration is a related classical problem [14, 15].

Approaching the problem of waves in three–dimensional systems in the presence of sheared flows, standard methods to calculate waves and motions of floating bodies must be immediately discarded, based as they are on potential theory. No satisfactory theory of creating bodies from submerged sources and sinks exist even in the simplest shear currents exists, not to mention advanced panel methods [16]. A feasible approach for our purposes is however to create a "ship–shaped footprint" in the surface by introducing an external surface pressure. The approach goes back over a century [17] and has recently been employed in wave resistance studies [9]. Such a model, only affects the dynamic boundary condition, not the equations of motion, thus does not in principle pose any restrictions on the flow vorticity.

1.1. Outline

The investigated system is presented in Section 1.2 along with the basic formalism. Section 2 then goes on to develop the general theory of waves from moving, time–dependent surface disturbances upon a horizontal background current which may vary arbitrarily with depth, both in direction and magnitude. In particular, a suitable formalism for working with a general (not explicitly known) dispersion relation is derived in Section 2.1, and applied to the general problem in Section 2.2. In Section 2.3 practical considerations are presented concerning numerical evaluation of the dispersion relation for arbitrary velocity profiles, and the formalism for calculating wave resistance and lateral radiation force is derived and discussed in Section 2.4.

Section 3 is of a more applied nature and presents numerical results for particular situations. A measured velocity profile from the Columbia River estuary is used, and pressure distributions modelling ships of realistic dimensions are employed in order to provide reasonably realistic estimates of the effect of shear in these waters while retaining some generality. For comparison, and to illustrate the effect of shear without the large number of lengthscales and parameters, corresponding results for the simple case of a linearly depth–dependent current are given in Section 3.1 before conclusions are drawn. Some further details on derivation and numerical procedures are found in appendices.

1.2. System definition

In this section the system under scrutiny is defined, along with general formalism used in the paper. The system is a generalisation of that considered in Ref. [18].

We consider infinitesimal wave amplitudes described by the surface elevation function $\hat{\zeta}(\mathbf{r}, t)$ with horizontal position $\mathbf{r} = (x, y) = r(\cos\varphi, \sin\varphi)$ and time t. The waves are superimposed on a depth-varying background flow $\mathbf{U}(z)$. In our general theory in Section 2, $\mathbf{U}(z)$ may vary both in magnitude and direction, although our numerical examples in Section 3 will all be unidirectional. We use the shorthand $\mathbf{U}(0) = \mathbf{U}_0$. A sketch of the system is seen in

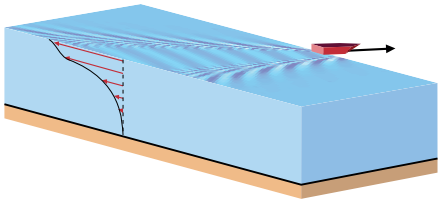

Figure 1: Schematic sketch of the system: a ship travelling with arbitrary, time–dependent velocity atop a shear current of arbitrary depth–dependence. Here a "lab" coordinate system is shown, fixed relative to the sea–bed.

Fig.1. We assume incompressible and inviscid flow. The three velocity components and pressure perturbation due to the waves we name $\hat{u}, \hat{v}, \hat{w}$, and $\hat{p}$, respectively, all functions of $\mathbf{r}, z$ and t. Hatted quantities are considered small, and we linearise with respect to these. The flow field is thus $[\mathbf{V}, P] = [\mathbf{U}(z) + \hat{u}\mathbf{e}_x + \hat{v}\mathbf{e}_y + \hat{w}\mathbf{e}_z, -\rho g z + \hat{p}]$, with $\mathbf{V}$ and P the total velocity and pressure fields, respectively, g the gravitational acceleration, and ρ the density of the water. The flow obeys the Euler equation

$$\partial_t \mathbf{V} + (\mathbf{V} \cdot \nabla)\mathbf{V} = -\nabla P/\rho - g\mathbf{e}_z. \tag{1}$$

We neglect surface tension. The physical quantities are defined in Fourier space of the horizontal plane as $[\hat{\zeta}, \hat{u}, \hat{v}, \hat{w}, \hat{p}](\mathbf{r}, z, t) \leftrightarrow [\zeta, u, v, w, p](\mathbf{k}, z, t)$ as

$$[\hat{\zeta}, \hat{u}, \hat{v}, \hat{w}, \hat{p}](\mathbf{r}, z, t) = \int \frac{\mathrm{d}^2 k}{(2\pi)^2} [\zeta, u, v, w, p](\mathbf{k}, z, t) \mathrm{e}^{\mathrm{i}\mathbf{k}\cdot\mathbf{r}} \tag{2}$$

so that $\mathbf{k} = (k_x, k_y) = (k\cos\theta, k\sin\theta)$ is the wave vector (It is understood that $\hat{\zeta}$ and ζ do not depend on z). The water depth h is constant, and may be allowed to tend to ∞.

In the system sketched in Fig. 1 no less than three different reference frames are natural, depending on the question under consideration. Fig. 1 shows the "lab" reference frame, i.e., as seen by an observer on shore. A second frame of reference which we use in Section 2.2 is that which is fixed on the moving model ship. Finally, in section 3 we will sometimes work in the frame of reference in which the water surface is at rest.

For this reason the oft used terms 'upstream' and 'downstream' are ambiguous as denotations of directions of motion. We will instead use the terms 'shear–assisted' and 'shear–inhibited' to describe directions of ship motion or wave motion relative to the sub-surface current. The motion is assisted by the current if, in a reference system where the water surface is at rest, the sub-surface current has a component along the direction of motion (this corresponds to the ship travelling upstream in the case of e.g. a river). Correspondingly, for shear–inhibited motion the sub–surface current has positive component against the ship's motion, in a system where the surface is at rest (corresponds to downstream motion on a river). These concepts are visualised in Fig. 2a. They are only strictly

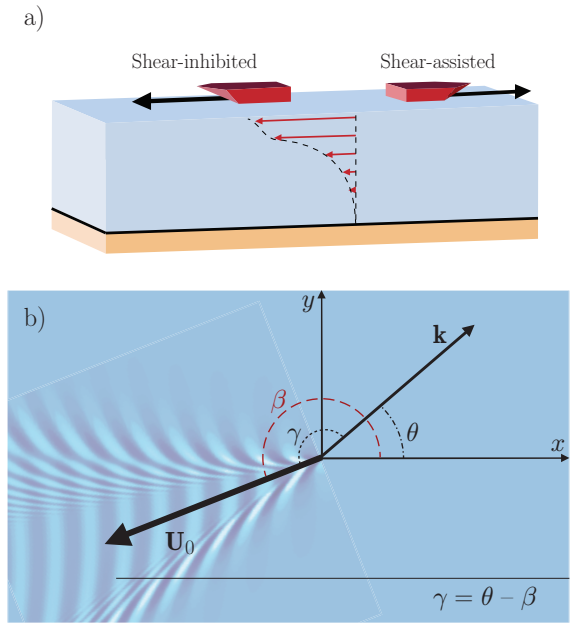

Figure 2: (a) Illustration of shear–assisted vs shear–inhibited ship motion; shown in the "lab" reference frame relative to the sea bed. (b) Definition of angles φ (coordinate angle in $\mathbf{r}$ plane), γ (angle between $\mathbf{k}$ and $\mathbf{U}_0$), β (angle between $\mathbf{U}_0$ and x axis, and θ (angle between $\mathbf{k}$ and x-axis). The reference frame is here at rest with respect to the ship. Note: $\beta = 0$ is the maximally shear assisted direction of motion, $\beta = \pi$ the maximally shear inhibited.

well defined for a monotonically varying velocity profiles, yet this is sufficient for our present purposes.

In later sections we shall make use of polar coordinates in the horizontal plane, which we define in figure 2, for a system in which the ship is at rest. Note carefully that the angle β differs by π from that used in [11, 10], where a reference system relative to the water surface was used. The angle between $\mathbf{k}$ and $\mathbf{U}_0$ is γ.

2. Theory: linear surface waves from an arbitrary time–varying wave source, propagating on an arbitrary shear current

In this section we present a theoretical framework for calculating waves from arbitrary wave sources on the surface, in flows with arbitrary dispersion relation $\omega(\mathbf{k})$, affected by sub-surface currents that may vary both with depth and direction. To our knowledge no theory this general has ever been presented. As a special case the theory provides a procedure for calculation and analysis of ship waves on arbitrary horizontal shear currents.

From the linearised Euler equations and continuity equation in $\mathbf{k}$-space we have the relations (cf. e.g. the pro-

cedure of [19])

$$(\partial_t + \mathrm{i}\mathbf{k}\cdot\mathbf{U})w'(z,t) - \mathrm{i}\mathbf{k}\cdot\mathbf{U}'w(z,t) = -k^2 p(z,t)/\rho, \tag{3a}$$

$$(\partial_t + \mathrm{i}\mathbf{k}\cdot\mathbf{U})w(z,t) = -p'(z,t)/\rho, \tag{3b}$$

where a prime denotes differentiation with respect to z, and the dependence on $\mathbf{k}$ of p and w is suppressed here and henceforth.

2.1. General form of surface wave dispersion relation

We will now present a general, implicit form of the dispersion relation for a waves atop a general depth–dependent shear flow $\mathbf{U}(z)$. The relation allows us to derive general expressions for surface waves from an arbitrary surface source in Section 2.2. Determining $\omega(\mathbf{k})$ for a specific situation is the topic of Section 2.3.

We use the physical values $\omega_\pm(\mathbf{k})$ to express the surface elevation for a given $\mathbf{k}$-component as:

$$\zeta(\mathbf{k},t) = Z_+(\mathbf{k})\mathrm{e}^{-\mathrm{i}\omega_+ t} + Z_-(\mathbf{k})\mathrm{e}^{-\mathrm{i}\omega_- t} \tag{4}$$

where $Z_\pm$ are unknown coefficients to be determined. Also the other perturbed quantities u, v, w and p will have time dependence $\propto \exp(-\mathrm{i}\omega_\pm t)$.

If the values of $Z_\pm$ are known from initial conditions, the full time dependent solution to the free surface elevation can be found from (4).

The phase velocities $\omega_+(\mathbf{k})/k$ and $\omega_-(\mathbf{k})/k$ correspond to partial waves propagating in directions $\mathbf{k}$ and $-\mathbf{k}$, respectively. They satisfy the relation

$$-\omega_-(\mathbf{k}) = \omega_+(-\mathbf{k}). \tag{5}$$

Hence there is a unique, positive phase velocity $\omega_+(\mathbf{k})$ in propagation direction $\mathbf{k}$, and the integral over all $\mathbf{k}$ effectively accounts for each mode twice. The relation (5) is general and holds for any shear current. We show in Appendix A.1 that the dispersion relation for a plane wave of small amplitude on a depth–dependent flow may be written

$$\Delta_R(\mathbf{k},\omega) \equiv (1+I_g)(\omega - \mathbf{k}\cdot\mathbf{U}_0)^2 + (\omega - \mathbf{k}\cdot\mathbf{U}_0)\mathbf{k}\cdot\mathbf{U}_0' \tanh kh/k - gk\tanh kh = 0, \tag{6}$$

where Δ_R is defined for later reference, and

$$I_g(\mathbf{k}) = \int_{-h}^{0} \mathrm{d}z \frac{\mathbf{k}\cdot\mathbf{U}''(z) w(z,0)\sinh k(z+h)}{k[\mathbf{k}\cdot\mathbf{U}(z)-\omega]w(0,0)\cosh kh}. \tag{7}$$

The implicit dispersion relation (6) is extremely useful for analytical purposes. It is not itself closed, since both $\omega(\mathbf{k})$ and $w(z,t)$ are unknowns. The two roots of the equation $\Delta_R = 0$ are $\omega = \omega_\pm(\mathbf{k})$. It is found e.g. in [20] that the zeros of Δ_R are simple, hence Eq. (6) may be written on the form

$$\Delta_R(\mathbf{k},\omega) = (1+I_g)(\omega-\omega_+)(\omega-\omega_-) = 0. \tag{8}$$

2.2. Waves from an arbitrary, time-dependent pressure distribution

We wish to find a solution to the surface pattern resulting from a time-dependent externally applied pressure distribution $\hat{p}_{\mathrm{ext}}(\mathbf{r},t) \leftrightarrow p_{\mathrm{ext}}(\mathbf{k},t)$ at the free surface.

The pressure, when positive, depresses the water surface thus modelling a moving wave source such as a ship. Using an applied surface pressure as wave source rather than e.g. potential theory with submerged sources such as are often used in the theory of ship motions [21], is advantageous since only the boundary conditions are directly affected. This is necessary in our system, since the flow we consider is inescapably rotational and potential theory is inapplicable.

By superposition, the response $G(\mathbf{k},t)$ of the system to an arbitrary time-dependent pressure distribution can be expressed as a time-integral of pressure pulses emitted at all previous times,

$$G(\mathbf{k},t) = \int_{-\infty}^{t} \mathrm{d}\tau p_{\mathrm{ext}}(\mathbf{k},\tau) H(\mathbf{k},t-\tau). \tag{9}$$

$H(\mathbf{k},t-t_0)$ is the system's response to an impulsive pressure rate $p_I(t) = I\delta(t)$ which imparts a finite impulse to the surface during an infinitesimally short time. I equals unity in units of pressure. G and H physically may represent any of the perturbation quantities u, v, w, p or ζ. Mathematically H plays the role of a Green's function.

We now proceed to finding the response of the free surface to a pressure impulse. In Eq. (9) we let $G \to \zeta$, and the correspondng response function we call $H_\zeta(\mathbf{k},t)$. The full time evolution $\zeta(\mathbf{k},t)$ for $t>0$ is then calculated from (9) as

$$\zeta(\mathbf{k},t) = \int_{-\infty}^{t} \mathrm{d}\tau p_{\mathrm{ext}}(\mathbf{k},\tau) H_\zeta(\mathbf{k},t-\tau) \tag{10}$$

with H_ζ derived in the following, given in (17).

The prescribed impulsive pressure enters the equation system via the dynamic free surface boundary condition, which can be written

$$\mathrm{i}\mathbf{k}\cdot\mathbf{U}_0' w - (\partial_t + \mathrm{i}\mathbf{k}\cdot\mathbf{U}_0)\, w' - k^2 g\zeta = k^2 I\delta(t)/\rho. \tag{11}$$

$$(\partial_t + \mathrm{i}\mathbf{k}\cdot\mathbf{U}_0)\,\zeta = w, \tag{12}$$

with w, w' evaluated at $z=0$. Here $\mathbf{U}_0$ is surface velocity, and a prime denotes differentiation with respect to z. Integration over an infinitesimal time interval $t = 0_-$ to 0_+ yields the following relations for $w(z,t)$ and $\zeta(t)$,

$$w'(0,0_+) = -k^2 I/\rho, \tag{13a}$$

$$\zeta(0_+) = 0, \tag{13b}$$

$$\dot{\zeta}(0_+) = w(0,0_+), \tag{13c}$$

using the assumptions that the system is completely at rest for $t<0$ and that all physical quantities have finite values at $t>0$, at $t=0_+$ in particular. We suppress the dependence of w and ω on $\mathbf{k}$ in this subsection.

When a current of arbitrary depth–variation is present, the primary challenge is that analytical expressions for $\omega_\pm(\mathbf{k})$ and $w(z,t)$ cannot be found. We show in Appendix A.1 the relations

$$w'(0,0_+) = k(1+I_g)w(0,0_+)\coth kh, \tag{14a}$$
$$= -\frac{\mathbf{k}\cdot\mathbf{U}_0'\tilde{\omega}+gk^2}{\tilde{\omega}^2}w(0,0_+), \tag{14b}$$
$$= \frac{k}{F(\mathbf{k})}w(0,0_+), \tag{14c}$$

where ω can be either of the roots of $\Delta_R = 0$, i.e. ω_+ or ω_-, and the intrinsic frequency is $\tilde{\omega} = \omega - \mathbf{k}\cdot\mathbf{U}_0$. Eq. (14c) defines the quantity $F(\mathbf{k})$ for later reference. We note that $F(\mathbf{k})$ can be written in several different forms,

$$F(\mathbf{k}) = \frac{kw(0,0_+)}{w'(0,0_+)} \tag{15a}$$
$$= \frac{\tanh kh}{1+I_g} \tag{15b}$$
$$= \frac{(\omega-\omega_-)(\omega-\omega_+)}{\Delta_R}\tanh kh \tag{15c}$$
$$= \frac{k\tilde{\omega}(\mathbf{k})^2}{gk^2 - \mathbf{k}\cdot\mathbf{U}_0'\tilde{\omega}(\mathbf{k})}. \tag{15d}$$

Which form of $F(\mathbf{k})$ is most convenient is different in different cases. The final form (15d) has the advantage that only the value of $\omega(\mathbf{k})$ is required when $\mathbf{U}(z)$ is known.

From (4), (13) and (14) then follows

$$Z_+ + Z_- = 0; \tag{16a}$$
$$\omega_+ Z_+ + \omega_- Z_- = -\mathrm{i}IkF(\mathbf{k})/\rho \tag{16b}$$

Solving for $Z_\pm$ and inserting into (4) yields the surface elevation H_ζ from an impulsive pressure pulse as

$$H_\zeta(\mathbf{k},t) = \frac{\mathrm{i}kF(\mathbf{k})}{2\rho\omega_{\mathrm{div}}(\mathbf{k})}(\mathrm{e}^{-\mathrm{i}\omega_- t} - \mathrm{e}^{-\mathrm{i}\omega_+ t}), \tag{17}$$

where the "divergence frequency" is, using (5),

$$\omega_{\mathrm{div}}(\mathbf{k}) = \frac{1}{2}[\omega_+(\mathbf{k}) - \omega_-(\mathbf{k})] = \frac{1}{2}[\omega_+(\mathbf{k}) + \omega_+(-\mathbf{k})], \tag{18}$$

so that ω_{div}/k is the phase speed with which oppositely propagating waves move apart.

2.2.1. Suddenly appearing ship

As a step towards modelling a ship during manoeuvring or acceleration in a simple manner, we consider the special case where p_{ext} is constant for $t > 0$ and zero at $t < 0$, i.e., a "ship" that is launched at $t = 0$ already having its final velocity and continuing in steady motion thereafter. This is the system considered long ago by Havelock [12]. It is an artificial situation, but one which can be used as a building block to model more realistic situations. Turning the arrow of time yields instead a suddenly disappearing ship, and adding at the same instance the appearence of the same ship but with a slightly different velocity, say, is a simple model of a rapidly turning and/or accelerating ship. In numerical examples we will consider the more realistic case of a suddenly starting ship.

We use a reference frame following the ship, so that the motion of the ship relative to the water surface is contained in the surface current velocity $\mathbf{U}_0$ as measured in this system. The time integral in (10) can be solved explicitly, and ζ splits naturally into a steady and a transient contribution

$$\hat{\zeta}(\mathbf{r},t) = \lim_{\epsilon\to 0}[\zeta_s(\mathbf{r}) + \zeta_t(\mathbf{r},t)], \tag{19a}$$
$$\hat{\zeta}_s(\mathbf{r}) = \frac{1}{\rho}\int \frac{\mathrm{d}^2k}{(2\pi)^2}\frac{kp_{\mathrm{ext}}(\mathbf{k})F(\mathbf{k})}{(\omega_+ - \mathrm{i}\epsilon)(\omega_- - \mathrm{i}\epsilon)}\mathrm{e}^{\mathrm{i}\mathbf{k}\cdot\mathbf{r}}, \tag{19b}$$
$$\hat{\zeta}_t(\mathbf{r},t) = \frac{1}{\rho}\int \frac{\mathrm{d}^2k}{(2\pi)^2}\frac{kp_{\mathrm{ext}}(\mathbf{k})F(\mathbf{k})\mathrm{e}^{\mathrm{i}\mathbf{k}\cdot\mathbf{r}}}{2\omega_{\mathrm{div}}(\mathbf{k})} \times\left(\frac{\mathrm{e}^{-\mathrm{i}\omega_+ t}}{\omega_+ - \mathrm{i}\epsilon} - \frac{\mathrm{e}^{-\mathrm{i}\omega_- t}}{\omega_- - \mathrm{i}\epsilon}\right). \tag{19c}$$

Subscripts s and t denote stationary and transient, respectively. Upon splitting into ζ_s and ζ_t it was necessary to employ a radiation condition by adding a small imaginary part $-\mathrm{i}\epsilon$ to wave frequencies, whereby $\omega_\pm \to \omega_\pm - \mathrm{i}\epsilon$ (see, e.g., [10]) assuring that waves can only be radiated away from the source. Mathematically this moves the poles to complex values of $\mathbf{k}$, rendering the integrals definite. Physically, it introduces an arrow of time by implying the time–independent $\hat{\zeta}_s$ was "switched on" some time in the far past, and consequently likewise the transient contribution which exactly cancels the steady one for $t < 0$.

Given a value for $\omega_\pm(\mathbf{k})$ (using any of various approximation schemes described below), equation (10) now produces $\hat{\zeta}(\mathbf{r},t)$ at all times; the Fourier transform is taken as in equation (2), for example using a fast Fourier transform (FFT) algorithm.

2.2.2. Stationary ship waves

The simplest case is the classical situation of a ship which has been travelling at constant velocity for a long time. The wave pattern in this case is readily obtained from (10) when taking the limit $t \to \infty$, which yields

$$\hat{\zeta}(\mathbf{r}) = \hat{\zeta}_s(\mathbf{r}) = \lim_{\epsilon\to 0}\int \frac{\mathrm{d}^2k}{(2\pi)^2}\frac{kp_{\mathrm{ext}}(\mathbf{k})\tanh kh}{\rho\Delta_R(\mathbf{k},\omega+\mathrm{i}\epsilon)}\mathrm{e}^{\mathrm{i}\mathbf{k}\cdot\mathbf{r}}, \tag{20}$$

Using Δ_R on the form (8) is instructive. Transient waves described by (19c) vanish at large times $t \to \infty$, as will be further discussed in §2.2.3. Eq. (20) is exactly the expression for ship waves from a ship moving with velocity $-\mathbf{U}_0$ relative to the water surface, as derived in [10] (note that angle β differs by π from that of [10, 11]), generalised to the case of general dispersion.

Figure 3: Super-Gaussian model ship pressure distributions from Eq. (21). Aspect ratios (left to right) $W = 3, 5, 8$.

2.2.3. Suddenly starting ship: wave patterns and asymptotics

We consider now the model of a ship which starts suddenly from rest. Formally this situation is created from the "suddenly appearing ship" model in Section 2.2.1 by superposing the ring wave from a ship at rest suddenly disappearing at $t = 0$, and reappearing in the same instance with velocity $\mathbf{U}_0$ relative to the water surface.

As a simple model "ship" we use an elliptical super-Gaussian pressure distribution with length L and beam (width) b of the form

$$p_{\text{ext}}(\mathbf{r}, t) = p_0 \exp\left\{-\pi^2 \left[(2x_\beta/L)^2 + (2y_\beta/b)^2\right]^3\right\}, \quad (21)$$

where

$$x_\beta(t) = [x - x_0(t)]\cos\beta(t) + [y - y_0(t)]\sin\beta(t), \quad (22a)$$
$$y_\beta(t) = -[x - x_0(t)]\sin\beta(t) + [y - y_0(t)]\cos\beta(t) \quad (22b)$$

expressed along the major and minor axes of the ellipse in a reference system (e.g. relative to the water surface) where the ship's position may be time–dependent. In a reference system fixed on the ship, $x_0 = y_0 = 0$ and $[x_\beta, y_\beta] = r[\cos(\varphi - \beta), \sin(\varphi - \beta)]$. The Froude number is $\text{Fr} = |\mathbf{U}_0|/\sqrt{gL}$. The super-Gaussian is a fairly realistic model of the submerged part of a hull shape, while avoiding having to specialise to a particular type of hull. Model "ship" pressure distributions for some aspect ratios are shown in Fig. 3.

When first set in motion, the ship creates an initial ring wave which propagates away. After some time the transient ring wave, ζ_t, has disappeared from sight and only a stationary ship wave pattern behind the travelling ship, ζ_s, remains. This is clear from Fig. 4, where the wave patterns are shown for increasing times after appearence, for different directions of motion atop a linear shear profile in deep water.

For large times the transient surface wave $\hat{\zeta}_t$ at some point far from the origin will vanish as $t^{-1/2}$. This can be shown rigorously with path integral methods and the stationary phase approximation, but is also physically clear from noting that the full transient wave energy will eventually radiate through any circular surface of radius R, and wave energy must thus fall off as $R_r(r)^{-1}$ for a ring wave of radius $\sim R_r$. Since wave energy of each Fourier mode moves outward in the far-field at a constant, k-dependent group velocity, $R_r \sim c_g t$, and since wave energy is $\propto \hat{\zeta}^2$, the time dependence $\hat{\zeta}_t \sim t^{-1/2}$ follows for large t.

2.3. Practical calculation techiques for arbitrary velocity profiles

To calculate the surface elevation (10) one needs to find the roots $\omega_\pm(\mathbf{k})$ of (6), which is itself not closed since both ω and $w(z)$ are unknowns. Analytical results are in general not available, except for the simplest current varying linearly with depth. There are several numerical or semi–analytical techniques that allow calculation of $\omega_\pm(\mathbf{k})$ for an arbitrary $\mathbf{U}(z)$ which we briefly review in this section.

2.3.1. Simplest case: linear profile

Consider first the simplest case of a linearly depth–dependent current. This is the only known case where an explicit, analytical dispersion relation is available for all $\mathbf{k}$. This idealised case is therefore instructive for analysis since analytical results can be derived.

To calculate ship waves during steady motion, say, one might work in a frame of reference where the model ship is at rest, and the ship's velocity relative to the water surface is $-\mathbf{U}_0$ where $\mathbf{U}_0 = [U_0, V_0] = |\mathbf{U}_0|[\cos\beta, \sin\beta]$ (see also Fig. 2). The current is unidirectional, i.e., $\mathbf{U}(z) = \mathbf{U}_0 + Sz\mathbf{e}_x$. (This corresponds a ship moving in direction $\beta + \pi$ relative to the water surface.) We define [11]

$$\text{Fr}_s = \frac{|\mathbf{U}_0|S}{g}. \quad (23)$$

For the linear shear profile one obtains [25, 26]

$$\omega_\pm = \omega_1 \pm \sqrt{\omega_1^2 + \omega_2^2}; \quad (24a)$$
$$\omega_1 = \mathbf{k}\cdot\mathbf{U}_0 - \tfrac{1}{2}S\tanh kh\cos\theta; \quad (24b)$$
$$\omega_2^2 = (S\cos\theta\mathbf{k}\cdot\mathbf{U}_0 + gk)\tanh kh - (\mathbf{k}\cdot\mathbf{U}_0)^2, \quad (24c)$$

hence $\omega_+\omega_- = -\omega_2^2$, and

$$\omega_{\text{div}} = \sqrt{gk\tanh kh + (S\tanh kh\cos\theta/2)^2}. \quad (25)$$

Since $I_g = 0$ when $\mathbf{U}''(z) = 0$, (15b) simply gives $F(\mathbf{k}) = \tanh kh$. Determining F and $\omega_\pm$ is sufficient for calculating all cases considered above, the most general case being (10) with (17).

2.3.2. The piecewise–linear approximation

A useful numerical scheme to this end is the piecewise–linear approximation (PLA), which was analysed in depth in [20], and which we will use herein to obtain numerical results. As described herein the PLA is restricted to unidirectional $\mathbf{U}(z)$; extension to shear currents changing direction is relatively straightforward. Alternative approximations to the dispersion relation are thereafter briefly discussed in section 2.3.3.

The piecewise–linear approximation (PLA), sometimes called the $N-$layer model, utilises the fact that explicit solutions are available when the velocity profile is linear as discussed above. A smooth velocity profile $u(z)$ is approximated by a series of linear segments inside N artificial

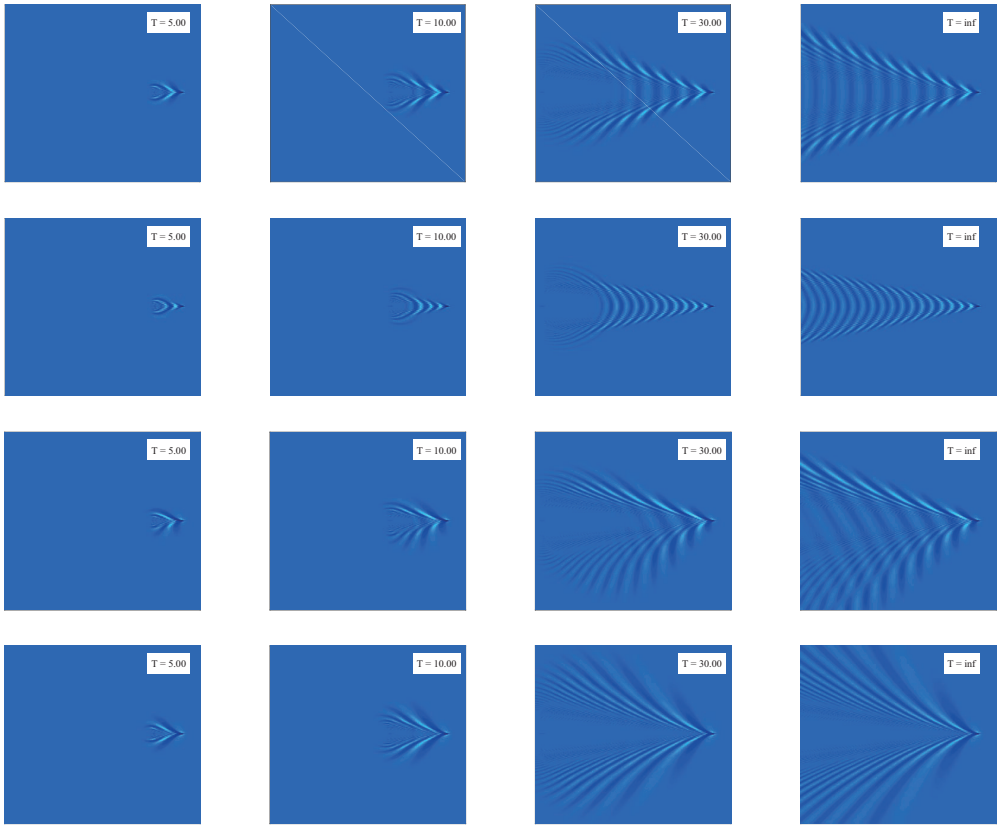

Figure 4: Wave patterns of model ship suddenly set in motion from rest at $T = 0$, at increasing nondimensional time $T = t\sqrt{g/L}$ where L is the ship length. The ship is modelled as a super–Gaussian of aspect ratio $L/b = 6$; see Eq. (21). First row: no shear; Second row: shear–assisted ($\beta = 0$); Third row: side–on shear ($\beta = \pi/2$); Fourth row: shear–inhibited ($\beta = \pi$). The shear Froude number is $\mathrm{Fr}_s = S|\mathbf{U}_0|/g = 0.8$ with $\mathbf{U}_0$ the ship velocity relative to the water surface. The reference system is relative to the ship, rotated so that ship motion is the same in all cases.

layers, allowing the solution to the vertical velocity to be expressed explicitly within each layer and matched at the artificial layer boundaries. We provide further details in Appendix A.2. Following the derivation process in [20], within the top layer the vertical velocity satisfies

$$w(\mathbf{k}, t) = A_1 \sinh k(z + h_1) + B_1 \cosh k(z + h_1), \quad \text{for} - h_1 < z < 0, \tag{26}$$

in which h_1 is the thickness of the top layer and A_1 and B_1 are coefficients depending on $\mathbf{k}$ and t, which are determined by the matching conditions at the $N - 1$ layer interfaces and from surface and bottom boundary conditions. Inserting (26) into the first form of $F(\mathbf{k})$ in (15a) yields

$$F(\mathbf{k}) = \frac{A_1 \sinh kh_1 + B_1 \cosh kh_1}{A_1 \cosh kh_1 + B_1 \sinh kh_1} \tag{27}$$

evaluated at $t = 0$.

The next essential step is to obtain solutions for $\omega_\pm$, exact or approximate, and to determine A_1 and B_1 via the PLA procedure [20]. The PLA is particularly suitable for problems which are solved in the Fourier plane since it provides a rapid and accurate solution to the dispersion relation $\omega(\mathbf{k})$ equally well for all wavelengths, converging to the exact value as N increases [20, 22]. For our numerical demonstrations we find that 4-5 layers are typically enough at the 1% accuracy level.

2.3.3. Alternative approximations to the dispersion relation

A simpler approach than the PLA can be obtained by evaluating $\omega_+(\mathbf{k})$ using an explicit, approximate dispersion relation. The accuracy of such approximations is not so easily predicted, however, and is different in different areas of the $\mathbf{k}$ plane. A much used approximation which is accurate to within a few percent for all $\mathbf{k}$ in many cases, is the relation by Kirby & Chen [23]

$$\omega_+(\mathbf{k}) \approx \omega_0(k) + \int_{-h}^{0} \mathrm{d}z \frac{2\mathbf{k}\cdot\mathbf{U}(z)\cosh 2k(z+h)}{\sinh 2kh} \quad (28)$$

where h is the total depth of the flow and $\omega_0 = \sqrt{gk\tanh kh}$ (note that this 3D generalization of the Kirby & Chen expression also allows the direction of $\mathbf{U}$ to vary with z). The approximate value for $\omega_+(\mathbf{k})$ is inserted into equations (10) via (15d).

We recently made progress on the question of analytical approximations to dispersion relations, deriving error estimates for (28) and also presenting a more robust alternative to (28) in Ref. [24]. Two of us (YL & SÅE) have also developed and implemented another numerical method, a simple and promising alternative to the PLA based on direct integration of (3a) and (6) (manuscript in preparation).

2.4. Transient wave resistance and radiation force

A travelling ship imparts momentum to the water around it to create waves, giving rise to a wave radiation force acting on the ship in the opposite direction. In the absence of shear the wave radiation force always points sternwards for ships in rectilinear motion, and is called wave resistance, or wave–making resistance. Wave resistance typically accounts for more than 30% of the energy consumption of ocean going vessels [1].

We work in a reference frame where the ship is at rest, and the water surface moves at velocity $\mathbf{U}_0$ as shown in Fig. 2. Following Havelock [12] the wave radiation force created by a travelling pressure distribution is the force exerted by the external pressure $\hat{p}_{\mathrm{ext}}(\mathbf{r},t)$ acting on vertical projections of the moving surface $\hat{\zeta}(\mathbf{r},t)$. The force along unit vector $\mathbf{e}_f$ acting on horizontal area d^2r at $\mathbf{r}$ is thus

$$\mathrm{d}f(\mathbf{r},t) = \hat{p}_{\mathrm{ext}}(\mathbf{r},t)(\mathbf{e}_f\cdot\nabla)\hat{\zeta}(\mathbf{r},t)\mathrm{d}^2r. \quad (29)$$

A ship travelling at an oblique angle with a sub-surface shear current will in general radiate waves asymmetrically around its line of motion, and the radiation force will consequently have both a sternward and a lateral component. The two components are derived with the methods laid out in [10], to yield

$$\begin{aligned} \begin{matrix} R_\parallel(t) \\ R_\perp(t) \end{matrix} &= -\frac{1}{U_0}\int \mathrm{d}^2r\hat{p}_{\mathrm{ext}}(\mathbf{r},t)\begin{pmatrix}\mathbf{U}_0\\ \mathbf{e}_z\times\mathbf{U}_0\end{pmatrix}\cdot\nabla\hat{\zeta}(\mathbf{r},t) \\ &= -\mathrm{i}\int\frac{\mathrm{d}^2k}{(2\pi)^2}\begin{pmatrix}k\cos\gamma\\ k\sin\gamma\end{pmatrix}p^*_{\mathrm{ext}}(\mathbf{k},t)\zeta(\mathbf{k}) \end{aligned} \quad (30)$$

where an asterisk denotes the complex conjugate and $\parallel$ and $\perp$ denote sternward resistance and lateral radiation force towards starboard (towards the right), respectively.

The transient radiation forces may thus be evaluated by inserting $\zeta_t(\mathbf{r},t)$ from (19c) into (30), giving

$$\begin{matrix} R_{\parallel,t}(t) \\ R_{\perp,t}(t) \end{matrix} = -\frac{\mathrm{i}}{8\pi^2\rho}\lim_{\epsilon\to 0}\int_{-\pi}^{\pi}\mathrm{d}\gamma I(\gamma,t); \quad (31a)$$

$$I(\gamma,t) = \int_0^\infty \mathrm{d}k\frac{k^3|p_{\mathrm{ext}}(\mathbf{k},t)|^2F(\mathbf{k})}{\omega_{\mathrm{div}}(\mathbf{k})}\begin{pmatrix}\cos\gamma\\ \sin\gamma\end{pmatrix} \times\left(\frac{\mathrm{e}^{-\mathrm{i}\omega_+t}}{\omega_+-\mathrm{i}\epsilon}-\frac{\mathrm{e}^{-\mathrm{i}\omega_-t}}{\omega_--\mathrm{i}\epsilon}\right). \quad (31b)$$

Expressing radiation forces in the form (31a) is useful for analytical purposes. For numerical purposes we use (30) more directly using a fast Fourier transform (FFT) method.

The static part of the wave resistance is obtained by inserting ζ_s into (30). We refer to [10] for further details on the evaluation of the static part of the wave resistance.

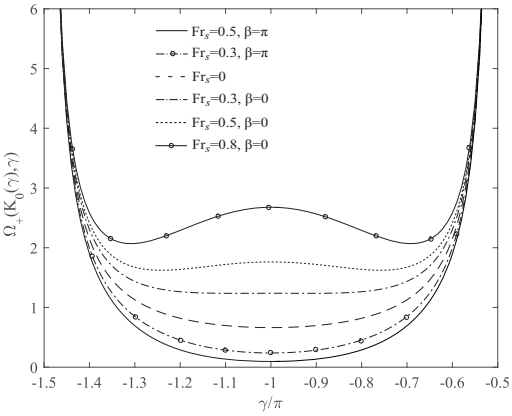

Figure 5: The intrinsic wave frequency $\tilde{\omega}_+(k_0(\gamma),\gamma)$, in units of $\sqrt{L/g}$, which solves the dispersion relation in direction γ under different conditions of a linear shear profile.

2.4.1. Wave resistance oscillations

The transient behaviour of the wave resistance after the ship is set in motion, is to oscillate around its ultimate static value, at a frequency which varies greatly with direction or motion as well as shear strength. We will now explain what decides the oscillation frequency.

The integral (31b) is given solely by the contribution from the poles (infinitesimally close to) where $\omega_\pm(\mathbf{k})$ are zero. Since $\omega_+(\mathbf{k})$ and $\omega_-(\mathbf{k})$ are related through relation (5), and we are free to replace $\mathbf{k}\leftrightarrow-\mathbf{k}$ under the integranl sign, considering the zeros of the positive frequency $\omega_+(\mathbf{k})$ is sufficient. Taking the k integral first as written out in (31a), the pole picks out a value $k_0(\gamma)$ so that

$$\omega_+(k_0(\gamma),\gamma) = 0. \quad (32)$$

Thus the particular frequency is picked out which satisfies the dispersion relation, which is to say that only waves which are able to propagate towards infinity along direction γ may contribute to the wave resistance.

When t grows large (while keeping r constant), the exponential factor $\exp[-\mathrm{i}\omega_+(k_0(\gamma),\gamma)t]$ in the integrand of (31b), and is therefore dominated by the contribution from the value of γ where the phase is stationary, that is, the value of γ where

$$\partial_\gamma \omega_+(k_0(\gamma),\gamma) = 0. \tag{33}$$

Some time after $t = 0$, the transient contribution to the wave resistance will therefore oscillate in time with the frequency of a stationary point, a maximum or minimum of $\omega_+(k_0(\gamma),\gamma)$ with respect to γ.

Let intrinsic frequencies be denoted with a tilde,

$$\tilde{\omega} = \omega - \mathbf{k}\cdot\mathbf{U}_0. \tag{34}$$

For the case of a linear shear current, we plot $\tilde{\omega}_+(k_0(\gamma),\gamma)$ in units of $\sqrt{g/L}$ as a functon of γ in Fig. 5; L is a characteristic length of the wave disturbance to be specified in particular examples below. We see that in all cases there is a stationary point at $\gamma = -\pi$. In the most shear–assisted direction ($\beta = 0$), this frequency is enhanced compared to no shear, giving a faster oscillation of the wave resistance, whereas the opposite is the case in the maximally shear inhibited direction ($\beta = \pi$), where the oscillation can become very slow. For shear–assisted motion there are also two other stationary phase points at angles either side of $\gamma = \pi$, as is evident in Fig. 5. Notably, the presence of shear which inhibits motion can dramatically decrease the oscillation frequency compared to still water, even at moderate shear.

3. Numerical results

In this section we present numerical calculations of transient wave resistance on different model ships. While retaining generality by not specialising to particular real hull shapes, we have emphasised realism: a reasonably realistic model is used for the shape of the ship hull, and calculations are performed for a real velocity profile measured in the Columbia River estuary, where there is high traffic of vessels of many types. Parameters for vessel length and beam are taken from real ships known to travel in these waters.

The choice of the Columbia River delta for our data is primarily due to the excellent shear profile data available [27], although the loacation is also particularly apt for studies of ship wave effects. Thousands of ships ranging from carrier ships of more than 1000 ft to small boats, are piloted up and down the Columbia river each year, in waters which are considered particularly trecherous, sometimes referred to as the Graveyard of the Pacific.

Following [10, 9] we plot wave resistance relative to the constant

$$R_0 = \frac{p_0^2}{2\pi^3\rho g}.$$

3.1. Linear velocity profile

In order to better highlight the underlying physics of the effect of shear on wave resistance, we begin by considering the simplest shear flow, which varies linearly as a function of depth, $U(z) = U_0 + Sz$. Realistic shear profiles are considered in Section 3.2.

3.1.1. Suddenly starting ship

For the simplest, linearly varying velocity profile considered in section 2.3.1 we calculate the transient wave resistance for a ship modelled as in equation (21), whose velocity goes suddenly from zero to a constant value V. While idealised, this models a starting ship without the need for further parameterisation of the acceleration phase. An example of what the transient wave resistance looks like is shown in figure 6. The model ship is elliptical with aspect ratio 6 and length $L = 1$ (arbitrary units since the problem is intrinsically scale–free), and calculation is performed for $\mathrm{Fr} = 0.3$ and shear strengths varying from $\mathrm{Fr}_s = 0$ to 0.8.

The oscillation frequencies of the transient wave resistance are found to agree well with the stationary phase values of $\omega_+(k_+(\gamma),\gamma)$ in figure 5 as expected.

The transient wave resistance is seen to go through a sharp peak shortly after the ship is set in motion, and then relax in an underdamped manner towards its steady–motion value. For shear–assisted motion ($\beta = 0$), the initial peak can be much higher than its static value, whereas this effect is weaker in the case without shear ($\mathrm{Fr}_s = 0$) and for shear–inhibited ship motion. Letting the shear vary from strongly inhibiting (high Fr_s, $\beta = \pi$) via no shear to fairly strongly assisting, we see that the transient oscillations increase both in amplitude and frequency, whereas the static wave resistance decreases. An interesting observation is that for very strongly motion-assisting current ($\mathrm{Fr}_s = 0.8$ in this case), the total wave resistance can actually be negative during some time intervals, since oscillation amplitudes are large and the static wave resistance correspondingly small.

Both the difference in oscillation frequency and the magnitude of the steady motion wave resistance can be understood by considering the relative values of phase velocity and group velocity in different directions of wave propagation. A detailed discussion of this may be found in Ref. [26]. For a linear shear current, where the dispersion relation (24) is known analytically, one finds that in a reference frame following the surface, the group velocity is quite similar in all directions of motion, whereas phase velocity can differ greatly. In shear–inhibited directions dispersion is weakened and an emitted wave group will retain its initial shape and width to a greater extent than in quiescent water. The opposite is the case for shear–assisted wave propagation; here the phase velocity can far

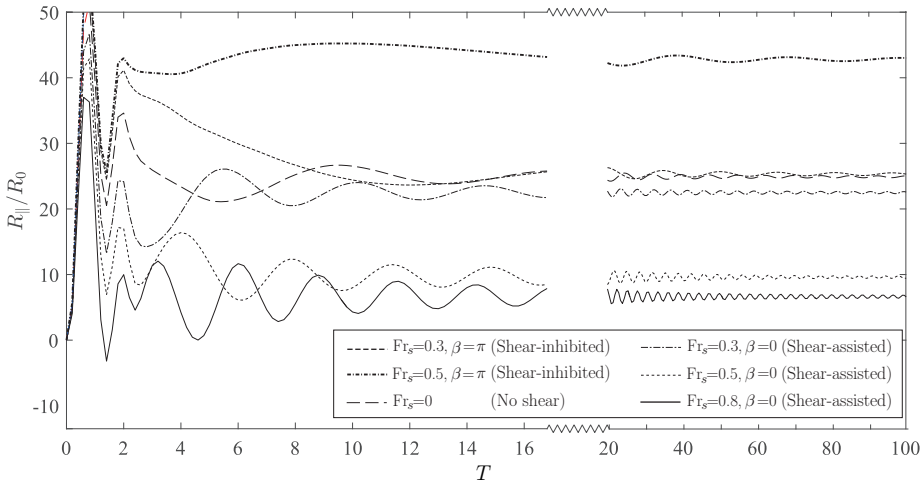

Figure 6: Transient wave resistance on a ship set suddenly in motion as a function of nondimensional time $T = t\sqrt{L/g}$, for different cases where a linearly depth-dependent shear current is present in deep water. The "ship" is modelled as an ellipsoidal, super-Gaussian surface pressure of aspect ratio 6 and $L = 1$ (arbitrary units), moving with Fr = 0.3. Note that the abcissa is scaled differently for $T > 20$. Note furthermore that $R_{\|}$ scales linearly with L, which is arbitrary in this scale–free system, hence so is the scaling of the ordinate axis.

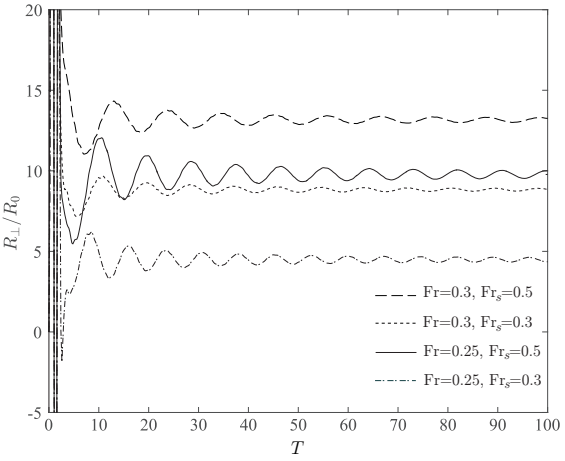

Figure 7: Same as Fig. 6, but for the transient lateral wave radiation force $R_{\perp}$, for motion normal to a the shear current in a reference frame following the water surface; $\beta = \pi/2$ (see Fig. 1). The scaling of the ordinate is arbitrary (see Fig. 6).

exceed group velocity, so wave groups quickly spread and have a rapidly changing, volatile appearence.

When the ship suddenly starts, an initial ring wave is emitted, as seen in Fig. 4. Wave resistance will continue to oscillate for as long as this ring wave remains in the ship's near–zone. The fact that group velocity is fairly isotropic means that it takes approximately the same time for the ring wave to disappear from sight, matching the observation that the oscillations in Fig. 6 die off at a similar rate in all cases. The frequency of oscillation, however, depends on the phase speed of the transient waves *within* the ring wave group, and the higher phase velocity for shear–assisted propagation means faster oscillations, as also observed in Fig. 6, and explained in connection with Fig. 5.

Finally, we found in Ref. [10] that the effect on shear on wave resistance is, in a rough sense, to effectively change the Froude number to a value based on the ship velocity relative to some depth–average current speed rather than its surface value. The Froude number is effectively lowered in shear–assisted motion, and increased in shear–inhibited motion. A detailed discussion is found in section 3.2.1 where we compare a real velocity profile to a linear approximation in this respect. Since the general trend is that wave resistance increases with increasing Fr for Fr ~ 0.3, this explains why the resistance in steady motion is typically decreased for shear–assisted motion and increased for shear–inhibited motion. However, this does not always hold true, due to interference effects between waves from bow and stern.

We go on to calculate the transient lateral radiation force for the same ship, shown in Fig. 7. The Froude numbers 0.25 and 0.3 are chosen as realistic examples. The ship motion is now across the shear current, $\beta = \pi/2$ as defined in figure 1. For an aspect ratio of 6 the lateral force is roughly half the magnitude of the sternward force. We find the relative magnitude of lateral to sternward force to vary strongly with Froude number and aspect ratio, as indicated for the former case by the large effect of lowering Fr from 0.30 to 0.25.

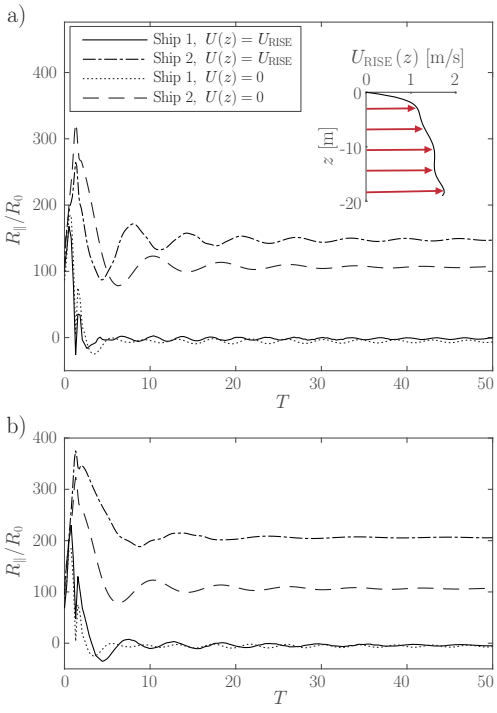

Figure 8: Transient wave resistance for motion in the shear assisted (a) and inhibited (b) directions atop the measured current in the Columbia River delta, as a function of nondimensional time $T = t\sqrt{g/L}$. Three ships are modelled with equation (21) with dimensions as given in Table 1. The wave resistance in quiescent waters is shown for comparison. Inset to (a): measured Columbia River velocity profile $U_{\mathrm{RISE}}(z)$ [27] approximated with a 6th order polynomial, in a reference frame moving with the surface current. The legend applies to both a) and b).

3.2. General, realistic velocity profiles

We now compute the transient wave resistance using a real, measured velocity profile. The shear current is that measured by the RISE project, a tidal current in the mouth of the Columbia River [27][1]. Buoyant fresh water from the river creates a strong surface jet as it enters the salt water of the Pacific Ocean. We approximate the measured data with a 6th order polynomial which is then subjected to the piecewise-linear procedure to calculate the dispersion relation numerically, as described in section 2 and detailed in Appendix A.2. The current profile $U_{\mathrm{RISE}}(z)$ in a reference frame where the surface current is zero is shown in the inset of figure 8a. We model various ships using Eq. (21) with dimensions L (length) and b (beam) representative of typical vessels traveling at the Columbia River mouth, tabulated in Table 1.

[1]Since measurements begin at 2m depth, we presume this point to be at the surface, thus offsetting all data by 2m. This should be a conservative procedure since shear strength increases closer to the surface.

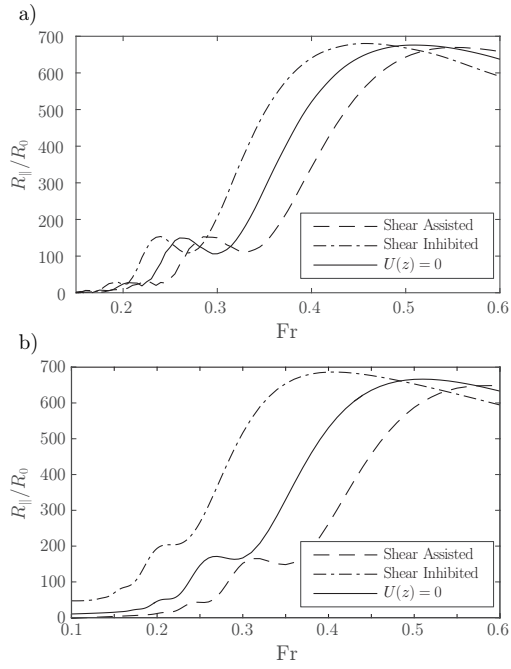

Figure 9: Wave resistance force in steady motion for Ship 2 (tugboat) as a function of Froude number for the maximally shear assisted ($\beta = 0$) and inhibited ($\beta = \pi$) directions of motion. a) The Columbia River velocity profile, b) Linearly varying profile $U(z) = U_0 + Sz$ with $\mathrm{Fr}_s \equiv U_0 S/g = 0.4$.

3.2.1. Suddenly starting ship

Results for transient sternward wave resistance for a ship starting suddenly in maximally shear-assisted and shear-inhibited directions of motion (corresponding to upstream and downstream motion in the Columbia delta, respectively) are shown in figure 8. Two ships are modelled, a bulk carrier ship, and a smaller vessel typical of a tugboat; Ships 1 and 2 in Table 1, respectively. The wave resistance in quiescent waters is shown for comparison.

ID	Ship Type	Length L [m]	Beam b [m]	Speed [Knots]	Aspect ratio
1	Bulk carrier	170	28	11.9	6.07
2	Tugboat	32	10.4	10.3	3.08
3	Fishing boat	19	6	8.0	3.17

Table 1: Parameters of the modeled ships, chosen as representative dimensions from boat traffic on the Columbia River. Real-time data on vessels in these waters is available at http://www.columbiariverbarpilots.com. Froude numbers for ships $1, 2, 3$ are $0.15, 0.3$ and 0.3, respectively.

The behaviour of the smaller ship ('Ship 2') is similar to that observed for the simple linear shear current, with wave resistance exhibiting a sharp peak shortly after the ship is set in motion, whereupon it relaxes in an underdamped way to the steady motion value with a frequency which is higher for shear assisted than for shear inhibited motion. Fluctuations are stronger for shear assisted (upstream) motion as was also noted in Fig. 6, and amount to transient variations in the order of 10% of the static value in this case. The wave resistance of the larger vessel ('Ship 1') approaches an insignificantly small value at large times, attributed to the lower Froude number (0.15) for this modelled vessel.

The most interesting observation made in Fig. 8 might concern the steady motion value of wave resistance. Untypically, wave resistance is increased compared to quiescent waters both for shear–assisted and shear–inhibited ship motion. This appears to run counter to lessons learned from a previous, much simpler and less realistic model study [10], where shear–assisted motion was always found to decrease wave resistance in this Froude number range. The reason is that our present, more realistic ship model (21) has a sharper bow and stern than the circular "ship" considered in [10], leading to interference effects between bow and stern waves such as are found for real ships. Indeed these interferences must be taken into account when choosing optimal operational speed in ship design [28]. We plot the Froude number dependence of the steady motion wave resistance for different Fr for the Colubia current profile in Fig. 9a for the tugboat (Ship 2). The plot clearly demonstrates that wave resistance in steady motion depends very strongly on direction and Froude number. Fr = 0.3, the speed of Ship 2 in Fig. 8, is a special case where shear increases wave resistance in both directions. Increasing the velocity a little to Fr = 0.33, a very different conclusion is reached: here, shear-inhibited wave resistance (ship travelling downstream) is more than a factor 3 greater than in the opposite direction.

Corresponding results for the lateral radiation force for motion across the shear current ($\beta = \pi/2$, measured in a reference frame in which the water surface is at rest) is shown in figure 10 for the three different ships in Table 1. In order to make the values comparable, we divide the force by the length of the ship. The lateral radiation force shows similar oscillations for short times as the sternward resistance in Fig. 8a, with the exception of the large carrier ship (Ship 1) which displays far stronger transient oscillations initially. Indeed, while the sternward resistance force is likely to be negligible for Ship 1, this needs not be the case for the early transient shortly after start.

In Fig. 10b we show the lateral radiation force relative to the sternward resistance force for cross–current motion, for Ships 2 and 3. The relative strength has very weak oscillations, but a highly conspicuous trait is how the relative strength of the transient force is more than twice as strong just after appearance of the "ship" compared to its asymptotic value, about $50-60\%$ percent of the transient sternward force at the time of the initial peak that is present in both force components. Again this indicates that the transient behavior of the lateral force could well have a bearing on seakeeping performance during manoeuvering, when transient waves will be emitted by the ship. We note furthermore that when stationary conditions have been reached, the radiation force is approximately 20% of the sternward component. This is a significant laterally directed force which must be compensated by steering (it is not to be confused, of course, with the lateral drag force which will also be present due to the shear flow between surface level and the ship's draught, a separate question not studied here. With no shear there is neither a net lateral drag nor radiation force when $\beta = \pi/2$.)

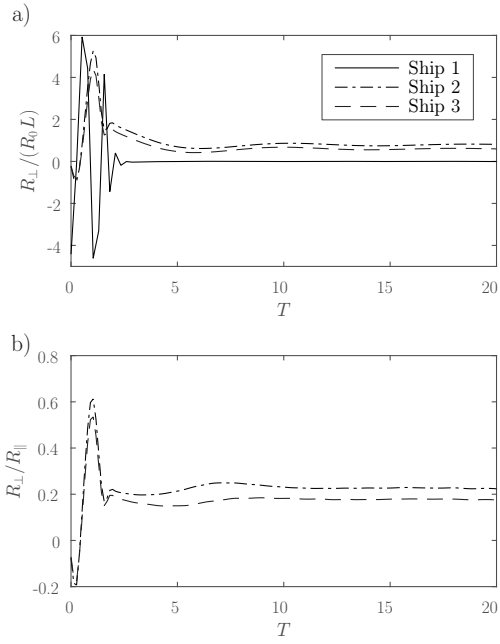

Figure 10: a) Transient lateral radiation force per unit ship length $R_\perp/(R_0L)$ for motion normal to the measured current in the Columbia River delta, in a reference system where the surface is at rest ($\beta = \pi/2$), as a function of nondimensional time $T = t\sqrt{g/L}$. Three ships are modeled using (21) with dimensions L and b and Froude number Fr as indicated. b) Transient lateral radiation force relative to transient wave resistance for the two smaller modeled ships. The legend applies to both a) and b).

The simplicity of working with the linearly dependent velocity profile as a model for a real current makes it tempting in practice to eschew the need to calculate $\omega(\mathbf{k})$ for a general shear flow, and instead approximate the real profile by a linear one with a representative constant shear. However, if we were to approximate the Columbia profile by a linear profile with a shear approximately that at the water surface — giving $\mathrm{Fr}_s \sim 0.4$ for our parameters — one could make a very great error in calculating the steady-motion wave resistance. In Fig. 9b we plot the

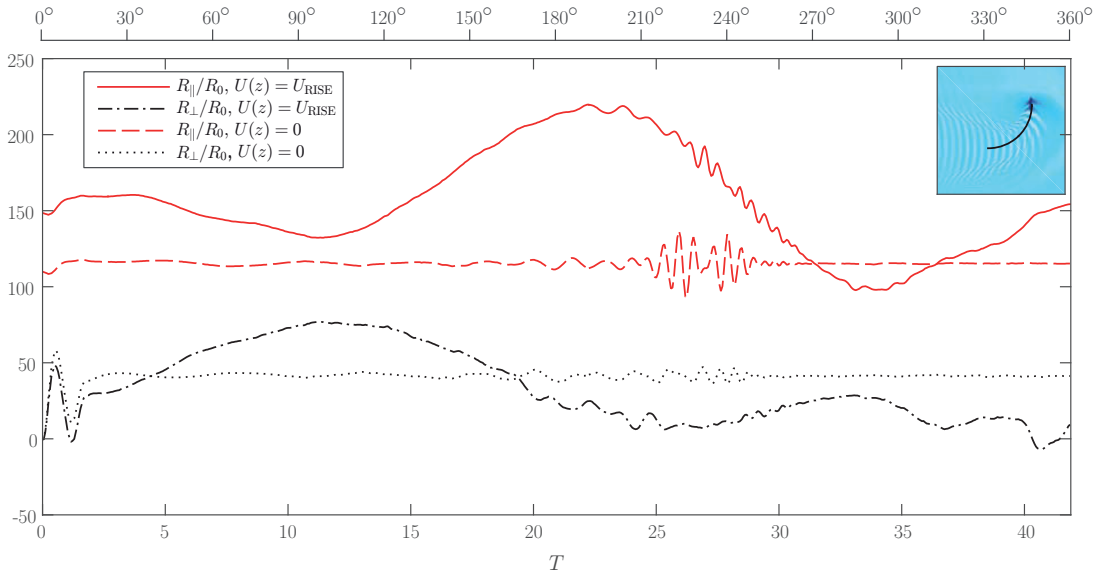

Figure 11: Transient wave resistance as a function of nondimensional time $T = t\sqrt{g/L}$ for a ship beginning a circular manoeuvring motion atop the measured shear current in the Columbia River delta. The ship dimensions are typical of a tugboat operating in these waters, 'Ship 2' in Table 1, initiating a turn of radius $4L$ at $T = 0$, from having traveled in a straight path in the shear–assisted direction (upstream). The path is circular thereafter, as seen in a reference system where the water surface is at rest. The angle the ship has turned is shown above the figure. The situation at 90° is shown in the inset for illustration. Also shown is the same manoeuvre in quiescent waters ($U(z) = 0$).

steady–motion wave resistance as a function of Fr using this model. It is clear that while the trend and general behaviour is similar, the rapid variation of $R_{\parallel}$ with Fr for $0.2 \lesssim \mathrm{Fr} \lesssim 0.4$ means the error can be several hundred percent. Clearly a better job can be made with a better choice of Fr_s, yet choosing a sufficiently good value in practice (if such exists) will require the use of knowledge of the full velocity profile and moreover be specific to each vessel. In our opinion this may not be any simpler nor numerically cheaper than a full calculation such as we have performed, and for which an effective calculation tool is already now developed.

We note, however, the possibility that a two–layer model might be a compromise which is the best of both worlds. In such a model a surface layer is given one constant shear value, and deeper waters another. It is well suited for modelling a surface shear layer due to wind or tides for many practical purposes. Such a model is analytically tractable while containing the key parameter of the vertical extent of the surface shear layer, whose relation to the ship length is a determining parameter. Analysis of such a model in the context studied here is beyond our present scope; the dispersion relation that can be used directly in the formalism of Section 2 may however be found in Ref. [29].

3.2.2. Turning ship

Analysis of a suddenly moving ship yields insight into transient wave resistance forces due to sudden changes in velocity along a straight course. It is of interest to consider another example of a ship manoeuvre; a turning motion. Figure 11 shows the wave resistance for a ship initially traveling along a straight path upstream in the Columbia River delta (shear–assisted direction), which begins a circular turning manoeuvre of radius $4L$ at $T = 0$. The forward velocity $\mathrm{Fr} = 0.3$ remains unchanged through the manoeuvre. We consider as example a typical tugboat operating in these waters, Ship 2 in Table 1. In order to given an impresson of all different directions of motion, we let the ship do a full 360° turn; a snapshot at 90° is shown in the inset. The same ship manoeuvre in quiescent waters is shown for comparison.

All graphs display certain oscillations at different times during the manoeuvre, due to the sudden change in lateral acceleration after $T = 0$, and later because the ship encounters its own previously emitted waves.

In quiescent water the lateral radiation force fluctuates around a constant value of, in this case, approximately $40R_0$ due to the now asymmetric wave field; another way of seeing it is that the turning ship must accelerate water towards the centre of the arc, resulting in an outwardly directed lateral added mass force. The sternward force without shear also fluctuates around a constant as it should. A different behaviour is observed for both force components, however, when the measured Columbia River shear current is present. Both resistance and lateral force vary greatly throughout, both peaking at around twice their quiescent

value, and the lateral force at times dropping to zero and even small negative values. For a ship to follow such a path with precision will thus require considerably greater skill than in quiescent water, having to account for the changing lateral and sternward forces. The lateral force can also reach more than 50% of the resistance force for a part of the circle with our parameters, typical of boat traffic in the area, by no means a small force in a manoeuvring context.

4. Conclusions

We have studied the wave radiation forces, including wave–making resistance, for different model ships in a real, measured current in the Columbia River delta. We calculate transient wave resistance on a "ship" modeled as a traveling pressure distribution in the form of an elliptic super–Gaussian. Choosing values of length/beam typical of smaller vessels (tugboats, fishing boats) we find that wave resistance can vary drastically depending on direction of motion, upstream or downstream, showing a strong dependence on Froude number. For typical Froude numbers — Fr $\sim$ 0.2 to 0.4 — we find that wave resistance can differ by more than a factor 3 between upstream and downstream motion. Appropriate choice of vessel velocity can thus make a large difference to resistance in strongly sheared waters.

When there is an oblique angle between the ship's line of motion and the shear current, the emitted ship wave pattern will be asymmetric, with more waves propagating to one side than the other. The total wave radiation (or wave–making) force then also has a lateral component. For our example model ships representative of tugboats or fishing boats, the lateral force was found to be approximately 20% of the sternward resistance force for a ship in steady motion.

We also study the transient behaviour of wave radiation forces acting on ships which change their velocity. As a simple example we consider ships that are set suddenly in motion. Both components of the wave radiation force undergo an initial peak as an initial ring wave is created, whereupon they oscillate in an underdamped manner towards their steady–motion values. For motion across the shear current the lateral force is found to have a stronger initial peak, and the lateral force momentarily reaches more than 50% of the value of the sternward force just after motion commences.

The general trend for typical small–ship operational Froude numbers is that compared to quiescent water, wave resistance decreases for upstream (shear–assisted) ship motion, and increases for downstream (shear–inhibited) motion, although interference effects between bow waves and stern waves can alter this for certain Froude numbers.

We also considered a circular manoeuvring motion atop the Columbia River current seen from a reference system following the water surface, for a small ship (tugboat). Unlike on quiescent water were both resistance and lateral force are constant through the motion (modulo small oscillations due to encountering the ship's own waves), these vary greatly through the circular path on the Columbia River mouth. Variations of amplitude of approximately 100% of the quiescent values of the forces are found. For a ship to follow such a path with precision will thus require considerably greater skill. The lateral force can also reach more than 50% of the resistance force for a part of the circle with our parameters, typical of boat traffic in the area.

The second main achievement reported in this manuscript is the development of a theory that allows calculation of waves from a general, time-dependent applied surface pressure acting on the surface of a horizontally directed shear current which may vary arbitrarily with depth in both direction and magnitude. We present a framework which provides the means to effectively calculate ship waves and wave resistance without undue difficulty. The theory is based on deriving the response of a water surface satisfying an arbitrary dispersion relation, to an impulsive applied pressure. The wave pattern is then calculated as the integral of emitted waves at all previous times. It is necessary to devise a scheme to obtain the dispersion relation numerically; in this paper we used the piecewise–linear approximation [20], but several other options are available.

Acknowledgements

SÅE is funded by the Norwegian Research Council (FRINATEK), project number 249740. We are grateful to Peter Maxwell for improvements to the PLA numerical code.

Appendix A. Derivation details

Appendix A.1. The implicit dispersion relation

We here derive in detail the implicit dispersion relations (6) and (14). We first make the ansatz that for a progressive wave of oscillating frequency ω and wave vector $\mathbf{k}$, w and p are of the following form,

$$[w(\mathbf{r},z,t),p(\mathbf{r},z,t)] = [\tilde{w}(\mathbf{k},z),\tilde{p}(\mathbf{k},z)]\mathrm{e}^{-\mathrm{i}\omega t+\mathrm{i}\mathbf{k}\cdot\mathbf{r}}. \quad \text{(A.1)}$$

Eliminating $\tilde{p}$ after inserting (A.1) into (3a) and (3b) yields the Rayleigh equation

$$(\mathbf{k}\cdot\mathbf{U}-\omega)(\partial_z^2-k^2)\tilde{w} = \mathbf{k}\cdot\mathbf{U}''w, \quad \text{(A.2)}$$

We define $H_w(\mathbf{k},z) = \sinh k(z+h)/\sinh kh$, and notice that since $(\partial_z^2-k^2)H_w = 0$,

$$\begin{aligned}
&\int_{-h}^{0} \mathrm{d}z\left[H_w(\mathbf{k},z)(\partial_z^2-k^2)\tilde{w}+\tilde{w}(\partial_z^2-k^2)H_w(\mathbf{k},z)\right]\\
&= H_w(\mathbf{k},0)\tilde{w}'(\mathbf{k},0) - w(\mathbf{k},0)H_w'(\mathbf{k},0)\\
&= \int_{-h}^{0}\mathrm{d}z\frac{\mathbf{k}\cdot\mathbf{U}''\tilde{w}H_w(\mathbf{k},z)}{\mathbf{k}\cdot\mathbf{U}-\omega}, \quad \text{(A.3)}
\end{aligned}$$

where the seabed condition $\tilde{w}(\mathbf{k}, -h) = 0$ was applied. The homogeneous boundary condition for w at the free surface is found as

$$(\mathbf{k}\cdot\mathbf{U}_0 - \omega)^2\tilde{w}_0\prime - [\mathbf{k}\cdot\mathbf{U}_0\prime(\mathbf{k}\cdot\mathbf{U}_0 - \omega) + gk^2]\tilde{w}_0 = 0, \quad \text{(A.4)}$$

where the subscript 0 denotes the values at $z = 0$.

Inserting the condition (A.4) into (A.3) then yields (6). Moreover, (A.4) and the dispersion relation (6) further give (14) since $w' = \tilde{w}'$ at $t = 0^+$.

Appendix A.2. The piecewise linear approximation

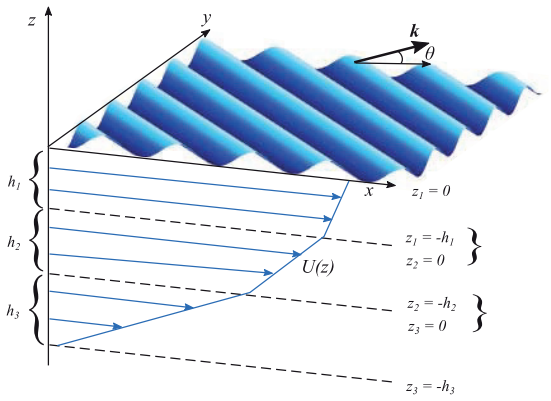

Figure A.12: Piecewise linear approximation (PLA): The velocity profile approximated by a piecewise-linear function, dividing the fluid ito N artificial layers.

Following [20], the fluid is artificially divided into N layers in the vertical direction each with thickness h_j and constant vorticity S_j as shown in Fig. A.12. A vertical coordinate z_j is defined within each layer where $z_j = 0$ and $-h_j$ at the top and bottom layer interfaces respectively. The approximate piecewise linear background velocity profile in each layer is

$$U_j^{PL} = U_{j-1} + S_j z_j.$$

A spatially uniform velocity V_0 in the y direction, corresponding to a translation of the frame of reference, can be added when needed, amounting only to the addition of a Doppler shift $k_y V_0$ to the wave frequencies $\omega(\mathbf{k})$ as calculated with the PLA.

As presented in more detail in [20], solutions u_j, v_j, w_j, p_j to the linearized Euler equations can now be found within each layer $j = 1, 2, ..., N$ modulo undetermined coefficients, and solutions are matched by requiring continuity of w and p (kinematic and dynamic boundary conditions, respectively) across the artificial layer boundaries, as well as free surface boundary conditions at $z = 0$ and vanishing w at $z = -h$ (or $z \to -\infty$). To wit one obtains

$$(\partial_t + \mathrm{i}\mathbf{k}\cdot\mathbf{U}_j)(\partial_{z_j}^2 - k^2)w_j = 0, \quad -h_j < z_j < 0, \quad \text{(A.5a)}$$
$$p_1 - \rho g\zeta = p_{\text{ext}}, \text{ at } z_1 = 0, \quad \text{(A.5b)}$$
$$w_1 = (\partial_t + \mathrm{i}\mathbf{k}\cdot\mathbf{U}_1)\zeta, \quad \text{at } z_1 = 0, \quad \text{(A.5c)}$$
$$w_j(z_j = -h_j) = w_{j+1}(z_{j+1} = 0), \quad \text{(A.5d)}$$
$$p_j(z_j = -h_j) = p_{j+1}(z_{j+1} = 0), \quad \text{(A.5e)}$$
$$w_N = 0, \; z_N = -h_N. \quad \text{(A.5f)}$$

where (A.5a) holds for $1 \le j \le N$, and (A.5d) and (A.5e) hold for $1 \le j \le N - 1$.

In particular, the vertical velocity perturbation and the dynamic pressure distribution are of the following forms, respectively

$$w_j = A_j(\mathbf{k}, t)\sinh k(z_j + h_j) + B_j(\mathbf{k}, t)\cosh k(z_j + h_j), \quad \text{(A.6a)}$$
$$-kp_j/\rho = (\partial_t + \mathrm{i}\mathbf{k}\cdot\mathbf{U}_j)w_j' - \mathrm{i}k_x S w_j. \quad \text{(A.6b)}$$

Inserting (A.6) into (A.5) and eliminating the B coefficients yields set of $N + 1$ linear equations. The eigenvalues of $\omega(\mathbf{k})$ are found from requiring the determinant of the system matrix be zero, the criterion for nontrivial solutions of the homogeneous system to exist. This gives, in general $N + 1$ eigenvalues, of which two are physical and an appropriate procedure must be employed to choose the correct values, as detailed and discussed in [20]. The procedure moreover automatically provides the coefficients A_1 and B_1 required in Eq. (27).

References

[1] O. M. Faltinsen, Hydrodynamics of High-Speed Marine Vehicles, Cambridge University Press (2005).

[2] J. H. Michell, The wave-resistance of a ship, The London, Edinburgh, and Dublin Phil. Mag. J. Sci. 45 (1898), 106–123.

[3] T. H. Havelock, The wave making resistance of ships: a theoretical and practical analysis, Proc. R. Soc. London A, 82 (1909), 197–208.

[4] T. H. Havelock, Ship resistance: the wave making properties of certain travelling pressure disturbances, Proc. R. Soc. London A, 89 (1914), 489–499.

[5] T. H. Havelock, Wave resistance: some cases of three-dimensional fluid motion, Proc. R. Soc. London A, 95 (1919), 354–365.

[6] T. H. Havelock, The effect of shallow water on wave resistance, Proc. R. Soc. London A, 95 (1922), 499–505.

[7] J. V. Wehausen, The wave resistance of ships, Adv. Appl. Mech. 13 (1973) 93–245.

[8] F. Noblesse, A slender–ship theory of wave resistance, J. Ship Res. 27 (1983), 13–33.

[9] M. Benzaquen, A. Darmon, and E. Raphaël, Wake pattern and wave resistance for anisotropic moving disturbances, Phys. Fluids, 26 (2014) 092106.

[10] Y. Li and S. Å. Ellingsen, Ship waves on uniform shear current at finite depth: wave resistance and critical velocity, J. Fluid Mech. 791 (2016), 539–567.

[11] S. Å. Ellingsen, Ship waves in the presence of uniform vorticity, J. Fluid Mech. 742 (2014) R2.

[12] T. H. Havelock, The initial wave resistance of a moving surface pressure, Proc. R. Soc. London A, 93 (1917), 240–253.

[13] T. H. Havelock, The wave resistance of a cylinder started from rest, Quart. J. Mech. Appl. Math., 2 (1949), 325–334.
[14] R. N. Bhattacharyya, Waves Produced by a Pressure System moving with an Acceleration over the Surface of Deep Water, Proc. Ind. Nat. Sci. Acad. 22 (1956) 155–169.
[15] J. V. Wehausen and E. V. Laitone, Surface Waves, in Encyclopedia of Physics vol 9 (Springer, 1960)
[16] S. Å. Ellingsen and P. A. Tyvand, Waves from an oscillating point source with a free surface in the presence of a shear current, J. Fluid Mech. 798 (2016) 232–255.
[17] T. H. Havelock, The propagation of groups of waves in dispersive media, with application to waves on water produced by a travelling disturbance, Proc. R. Soc. London A 81 (1908) 398–430.
[18] Y. Li and S. Å. Ellingsen, Effect of anisotropic shape on ship wakes in presence of shear current of uniform vorticity, in Proceedings of the 35th International Conference on Ocean, Offshore and Arctic Engineering (2016) OMAE2016-54250.
[19] V. I. Shrira, Surface waves on shear currents: solution of the boundary–value problem, J. Fluid Mech. 252 (1993), 565–584.
[20] B. K. Smeltzer and S. Å. Ellingsen, Surface waves on arbitrary vertically-sheared currents, Phys. Fluids 29 (2017) 047102 .
[21] O. M. Faltinsen, Sea Loads on Ships and Offshore Structures, Cambridge University Press (1990).
[22] X. Zhang, Short surface waves on surface shear, J. Fluid Mech. 541 (2005), 345–370.
[23] J. T. Kirby and T. M. Chen, Surface waves on vertically sheared flows: approximate dispersion relations, J. Geophys. Res. 94 (1989), 1013–1027.
[24] S. Å. Ellingsen and Y. Li, Approximate dispersion relations for waves on an arbitrary shear flow, (submitted).
[25] Y. Li and S. Å. Ellingsen, Initial value problems for water waves in the presence of a shear current, in Proceedings of the 25th International Ocean and Polar Engineering Conference (2015), Vol. 3 pp. 243–250.
[26] S. Å. Ellingsen, Initial surface disturbance on a shear current: The Cauchy–Poisson problem with a twist, Phys. Fluids 26 (2014) 082104.
[27] L. F. Kilcher and J. D. Nash, Structure and dynamics of the Columbia River tidal plume front, J. Geophys. Res. Oceans 115 (2010) C05590. Data sets available from `http://makani.coas.oregonstate.edu/rise/`.
[28] H. Schneekluth and V. Bertram, Ship Design for Efficiency & Economy, 2nd ed., Butterworth–Heinemann (1998).
[29] B. K. Smeltzer, Y. Li and S. Å. Ellingsen, Effect on Doppler resonance from a near–surface shear layer, in Proceedings of the 36th International Conference on Ocean, Offshore and Arctic Engineering (2017) OMAE2017-61231.

Paper VII

Initial value problems for water waves in the presence of a shear current

Is not included due to copyright

Paper VIII

Effect of Anisotropic Shape on Ship Wakes in Presence of Shear Current of Uniform Vorticity

---

Is not included due to copyright